

**THE TECTONIC EVOLUTION OF THE INGENIKA GROUP AND
ITS IMPLICATIONS FOR THE BOUNDARY BETWEEN THE
OMINECA AND INTERMONTANE BELTS,
NORTH-CENTRAL BRITISH COLUMBIA**

by

KIM ANGELINA BELLEFONTAINE

**DEPARTMENT OF GEOLOGICAL SCIENCES
MCGILL UNIVERSITY
MONTREAL, QUEBEC**

**A THESIS SUBMITTED IN PARTIAL FULFILLMENT OF
THE REQUIREMENTS FOR THE DEGREE OF
MASTER OF SCIENCE**

DECEMBER, 1990

© KIM ANGELINA BELLEFONTAINE, 1990

ABSTRACT

The Ingenika Range forms part of a large zone of structural divergence that roughly coincides with the boundary between North America and Superterrane I. Contrasting tectonic histories from the Intermontane, Omineca and Foreland Belts at the latitude of the thesis area are consistent with a collisional model involving tectonic wedging, delamination and large-scale backthrusting.

The Upper Proterozoic Ingenika Group in the Ingenika Range has undergone a progressive deformational history involving pre-, syn-, and post-metamorphic structures. During the Middle Jurassic regional structural vergence changed from northeast- to southwest-directed folds and faults. Regional metamorphism reached amphibolite ^{facies} grade and was synchronous with west-vergent deformation. Minor structures in the study area suggest that the Swannell fault was an east-dipping thrust fault that emplaced North American strata over allochthonous rocks of Quesnellia. The Swannell fault was probably also active during the Middle Jurassic and may have acted as the structural discontinuity between a backthrustured crustal flake and an underlying, eastward moving wedge.

RESUME

La chaîne Ingenika fait partie d'une zone structurale en extension qui correspond à la frontière entre le continent nord-américain et le superterrain I. L'évolution de chacune des ceintures tectoniques Intermontane, Omineca, et Foreland au niveau de la région d'étude est différente bien qu'elles soient en accord avec un modèle tectonique global en collision impliquant un prisme d'accrétion tectonique, une délamination et un r trocharriage   grande  chelle.

Dans la cha ne Ingenika, le Groupe Ingenika d' ge Prot rozoique sup rieur a subi une d formation progressive impliquant des structures pr -, syn- et post-m tamorphiques. Au Jurassique moyen, le d versement r gional des failles et plis a chang  du nord-est au sud-ouest. Le m tamorphisme r gional a atteint le facies amphibolitique tout en  tant contemporain au d versement vers l'ouest des unit s. Dans la r gion d' tude, les structures g ologiques mineures sugg rent que la faille Swannell  tait   l'origine une faille de chevauchement   pendage vers l'est qui mettait en contact les strates du continent nord-am ricain surmontant les strates allochtones du Quesnellia. La faille Swannell qui  tait probablement aussi active au Jurassique moyen, peut avoir agi en tant que discontinuit  structurale entre une couche crustale de r trocharriage et une unit  sous-jacente se d pla ant vers l'est.

ACKNOWLEDGEMENTS

I am grateful to Dr. Andrew Hynes for financial support for the project, rigorous discussions in the field and out, review of this manuscript and most of all for being a patient and understanding supervisor. Personal communications with Hugh Gabrielse, Graham Nixon, Filippo Ferri and JoAnne Nelson have greatly improved my geological knowledge of north-central British Columbia. They are sincerely appreciated for their discussions. Kathy Minehan is thanked for many conversations about the project and for assistance and company in the field. Microcomputer programs, and the expertise to go with them were provided by Glenn Poirier and Serge Perreault. Discussions with them and Roland Dechesne have helped in the compilation and interpretation of data. The french translation of the abstract was prepared by Bill McMillan, S.P., G.S., and Mark Soiseth. Merci beaucoup!

The contributions of many other individuals have been essential for the completion of this thesis. George Panagiotidis prepared polished thin sections of samples, Dr. Moyra MacKinnon helped in the acquisition of microprobe analyses and Ed Hawco and Richard Yates provided photographs and slides. Northern Mountain Helicopter Ltd., Joe Martin & Sons, Skylark Resources and Esso Minerals provided logistical support, entertainment, and occasional hot showers and meals during the '87 and '88 field seasons. "Johansen Portable" gratefully acknowledges their generosity and hospitality. Additional funds were supplied by the British Columbia Ministry of Energy Mines and Petroleum Resources in the form of research grants.

I am also indebted to my family and friends for their support during the course of this project. The Montréal chapter includes Adrien and Judy Doucette, Gary Nassif, Kate MacLachlan, Anne Kowsloski, Jennifer Springer, François Legault, Scott Green, Jim Rowland and Stephane Bunton. The B.C. contingent

includes Filippo Ferri, Ron Arksey and JoAnne Nelson. And last but not least, thanks to my parents Danny and Judy, for supporting me in everything I do and for moving "me and my rocks" across the country countless times.

THANKS TO ALL!!

TABLE OF CONTENTS

Abstract.....	ii
Resume	iii
Acknowledgements	iv
Table of Contents.....	vi
List of Figures	ix
List of Plates.....	x
List of Tables.....	xii

CHAPTER I INTRODUCTION

1.1 Regional Geology	1
1.2 Purpose of Study	3
1.3 Location Accessibility	4
1.4 Local Geology	4
1.5 Previous Work.....	6

CHAPTER II STRATIGRAPHY

2.1 Introduction	9
2.2 Distribution of Lithologies.....	9
2.3 Stratigraphic Terminology and Interpretation.....	11
2.4 Correlations with Windermere Stratigraphy.....	17

CHAPTER III STRUCTURE

3.1 Introduction	21
3.2 D ₁ Structures	21
3.3 D ₂ Structures	25

TABLE OF CONTENTS CONT'D

3.4	D ₃ Structures	27
3.4.1	D ₃ Structures on Southwest Limb	27
3.4.2	D ₃ Structures on Northeast Limb	33
3.5	D ₄ Structures	33
3.6	Structural Summary	42

CHAPTER IV METAMORPHISM AND GEOTHERMOBAROMETRY

4.1	Introduction	43
4.2	Distribution of Metamorphic Isograds	43
4.3	Petrology	45
4.4	Relationship of Metamorphism to Deformation	48
4.5	Geothermobarometry	49
4.5.1	Introduction	49
4.5.2	Mineral Chemistry	51
4.5.3	Garnet-Biotite Geothermometer	52
4.5.4	Plagioclase-Biotite-Garnet-Muscovite Geobarometer	53
4.6	Results of Thermobarometry	57
4.7	Metamorphic Summary	59

CHAPTER V DISCUSSION AND CONCLUSIONS

5.1	Introduction	61
5.2	Geochronology of the Ingenika Range	61
5.3	Important Observations near Terrane Suture	63
5.3.1	Northern Omineca Belt - Swannell Ranges	64
5.3.2	Foreland Belt - Northern Rocky Mountains	65
5.3.3	Intermontane Belt - Lay Range	65

TABLE OF CONTENTS CONT'D

5.4	Synthesis and Interpretation	66
5.5	Tectonic Model	67
5.6	Discussion	69
5.7	Conclusions	71
Bibliography		73
Appendix A - Mineral Chemistries		84
A.1	Analytical Procedure	84
A.2	Analyses	84
Appendix B - Structural Map		In Rear Pocket

LIST OF FIGURES

- Figure 1:** Regional geology of north-central British Columbia.
- Figure 2:** Physiographic map of the Omineca Mountains.
- Figure 3:** Stratigraphic interpretation of Roots (1954).
- Figure 4:** Stratigraphy of the Ingenika Group.
- Figure 5:** Distribution of Ingenika Group in the southern Swannell Ranges.
- Figure 6:** Distribution of Windermere Supergroup in Canadian Cordillera.
- Figure 7:** Correlations of Windermere Stratigraphy.
- Figure 8:** Stereonet plot of F_1 fold axes.
- Figure 9:** Stereonet plot of Swannell antiform.
- Figure 10:** Stereonet plot of F_3 folds associated with minor thrust faults.
- Figure 11:** Schematic cross-section of the Ingenika Range.
- Figure 12:** Equal area stereonet plot of fold axes of small-scale kink folds.
- Figure 13:** Stereonet plot of axial planes of small-scale kink folds.
- Figure 14:** Possible stress fields produced with minor strike-slip motion on Swannell fault.
- Figure 15:** Structural data of megascopic kink fold.
- Figure 16:** Distribution of mineral isograds, and thermobarometry results.
- Figure 17:** Tectonic evolution of the Superterrane I - North American suture zone.

LIST OF PLATES

- Plate 1: Quartzites of lower Swannell Formation.
- Plate 2: Crenulated semi-pelitic schist of the Swannell Formation.
- Plate 3: Chloritic grits from the upper Swannell Formation.
- Plate 4: Carbonaceous sand of the Espee Formation(?).
- Plate 5: Green phyllite belonging to the Tsaydiz Formation(?).
- Plate 6: Crystalline limestone from the Espee Formation(?).
- Plate 7: Graded bedding in micaceous quartzite.
- Plate 8: Channelling in gritty sands.
- Plate 9: Isoclinal F_1 fold in metaquartzite.
- Plate 10: Large-scale F_1 fold in lower Swannell Formation.
- Plate 11: Cascading, rootless F_1 folds.
- Plate 12: F_1 fold defined by bedding-cleavage relationship.
- Plate 13: Southwesterly rotated, helicitic, syn-tectonic (D_2) garnet.
- Plate 14: Well developed crenulation cleavage.
- Plate 15: F_3 fold associated with slide plane.
- Plate 16: F_3 fold on southwest limb of antiform.
- Plate 17: Example of F_3 drag fold.
- Plate 18: F_3 fold evidenced by cross-cutting strata.
- Plate 19: Thrust fault about to form on southwest limb of Swannell antiform.
- Plate 20: Sub-horizontal benches marking thrust faults.
- Plate 21: Parasitic F_3 fold on northeast limb.
- Plate 22: Parasitic F_3 fold.
- Plate 23: D_3 bedding parallel thrust.
- Plate 24: Bedding parallel thrusts on northeast limb of Swannell antiform.
- Plate 25: Small-scale drag fold on northeast limb.
- Plate 26: Small-scale drag fold.

LIST OF PLATES CONT'D

- Plate 27: Dextral shear kink.
- Plate 28: Sinistral kink fold.
- Plate 29: Helicitic garnet preserving a straight S_1 schistosity.
- Plate 30: Spider garnet overgrowing S_1 and S_2 schistositities.
- Plate 31: Idioblastic garnet in garnet-sericite schist.
- Plate 32: Porphyroblastic biotite cross-cutting deformed schistosity planes.

LIST OF TABLES

- Table 1:** Metamorphic mineral assemblages.
- Table 2:** Results of geothermometry.
- Table 3:** Results of geobarometry.
- Table 4:** Summary of metamorphic conditions in the Ingenika Range.
- Table 5:** Tectonic history of the Ingenika Range.

CHAPTER I

INTRODUCTION

1.1 REGIONAL GEOLOGY

The Canadian Cordillera is divided into five morphogeologic (Figure 1, inset) composed of many distinct terranes (Gabrielse et al., in press). The research area lies near the boundary between the Omineca and Intermontane Belts, or more precisely, it straddles the suture zone between the accreted Intermontane Superterrane (Superterrane I - Stikinia, Cache Creek, Quesnellia, Harper Ranch, Slide Mountain) and the para-autochthonous cratonic rocks of the Cassiar terrane (Wheeler and McFeely, 1987; Wheeler et al. 1988). At the latitude of the study area, the terrane suture is defined by the Swannell fault.

East of the Swannell fault the Cassiar terrane consists of latest Precambrian miogeoclinal strata belonging to the Ingenika Group. These rocks are best exposed in a series of northwest trending, doubly plunging, elongate anticlinoria (Mansy and Dodds, 1976). West of the Swannell fault the Upper Paleozoic and Upper Triassic(?) Lay Range Assemblage is assigned to the Harper Ranch terrane and is thought to represent the basement of the Takla Group (Wheeler et al., 1988; Monger et al., in press). The Lay Range Assemblage consists of basaltic flows, cherts, volcanoclastics and argillites of oceanic affinity (Roots, 1954; Monger 1973; Irvine, 1974; Monger and Paterson, 1974) that have been intruded by the Late Triassic(?) Polaris Alaskan-type ultramafic body (Nixon et al., 1990a, 1990b). Late Triassic Takla Group east of the Pinchi-Finlay fault is part of the Quesnel terrane. It is composed of calc-alkaline island arc volcanics and probable comagmatic plutonic rocks and associated volcanoclastic sediments (Monger, 1977; K. Minehan, 1989b; Monger et al., in press). Late Triassic to early Jurassic rocks of similar

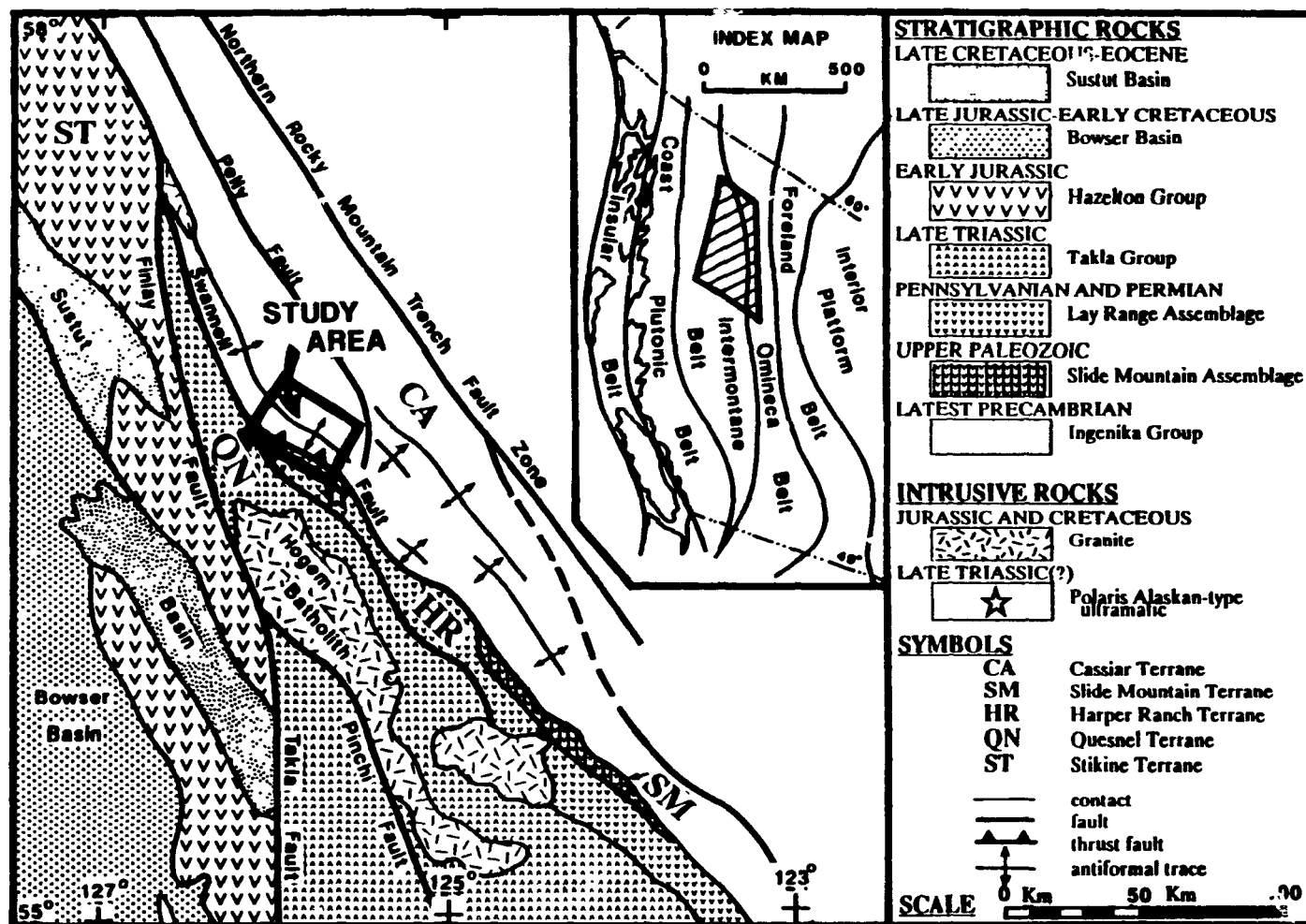


Figure 1: Regional geology of north-central British Columbia showing location of study area; map is modified after Wheeler and McFeely (1987) and Wheeler et al. (1988). Map inset displays the tectonostratigraphic zones of the Canadian Cordillera (Price et al., 1985).

chemistry west of the Pinchi-Finlay fault belong to the Takla and Hazelton Groups but are assigned to the Stikine terrane (Wheeler et al., 1988).

The structural style and prevailing metamorphic conditions of the Intermontane Belt are very different from those of the Omineca Belt. The former is characterized by northerly to northwesterly trending, steeply dipping strike slip faults with accompanying sub-greenschist to greenschist grade metamorphism (Monger, 1977; Bellefontaine and Minehan, 1988; Minehan, 1989a, 1989b). The latter has been subjected to polyphase deformation and regional metamorphism of amphibolite grade (Gabrielse et al., in press; Greenwood et al. in press).

The individual suspect terranes of the Intermontane Belt were probably assembled into Superterrane I by the end of the Triassic. Collision of this terrane with the paleomargin of North America occurred shortly thereafter (Wheeler and McFeely, 1987; Gabrielse and Yorath, in press). This thesis deals with the tectonic history of the cratonic rocks and the way in which Superterrane I and the North American continent collided in the area of study.

1.2 PURPOSE OF STUDY

The study area lies within the Proterozoic Ingenika Group at the boundary between cratonic North America (Omineca Belt) and rocks of the Intermontane Belt. The area is unique because it is nestled between the Finlay and Pinchi faults and the Northern Rocky Mountain Trench and appears to have been sheltered from any significant transcurrent movement (Gabrielse, 1985). Thus, it is a prime locality to study the original boundary relationship between ancestral North America and its first allochthonous terrane.

This project was undertaken for the following reasons:

1. to determine the nature of the contact (ie. Swannell fault) between the Omineca and Intermontane Belts in north-central British Columbia.
2. to document how and when motion occurred on the Swannell fault.
3. to unravel the complex structural and metamorphic history of the Ingenika Group.
4. to obtain the peak temperature and pressure conditions that affected the Ingenika rocks.
5. to compare the tectonic history of the Ingenika Range with other localities along the Superterrane I - North American suture zone.
6. to evaluate the tectonic implications of the findings.

1.3 LOCATION ACCESSIBILITY

The area of investigation is located in north-central British Columbia approximately 180 kilometres north-northwest of Prince George and 150 kilometres north-northeast of Smithers. The region can be accessed by plane or helicopter from both towns via the Sturdee Airstrip in the Toodoggone Valley. The area can also be reached using the Omineca Mining Road from Fort St. James as far as Johanson Lake. The last leg of the journey must be completed by helicopter. The trip is approximately one hour ferry time from the Sturdee Airstrip.

1.4 LOCAL GEOLOGY

The research area is located approximately 25 kilometres due north of Aiken Lake in the Ingenika Range of north-central British Columbia. The Ingenika Range is a subdivision of the Swannell Ranges of the Omineca Mountains (NTS 94C/12 - Orion Creek; Figure 2). The Upper Proterozoic Ingenika Group occupies a series of metamorphic culminations west of the Northern Rocky Mountain Trench. A

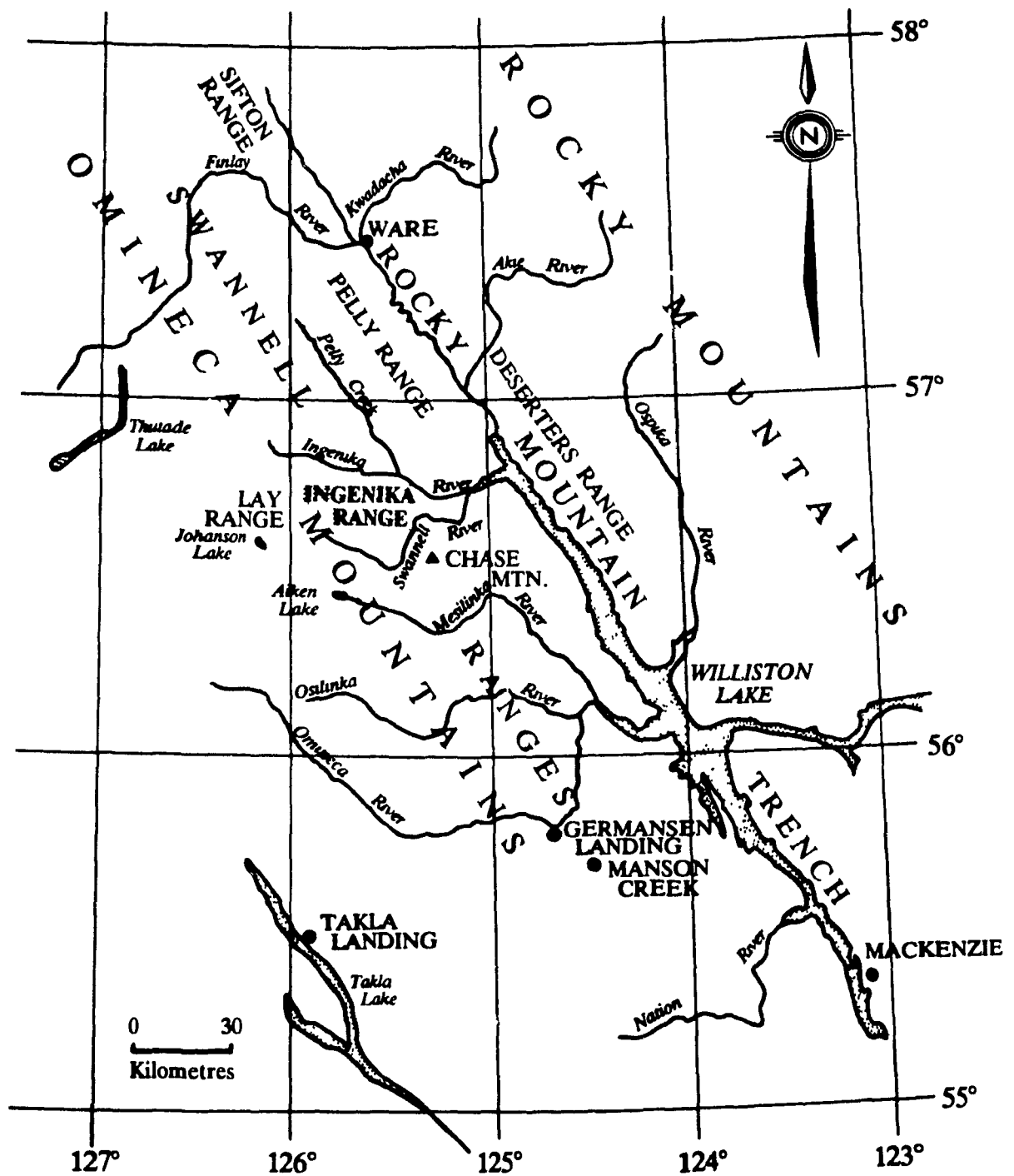


Figure 2: Physiographic map displaying major mountain ranges of the Omineca and Rocky Mountains in north-central British Columbia.

large post-metamorphic, doubly plunging antiform makes up the backbone of the Swannell Ranges. Although this antiform is slightly offset in places, it extends approximately 120 kilometres from the Wolverine Complex in the south to the crosscutting mid-Cretaceous Mount Whudzi granitic pluton in the north, located at the junction of the Swannell fault and the Finlay fault (Figure 1). The antiform is bounded to the east by the Pelly fault which brings similar clastic rocks into contact with the Ingenika Group. To the west it is limited by the Swannell fault, which is the suture that separates the cratonic rocks of North America from the suspect oceanic and island-arc terranes of the Intermontane Belt.

In the Ingenika Range the large-scale anticlinal structure is informally referred to as the Swannell antiform. This asymmetrical fold is slightly inclined to the southwest and folds the metamorphic isograds of the region. The highest-grade rocks are exposed in the core of the structure while the lowest grade rocks are present on the limbs. The isograds are evenly and widely spaced on the moderately dipping northeast limb (120/35NE) and closely spaced on the steeply dipping southwest limb (135/60SW) due to structural complexities. A segment from the northwest-plunging sector of the antiform between Wrede Creek and Swannell River was selected for detailed investigation.

1.5 PREVIOUS WORK

Work in the Aiken Lake map area (94/C west half - now Mesilinka) began in the mid 1940's with the studies of Armstrong (1946) and Armstrong and Roots (1948). Roots (1954) produced the first geological map of the area in which he defined two major stratigraphic units in the Ingenika Range and crudely delineated the major antiformal structure and metamorphic zonations of the region.

Operation Finlay marked the beginning of a regional-scale mapping project of the Omineca Mountains. Major contributions were made by Gabrielse (1971, 1972a, 1975), Gabrielse and Dodds (1974), Gabrielse et al. (1976, 1977), Mansy (1971, 1972, 1974), and Mansy and Dodds (1976). Regional studies in the Cassiar Mountains were conducted by Gabrielse (1962, 1963), Gabrielse and Mansy (1978, 1980), and Gabrielse and Dodds (1982). Compilation of much of this information by Mansy and Gabrielse (1978) led to a description of Upper Proterozoic stratigraphy exposed throughout the Omineca and Cassiar Mountains and these rocks were correlated with paleomargin strata along the entire orogen. More recently, Mansy (1986) completed an extensive regional stratigraphic and structural investigation of the miogeoclinal rocks present in the Omineca Mountains. He made broad interpretations of the structure and stratigraphy of the Ingenika Range and mapped the distribution of metamorphic isograds around the Swannell antiform.

Several graduate theses were carried out in neighbouring regions. Parrish (1976a, 1976b) researched the structure, metamorphism and geochronology of the Chase Mountain region directly southeast of the Ingenika Range. He documented doubly plunging structures in complexly deformed rocks at the northern edge of the high-grade Wolverine Complex. A follow-up paper (Parrish, 1979) discussed the geochronology of this area and its tectonic implications for the timing of deformation and metamorphism in the north-central part of the Omineca Crystalline Belt. Evenchick (1985, 1988) conducted a similar stratigraphic, structural, and metamorphic analysis of the Sifton and Deserters Ranges in the Cassiar and Northern Rocky Mountains.

Gabrielse (1985) reconstructed the Cordilleran orogen in north-central British Columbia by restoring displacements along the Northern Rocky Mountain

Trench and related faults. The orientation and movement on the Swannell fault, and its position in the overall tectonic framework of the Canadian Cordillera were discussed by Gabrielse.

The most recent studies of the cratonic rocks in the study area were done by Bellefontaine and Minehan (1988) and Bellefontaine (1989). These papers addressed some aspects of the tectonic history of the Ingenika Group and the probable strike and dip of the Swannell fault in the Ingenika Range. Bellefontaine and Hynes (1990) proposed a model for the Ingenika Range which is further developed in this paper.

Previous work on Intermontane rocks in contact with the Ingenika Group has not been substantial. The Lay Range Assemblage of oceanic rocks was examined primarily by Monger (1973) and Monger and Paterson (1974). The Polaris Alaskan-type ultramafic intrusion exposed in the Lay Range was treated in some detail by Irvine (1974, 1976) and most recently by Nixon et al. (1990a, 1990b). The Triassic Takla Group exposed in the Wrede Range directly north of Johanson Lake was studied by Monger (1977), Bellefontaine and Minehan (1988) and Minehan (1989a and 1989b).

The most recent regional-scale geologic mapping in the area was conducted near Germansen Landing and Manson Creek by Ferri and Melville (1988, 1989, 1990, in prep.) and Ferri et al. (1989).

CHAPTER II

STRATIGRAPHY

2.1 INTRODUCTION

Strata exposed in the Ingenika Range belong to the latest Hadrynian Ingenika Group of the Windermere Supergroup (Mansy and Gabrielse, 1978). The stratigraphic succession is dominated by monotonous sequences of metamorphosed quartz-rich clastic rocks and minor aluminous schists. The package contains no distinct marker units and no intrusive bodies. The rocks have experienced different styles and intensities of deformation as well as variable grades of metamorphism. Structural complexities in the area have disturbed stratigraphic relationships to such a large extent that sections and estimates of unit thicknesses by others (Mansy, 1972, 1974, 1986; Mansy and Dodds, 1976) are of questionable value.

The following discussion deals with the distribution of lithologies in the study area, the regional stratigraphic terminology proposed by Roots (1954) and Mansy and Gabrielse (1978), and the stratigraphic anomalies that exist along the western edge of the Swannell Ranges.

2.2 DISTRIBUTION OF LITHOLOGIES

Although the area is structurally complex, some general observations about the distribution of lithologies can be made. Rocks outcropping in the core of the Swannell antiform are significantly different from those exposed on each of the limbs. The core of the antiform is composed of repetitious sections of well bedded micaceous schist, quartzose schist, micaceous quartzite and pure quartzite interlayered with minor semi-pelitic schist and very rare amphibole-bearing quartzite (Plate 1). The quartz-rich rocks weather a variety of colours including



Plate 1: Well bedded, pure quartzites and semi-pelites of the lower Swannell Formation exposed in the core of the Swannell antiform

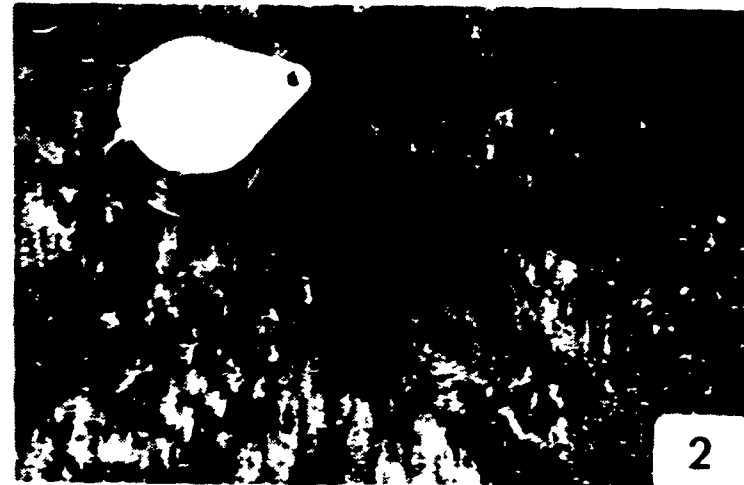


Plate 2: Crenulated semi-pelitic schist containing garnet, muscovite and biotite.



Plate 3. Grits exposed on the east limb of the antiform contain white feldspar and blue opalescent quartz grains



Plate 4. Buff coloured carbonaceous sand of the Espee Formation(?) displays bedding on the west flank of the Swannell antiform. View to the northwest; hammer for scale.

golden brown, grey, buff and white and are composed of sand-sized grains of quartz and minor feldspar. Semi-pelitic rocks typically contain muscovite, biotite, garnet \pm staurolite and are silver-grey in colour (Plate 2).

The eastern limb of the antiform is dominated by massive, well bedded (metre scale) grey-green grits and gritty sands that commonly contain chlorite, chalky white feldspar and blue opalescent quartz grains (Plate 3). The grits are interlayered with minor micaceous schist and blue-grey and green, well cleaved, laminated phyllites.

Grits and sands, commonly with a carbonaceous matrix, are overlain by several metres of green phyllite and a large limestone body on the west limb of the antiform (Plates 4 and 5). Grey-blue, massive, crystalline limestone displays sedimentary laminations in several localities and forms a ridge of outcrop close to the Swannell fault (Plate 6).

Sedimentary structures are not abundant in the study area. Rocks display bedding, graded bedding and very rare channelling (Plates 7 and 8).

2.3 STRATIGRAPHIC TERMINOLOGY AND INTERPRETATION

Roots (1954) introduced a two-fold stratigraphic classification for the Proterozoic strata in the Aiken Lake area. It included the lowermost Tenakihi Group, exposed in the core of the antiform, and the upper Ingenika Group present on the flanks of the fold (Figure 3). Gabrielse (1975) found that the distinction between the Ingenika and Tenakihi Groups was impossible to establish in the Fort Grahame map area. This led Mansy and Gabrielse (1978) to propose a new terminology for the upper Proterozoic strata exposed throughout the Cassiar and Omineca Mountains. The Ingenika Group was redefined as all strata that underlie the Cambrian Atan orthoquartzite and was subdivided into four formations named



Plate 5: Well cleaved, green phyllite on west limb of the antiform. May belong to the Tsaydiz Formation(?).



Plate 6. Blue-grey, massive crystalline limestone of the Espee Formation(?) on the west flank of Swannell antiform. View to the northwest.



Plate 7: Graded bedding in micaceous quartzite belonging to the lower Swannell Formation



Plate 8. Rare channelling in gritty sand suggests sediment transport from an eastern source.

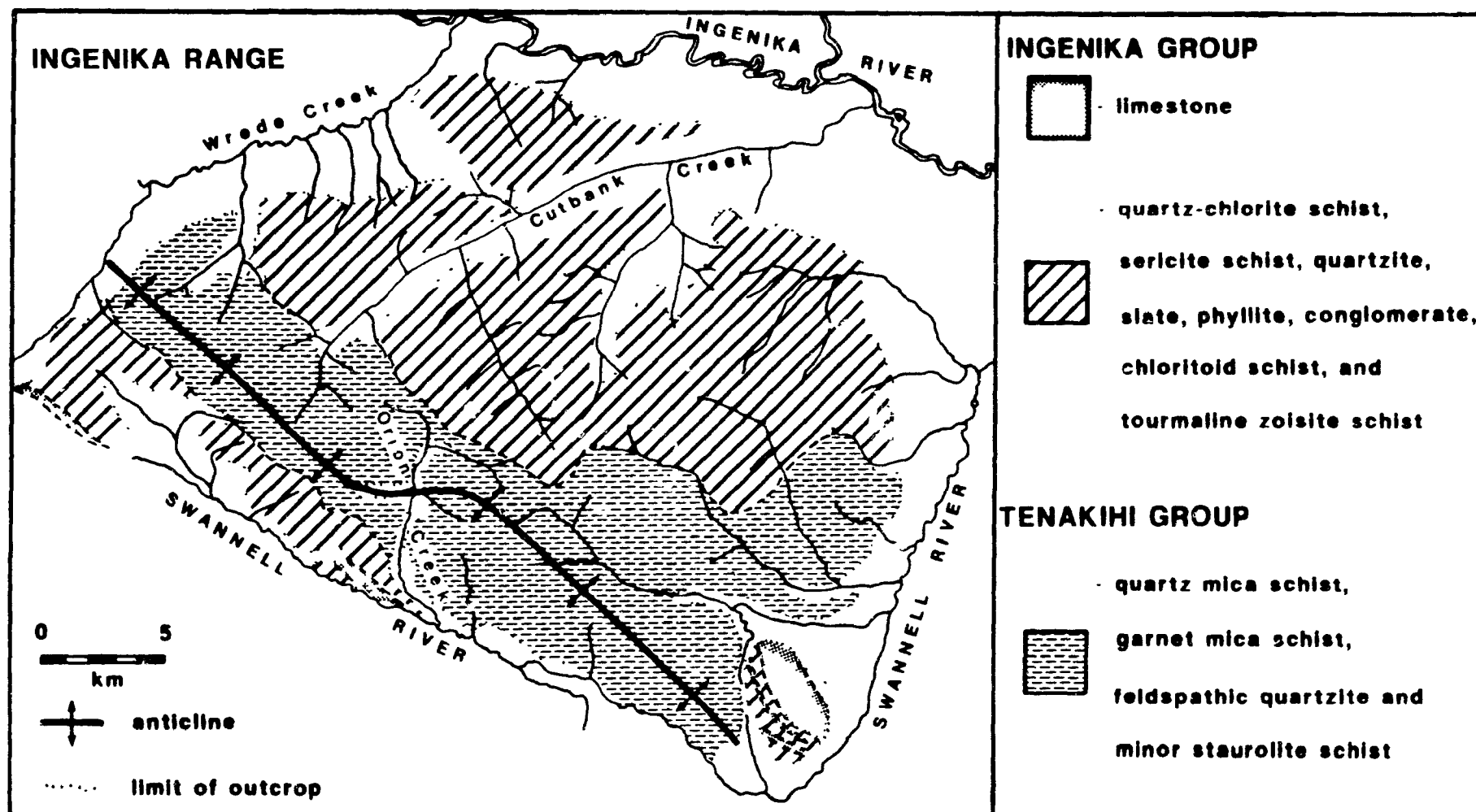


Figure 3: Twofold stratigraphic division of the Ingenika Range proposed by Roots (1954).

after the mountain ranges in which they are best exposed. From oldest to youngest these are the Swannell, Tsaydiz, Espee and Stelkuz Formations (Figure 4). This new stratigraphic terminology proved very effective when mapping Proterozoic strata in north-central British Columbia. However, difficulties in applying the scheme were encountered in the high-grade metamorphic rocks of the Wolverine Complex and in strata exposed along the western limb of the Swannell antiform (H. Gabrielse, pers. comm., 1989).

The lithologies on the west limb of the Swannell antiform do not correlate with those on the eastern limb (Mansy, 1986; H. Gabrielse, pers. comm., 1989; and this report). The eastern limb of the fold has significantly thicker exposures of middle and upper Swannell Formation than the west limb. Also, the west limb has a large carbonate body that does not outcrop to the east (Figure 5). Large bodies of carbonate have not been documented in the lower formations of the Ingenika Group. The first major limestone is found in the Espee Formation (Figure 4). The limestone on the west limb appears to be in contact with strata of the middle Swannell Formation. If the carbonate is part of the Espee Formation the upper member of the Swannell Formation and possibly the entire Tsaydiz Formation are missing from the section. Minor phyllite occurring on the west limb may represent a very thin Tsaydiz Formation or part of the middle or upper Swannell Formation. However, distinction between these possibilities is difficult since placement in the stratigraphic succession is dependent on a complete sequence of rock types and not the occurrence of a single lithology.

Differences in stratigraphy on the two limbs of the Swannell antiform have been attributed to facies variations by Mansy (1986). However, the structural data presented in Chapter 3 indicate that the stratigraphic succession on the west limb has been displaced along west-directed thrust faults. Thus, the large carbonate body

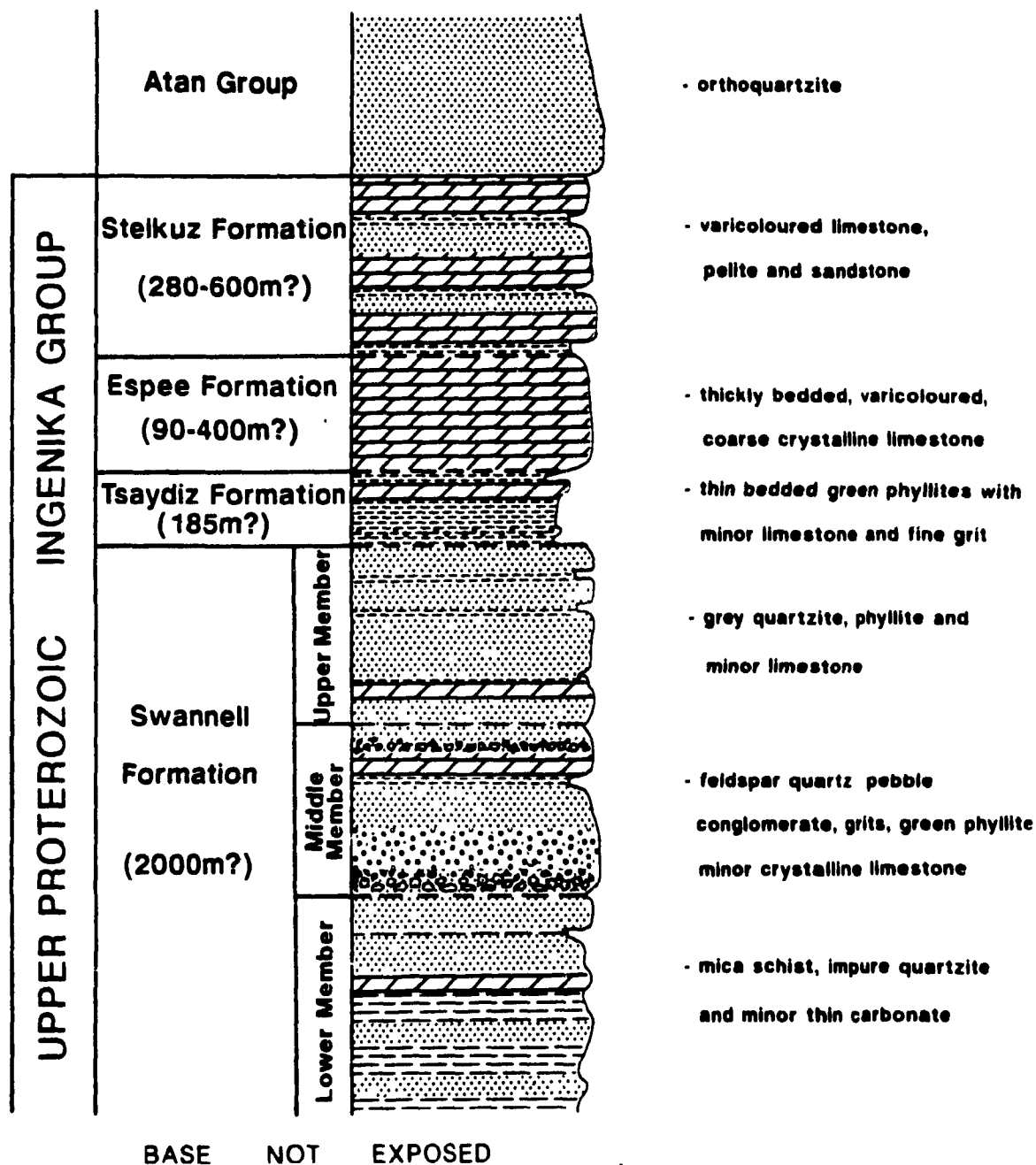


Figure 4: Stratigraphic succession proposed by Mansy and Gabrielse (1978) for upper Proterozoic strata in the Omineca and Cassiar Mountains. Thicknesses are suspect due to structural complexities.

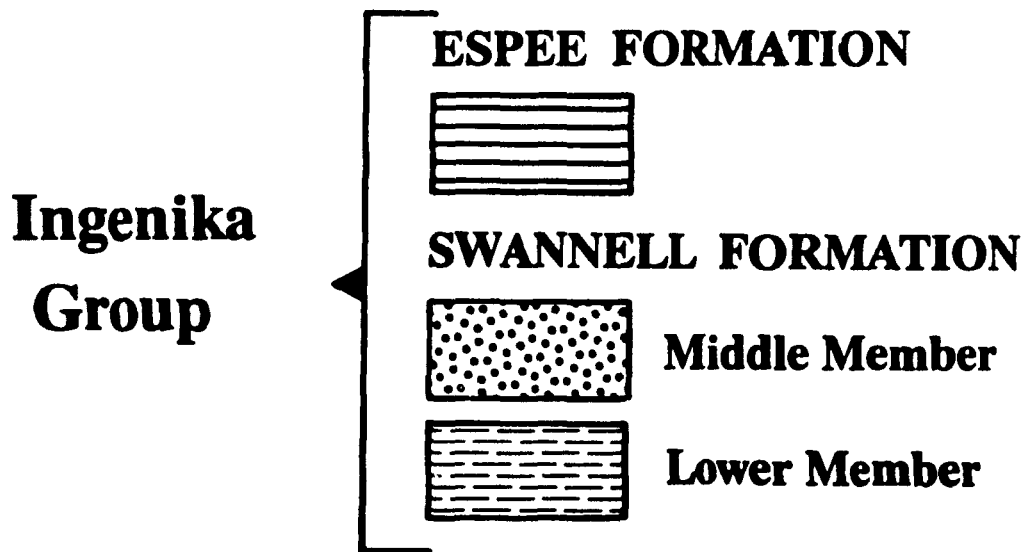
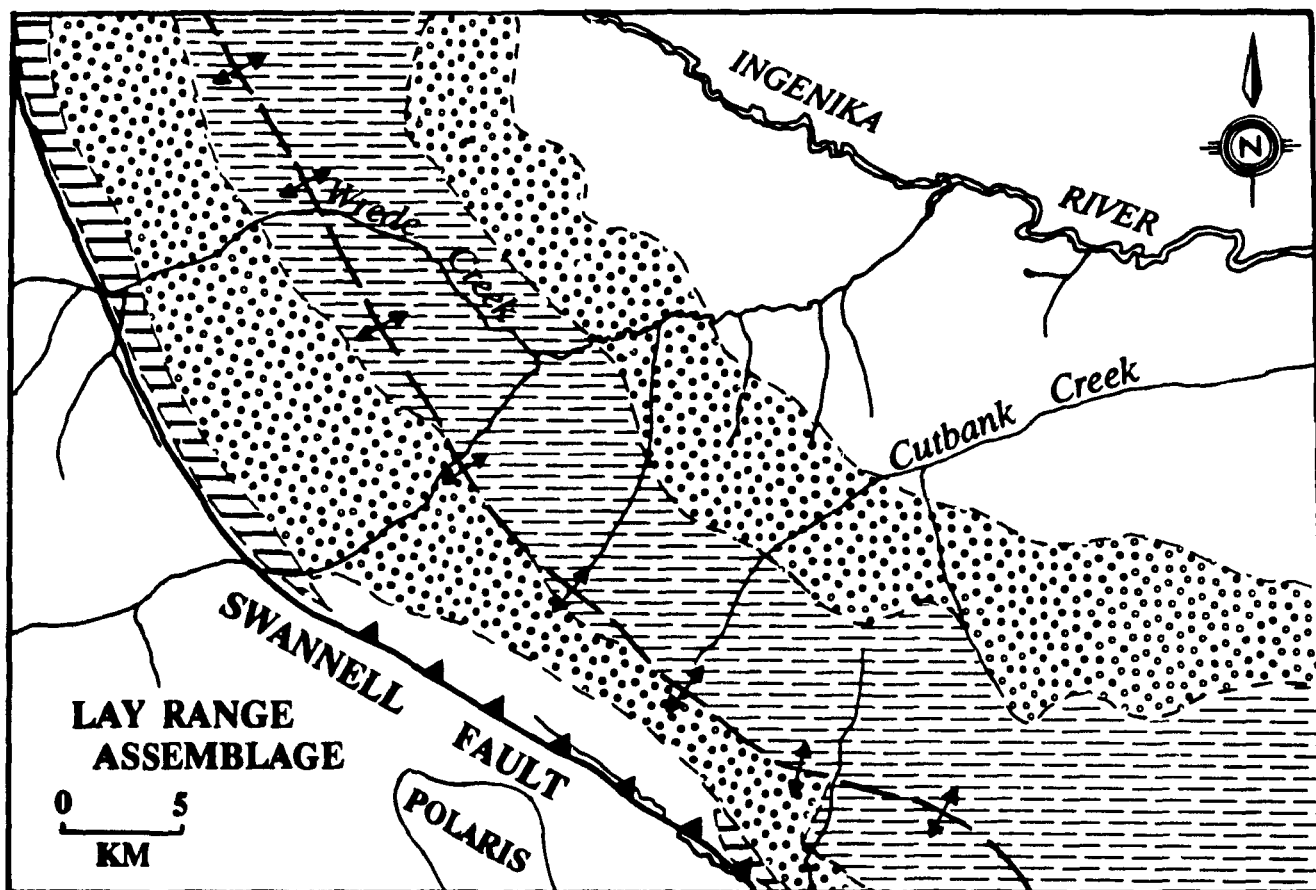


Figure 5: Distribution of Ingenika Group in the southern Swannell Ranges (modified after Roots, 1954; Mansy and Gabrielse, 1978; Mansy, 1986).

on the western limb probably belongs to the Espee Formation and is not a manifestation of facies changes. The Espee carbonate has been brought to the present level of erosion by thrust faulting (Figure 11).

2.4 CORRELATIONS WITH WINDERMERE STRATIGRAPHY

The Windermere Supergroup is a clastic wedge of miogeoclinal strata that extends the length of the Canadian Cordillera (Figure 6). It was deposited off the western margin of cratonic North America during late Proterozoic time (Mansy and Gabrielse, 1978). These rocks lie stratigraphically between older Precambrian units (Precambrian basement complexes and Belt Purcell sedimentary assemblages) and lower Cambrian quartzites (Young et al., 1973; Eisbacher, 1981). Windermere sequences are characterized by thick basal units of coarse grits and fine shales, overlain by thick carbonates and fine clastics. The lithological change from shales to carbonates marks the transition from deep-water to shallow-water conditions (Young et al., 1973; Mansy and Gabrielse, 1978).

Gabrielse (1972b) was the first to correlate Proterozoic strata in north-central British Columbia with the Windermere Supergroup. Mansy and Gabrielse (1978) assigned the Ingenika Group to the Windermere Supergroup on the basis of similar sedimentary characteristics. Poorly sorted, thickly bedded, monotonous clastic sequences derived from an eastern source indicate deposition in relatively deep water. Coarser beds and graded bedding are compatible with deposition by turbidity currents. The establishment of shallow-water conditions in the Ingenika Group is marked by the deposition of the Tsaydiz Formation and the Espee carbonates. These conditions existed through to the end of Proterozoic time (Mansy and Gabrielse, 1978).

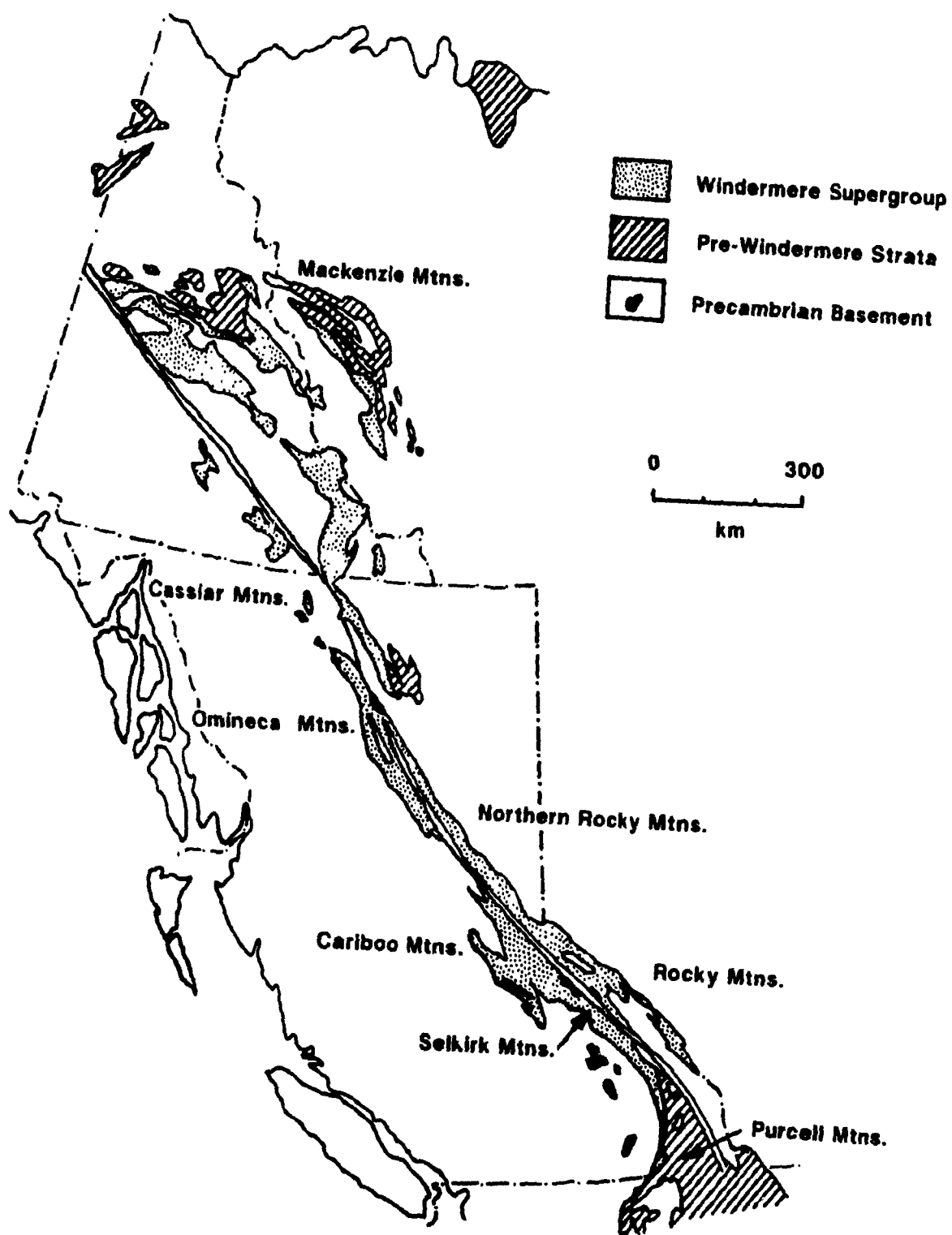


Figure 6: Distribution of Windermere Supergroup in Canadian Cordillera (after Eisebacher, 1981; Evenchick, 1985).

		CASSIAR, OMNECA MOUNTAINS		CARIBOO MOUNTAINS		NORTHERN PURCELL MOUNTAINS		CENTRAL PURCELL MOUNTAINS		SCUTHERN SELKIRK MOUNTAINS		ROCKY MOUNTAINS MOUNT ROBSON		NORTHERN ROCKY MOUNTAINS																																																																																																																																																																																																																																																																																																																																																																																																																																																																																																																																																																																																																																																																																																																																																																																																																																																																																																																																																																											
REF.		Mansy and Gabrielse, 1978		Campbell et al., 1973		Evans, 1933		Reesor, 1973		Little, 1960		Slind and Perkins, 1966		Irish, 1970 Taylor and Stott, 1973 Gabrielse, 1975																																																																																																																																																																																																																																																																																																																																																																																																																																																																																																																																																																																																																																																																																																																																																																																																																																																																																																																																																																											
LOWER €		ATAN GROUP		YANKS PEAK		HAMILL GROUP		HAMILL GROUP		QUARTZITE RANGE		GOG GROUP		ATAN GROUP																																																																																																																																																																																																																																																																																																																																																																																																																																																																																																																																																																																																																																																																																																																																																																																																																																																																																																																																																																											
UPPER PROTEROZOIC		WINDERMERE SUPERGROUP		INGENIKA GROUP		COMPLEX		CARIBOO GROUP		YANKEE BELLE		CUNNINGHAM		ISAAC		KAZA GROUP		base not exposed		WOLVERINE METAMORPHIC COMPLEX		SHUSWAP METAMORPHIC COMPLEX		HORSETHIEF CREEK GROUP		upper slate and quartzite unit		limestone unit		middle slate unit		lower feldspathic grit unit		base not exposed		PURCELL SUPERGROUP		PURCELL SUPERGROUP		TOBY		TOBY		MIETTE GROUP		BYNG		unit		middle unit		lower unit base not exposed		MISINCHINKA GROUP		upper phyllitic slate unit		limestone dolomite unit		lower phyllite and schist unit		feldspathic grit unit		base not exposed																																																																																																																																																																																																																																																																																																																																																																																																																																																																																																																																																																																																																																																																																																																																																																																																																																																																																																																									

Figure 7: Nomenclature and correlations of Windermere stratigraphy in Canadian Cordillera. Taken from Mansy and Gabrielse (1978).

The Ingenika Group and other Windermere successions have been correlated on the basis of lithology and stratigraphic position by Young et al. (1973) and Mansy and Gabrielse (1978; Figure 7). The Ingenika Group exposed in the Cassiar and Omineca Mountains is similar to the Cariboo Group of the Cariboo Mountains, the Horsethief Creek Group in the Purcell Mountains, the Miette Group in the Rocky Mountains, and the Misinchinka Group in the Northern Rocky Mountains.

CHAPTER III

STRUCTURE

3.1 INTRODUCTION

Ingenika Group rocks have experienced a complex structural history that involves at least four major sets of structures. They include pre-, syn-, and post-metamorphic folds that are all approximately colinear and plunge to the northwest. These structures may represent several distinct deformational events, or more likely, may be part of a progressive deformational process. In either case, a traditional numbering scheme has been employed for ease of reference to structural elements (F_1 , S_2 , D_3 , etc.). It should also be noted that many of structural observations presented here are corroborated by thin section studies. All samples collected in the thesis area were oriented so that thin sections could be viewed down the mineral lineation; that is to the northwest.

Each deformational/structural phase observed in the Ingenika Range is discussed separately below (See also Structural Geology Map - Appendix B) and the relative age and tectonic significance of the observations is dealt with in Chapter V.

3.2 D₁ STRUCTURES

The most prominent manifestations of the first phase of deformation are a well-developed, bedding-parallel (S_0), regional S_1 schistosity and a pervasive mineral lineation. These structural elements are very pronounced in the higher-grade rocks exposed in the core of the antiform. The foliation planes are defined by layers of phyllosilicate minerals including muscovite, biotite, sericite and chlorite. The schistosity is generally parallel to bedding and is much better developed in pelitic rocks than in quartz-rich lithologies. A pronounced mineral lineation is

present in the plane of the foliation and is defined by elongate quartz grains and laths of muscovite. The attitude of the lineation is very consistent over the entire study area; it plunges moderately at 330° .

F_1 folds are interpreted to be northeast-verging on the bases of local facing directions and the symmetry of the folds. They are typically northwest plunging, tight, recumbent and overturned folds that have axial planar S_1 schistosity (Figure 8; Plate 9). They are observed predominantly in very competent quartz-rich schists and metaquartzites in which only the noses of folds are commonly preserved (Plate 10). Outcrops consisting of isolated and flattened fold hinges, often with opposing senses of closure, are a consequence of major shearing parallel to the limbs of folds (Plate 11). Except for these rare F_1 closures, D_1 folds are apparent only from bedding-cleavage relationships (Plate 12).

One small-scale, northeast-verging fold possesses a folded uncrenulated S_1 schistosity and is interpreted to be a late D_1 structure.

D_1 deformation is synchronous with early metamorphic conditions (i.e. pre-peak conditions below garnet grade) since S_1 foliation planes contain phyllosilicate minerals such as chlorite, muscovite and biotite. The absence of higher-grade minerals like garnet suggests that D_1 deformation was probably not associated with significant crustal thickening.

The southern portion of the Swannell Ranges is one of few regions west of the Northern Rocky Mountain Trench in which northeast-vergent structures have been documented in miogeoclinal strata (Parrish, 1976a, 1976b; Bellefontaine, 1989; Ferri and Melville, in prep.). Since all F_1 folds observed are upward-facing and northeast-verging there is no evidence to support the development of large-scale recumbent structures during the first phase of deformation.

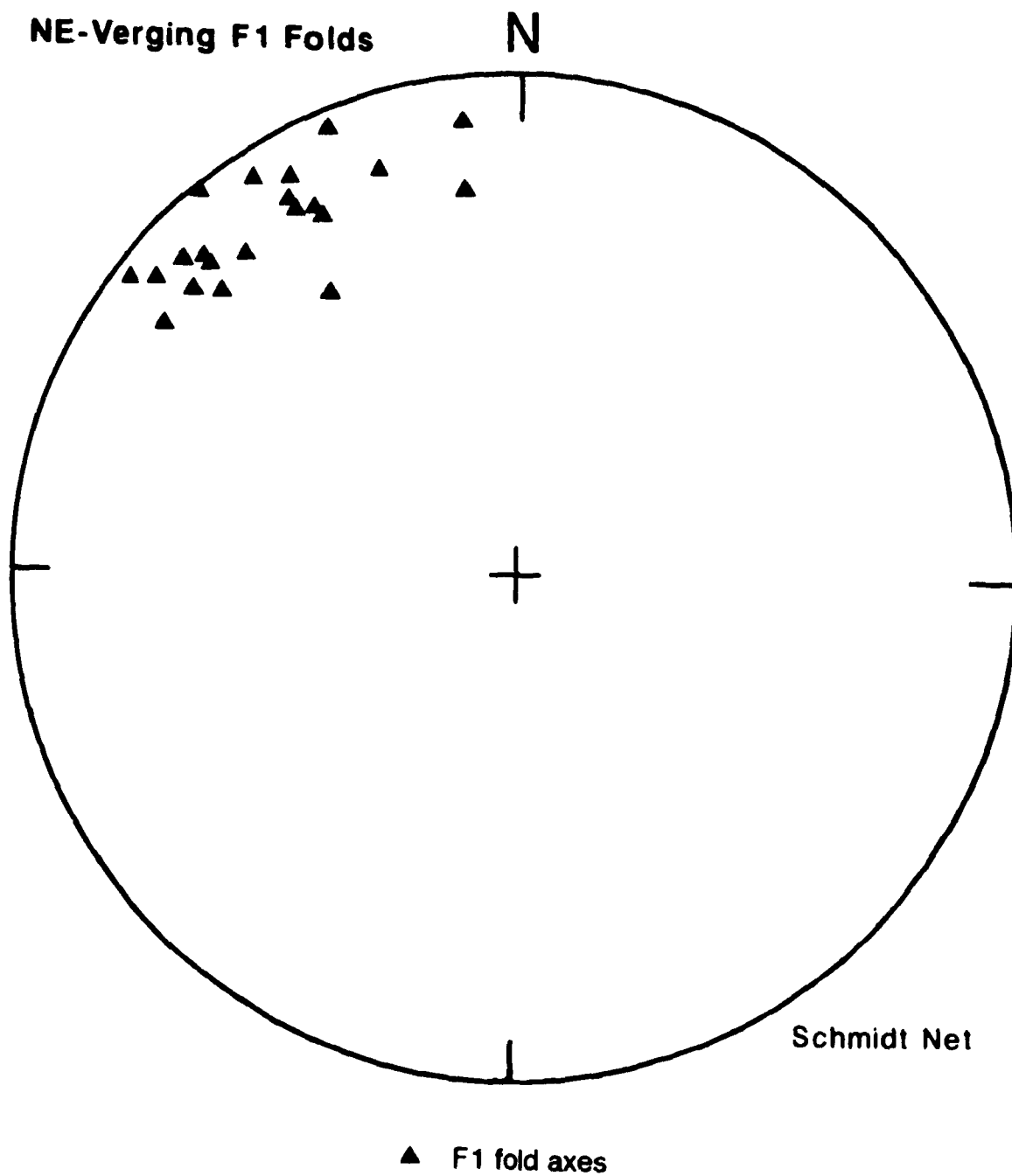


Figure 8: Equal area plot of F_1 fold axes in the Ingenika Range.



Plate 9: Isolated F_1 closure in metaquartzite of the lower Swannell Formation possesses a poorly developed axial planar schistosity. Photo viewed to the northwest.



Plate 10: Hinge of large-scale F_1 fold in weakly foliated metaquartzite. Photo looking northwest; person for scale



Plate 11: Opposing senses of closure in cascading, rootless, F_1 folds indicates major shear parallel to the limbs of folds. Photo looking northwest; person for scale.



Plate 12: Bedding-cleavage relationships in an upward facing package of rocks indicate the presence of a northeast-verging F_1 fold. Bedding is labelled S_0 in photo; cleavage is noted as S_1 . Photo taken from southwest limb of Swannell antiform; view to the northwest.

3.3 D₂ STRUCTURES

In contrast to D₁ structures, second phase structures include small-scale folds (and probably bedding-parallel thrusts) that verge towards the southwest. In outcrop F₂ folds are difficult to distinguish from folds produced during the third phase of deformation especially since D₂ structures were probably reactivated during D₃. The main difference between these two phases is that D₂ structures are syn-metamorphic and are associated with significant structural thickening whereas structural elements related to the third phase of deformation are post-metamorphic.

Evidence of D₂ is best observed in thin section. Garnets and staurolites from semi-pelitic schists in the core of the Swannell antiform overgrow crenulated S₁ schistosity. These fabrics consistently show top-to-the-west senses of rotation and indicate that metamorphism was synchronous with D₂ (Plate 13). A crenulation cleavage (S₂), defined by muscovite, chlorite, ± biotite, ± garnet (Plate 14), is often sufficiently developed in schistose lithologies to transpose S₁ completely. Several F₂ minor folds that deform a crenulated S₁ schistosity were observed in thin section. Muscovite and chlorite have grown axial planar to some of these folds to produce a weak second fabric (S₂). Axial planar quartz veinlets were also visible in thin section in the hinges of F₂ folds.

Evidence that deformation outlasted metamorphism includes continued rotation of garnet porphyroblasts after their formation and additional flattening of schistosity planes around these garnet crystals. Contrary evidence supporting outlasting metamorphism include post-tectonic staurolite rims that overgrow syntectonic inclusion-rich cores and large, randomly-oriented biotite and garnet porphyroblasts which overgrow and cut deformed metamorphic fabrics. These inconsistencies are probably best explained by progressive metamorphism and deformation in a strongly anisotropic package of rocks.

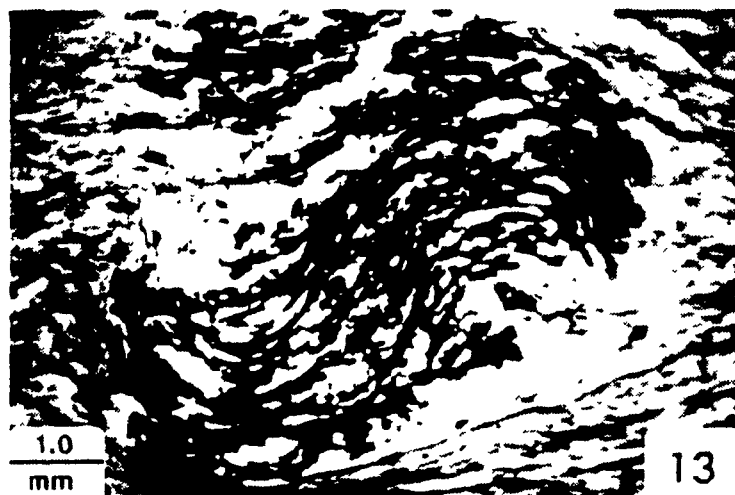


Plate 13: Rolled fabrics in syntectonic (D_2) garnet indicate top to the left (west-directed) transport; plane polarized light.



Plate 14: Crenulation cleavage (S_2) is superimposed on regional schistosity (S_1) in semi-pelitic schist from the core of Swannell antiform; plane polarized light.

Overall, D_2 structures are demonstrably syn-metamorphic and verge in a direction opposite to that of structures produced during D_1 . Folds and faults with southwesterly-directed asymmetry (D_2 and D_3) are very prominent west of the Northern Rocky Mountain Trench. They have been well documented throughout the Omineca Mountains by Gabrielse (1971, 1972a, 1972b), Mansy (1971, 1972, 1974, 1986), Mansy and Dodds (1976), Parrish (1976a, 1976b), and Evenchick (1985). However, these structures are typically better developed in other areas of the Omineca Mountains than in the Ingenika Range.

3.4 D_3 STRUCTURES

Third phase structures are characteristically open and upright folds that are commonly devoid of cleavage. They are associated with the Swannell antiform, which is itself a large F_3 fold. The antiform folds the metamorphic isograds associated with D_2 , as well as bedding and S_1 schistosity (Figures 9 and 16). Tight, recumbent and overturned F_1 folds are rotated around the antiform in a fashion similar to that of bedding and S_1 . The antiform has a steep southwestern limb (135/60SW), and a moderately dipping northeastern limb (120/35NE). The fold is weakly inclined toward the southwest and has a shallow northwesterly plunge. The axial surface trace of the antiform appears to have a major sinistral bend near Orion Creek (Figures 3 and 5).

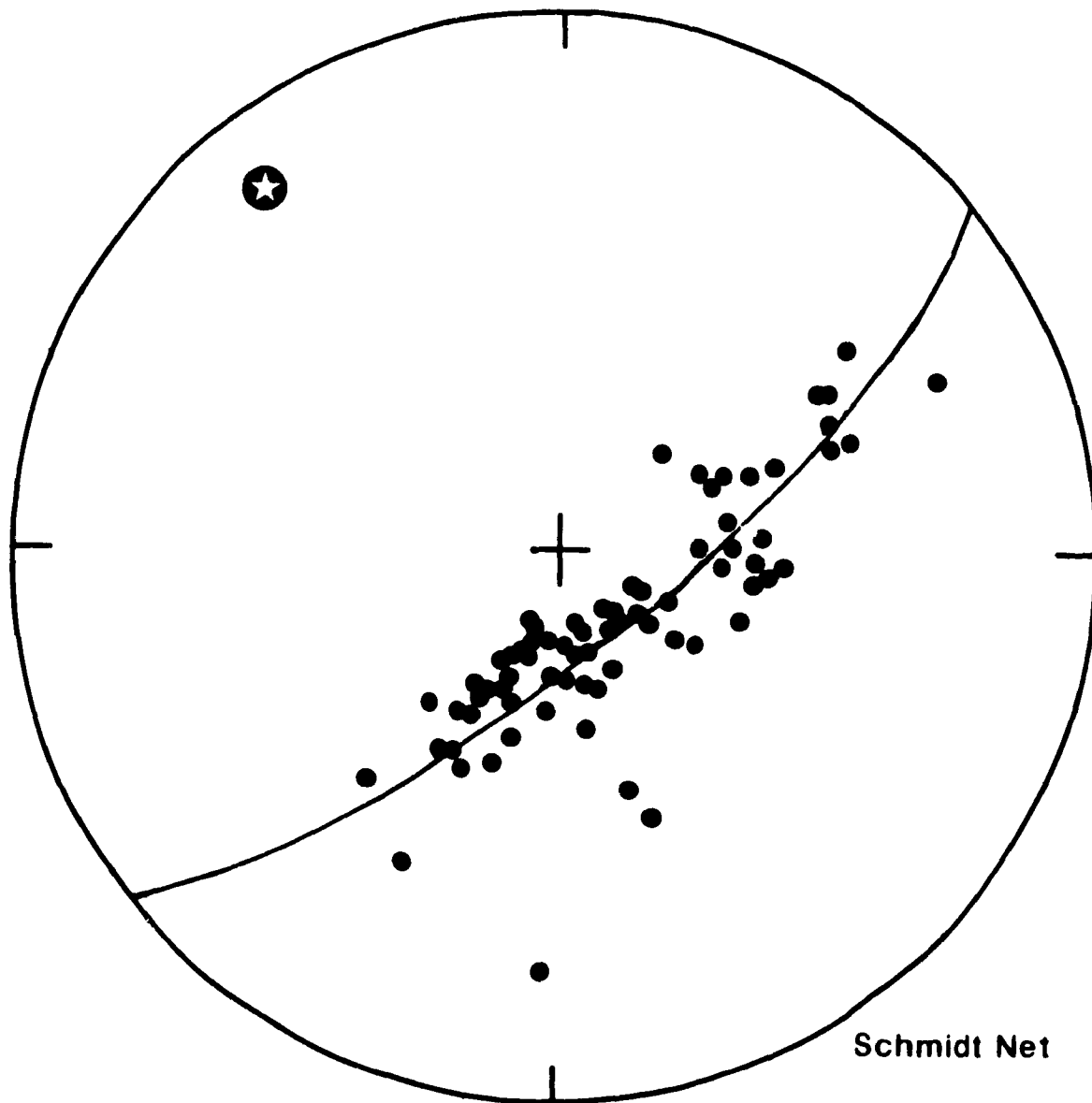
F_3 minor folds have very different geometries on the two limbs of the Swannell antiform. Each is discussed separately in the following sections.

3.4.1 D_3 Structures on Southwest Limb

Outcrop-scale F_3 folds are abundant on the southwestern limb of the antiform, which lies directly to the northeast of the Swannell fault. This limb is

Swannell Antiform

N



axis of antiform



poles to bedding and schistosity

Figure 9: Equal-area stereonet plot of structural data defining the Swannell antiform.

characterized by a cascade of southwest-vergent folds, in which bedding and S_1 steepen from the regional southwest-dipping limb orientation (135/60SW) through vertical and then turn over into shallow northeast-dipping strata that lie above minor thrust faults (Figure 10; Plates 15 to 17). These F_3 folds reflect drag due to southwest-vergent motion on the thrusts. The presence of F_3 thrust-related folds is commonly apparent only from cross-cutting stratigraphic relationships. Northeast-dipping, thrust-parallel strata crosscut underlying rocks with southwest-dipping limb orientations (Plate 18). The footwall strata do not appear to rotate into the slide zone with progressive shear (Plate 19).

The slide zones have an average strike of 125° and dip 45° northeast (Figure 10). They are generally localized in competent lithologies and are commonly recognized in the field by the occurrence of sub-horizontal benches that lack outcrop (Plate 20). Since these slides are abundant only in the immediate vicinity of the Swannell fault, and have strikes similar to that of the fault, it is probable that they developed in association with movement on it. If this is the case then the minor thrusts and associated drag folds present in the map area provide evidence for a southwesterly vergence of the Swannell fault.

The Swannell fault is not exposed in the region; it passes through the broad glaciated valley of the Swannell River. The dip of the fault is not known with certainty but the orientations of the minor thrusts indicate it may dip 45° northeast in the study area. The simplest interpretation based on available data is that the Swannell antiform is a large drag fold produced by a motion on the Swannell fault similar to that on the slide planes. The Swannell fault is probably a major basal thrust fault which transported Proterozoic Ingenika Group rocks southwesterly over the Paleozoic Lay Range Assemblage.

**SW-Verging F3-Slide
Related Folds**

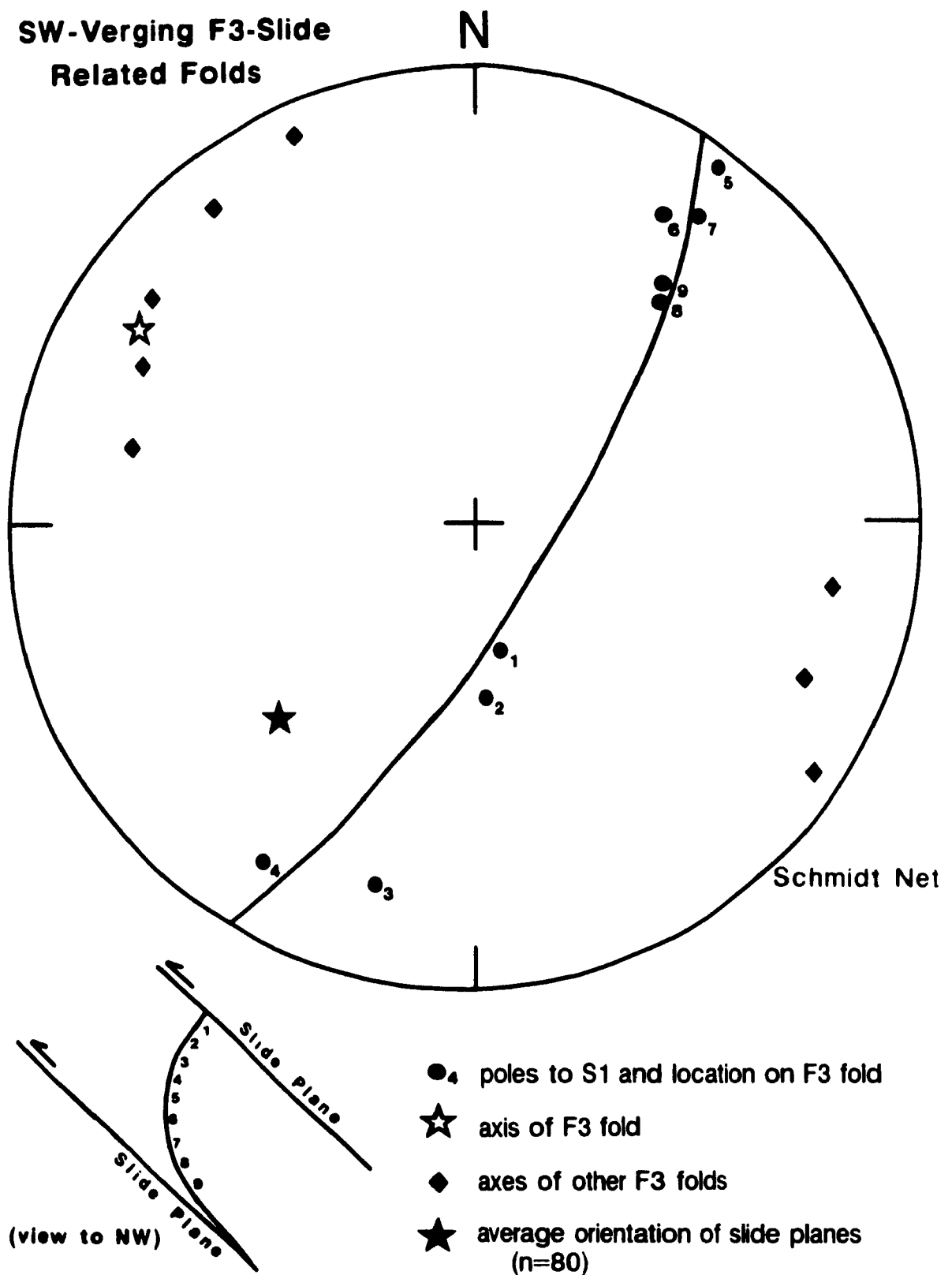


Figure 10: Stereonet plot of F_3 fold axes (drag folds) and associated slide zones from the southwestern limb of Swannell antiform.



Plate 15. F₃ drag folds and associated thrust/slide zone Photo viewed to the northwest; person for scale



Plate 16. Shallow northeast-dipping strata are parallel to a minor thrust fault and are part of an F₃ thrust-related drag fold. Underlying steeply southwest-dipping strata parallel the southwest limb of the Swannell antiform. View to the northwest.

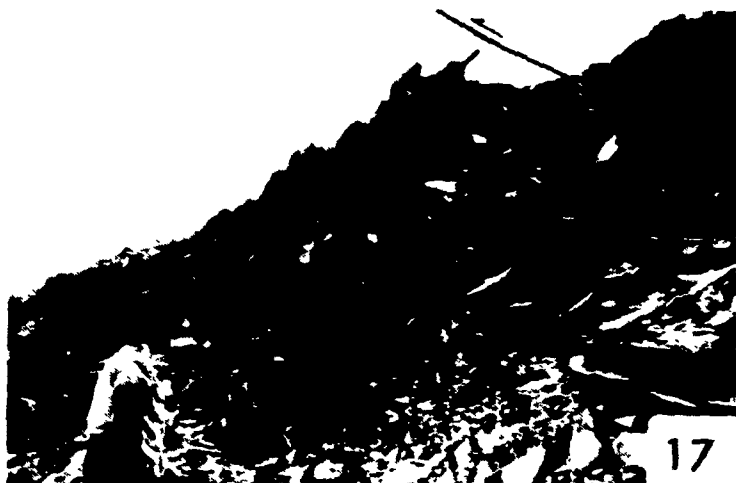


Plate 17. Example of thrust-related F₃ drag fold viewed to the northwest



Plate 18. Presence of thrust plane is evidenced by crosscutting stratigraphy on southwest limb of antiform Photo looking northwest

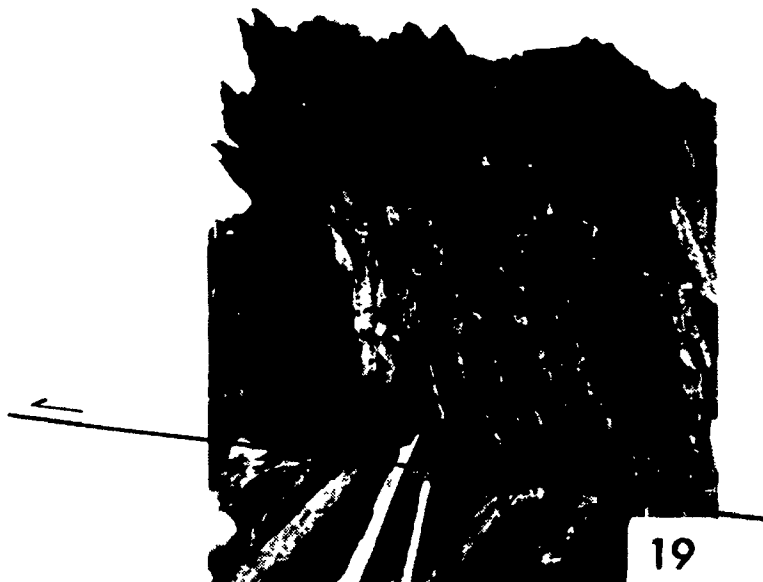


Plate 19: Slide plane about to form in thinly-bedded quartz schists. Strata above thrust plane will rotate into slide plane (ie. to the right in photo) with motion of hanging wall to the southwest. Photo looking northwest.



Plate 20: Sub-horizontal benches on southwest limb of antiform define the presence of slide zones. Photo looking northwest.



Plate 21: Parasitic F₃ fold on northeast limb of Swannell antiform. Photo viewed to the northwest.



Plate 22: F₃ fold is parasitic to northeast limb of antiform. Fold may be riding on a bedding-parallel thrust; view to the northwest.

A schematic cross-section of the Ingenika Range (Figure 11) shows the structural elements that deform the study area. The strata on the southwestern limb of the Swannell antiform have been displaced along minor west-directed thrust faults. The large carbonate body present on the west limb is thought to belong to the Espee Formation. Its juxtaposition against originally stratigraphically lower rocks to the northeast is probably due to thrust faulting instead of drastic facies changes as proposed by Mansy (1986).

3.4.2 D₃ Structures on Northeast Limb

In contrast to the southwestern limb, D₃ deformation on the northeastern limb of the Swannell antiform is restricted to southwest-vergent, open, upright folds that are parasitic to the antiform (Plates 21 and 22) and bedding-parallel slickensides (Plates 23 and 24) with small-scale drag folds displaying westerly vergence (Plates 25 and 26).

F₃ folds throughout the study area are broadly colinear with F₁ and F₂ structures, but are demonstrably post-metamorphic and related to deformation with a vergence in the opposite direction to that obtained in D₁. D₂ and D₃ have also produced several generations of crenulation folds and lineations in micaceous schists. However, similar orientations make them difficult to distinguish.

3.5 D₄ STRUCTURES

The most prominent late-stage structures in the study area are kink folds. Conjugate sinistral and dextral kinks occur at all scales and are concentrated in low grade rocks on the southwest limb of the Swannell antiform (Plates 27 and 28). Since these late folds occur only near the Swannell fault, it is probable that they developed in response to late-stage movement on the fault.

SCHEMATIC CROSS-SECTION

(View to NW)

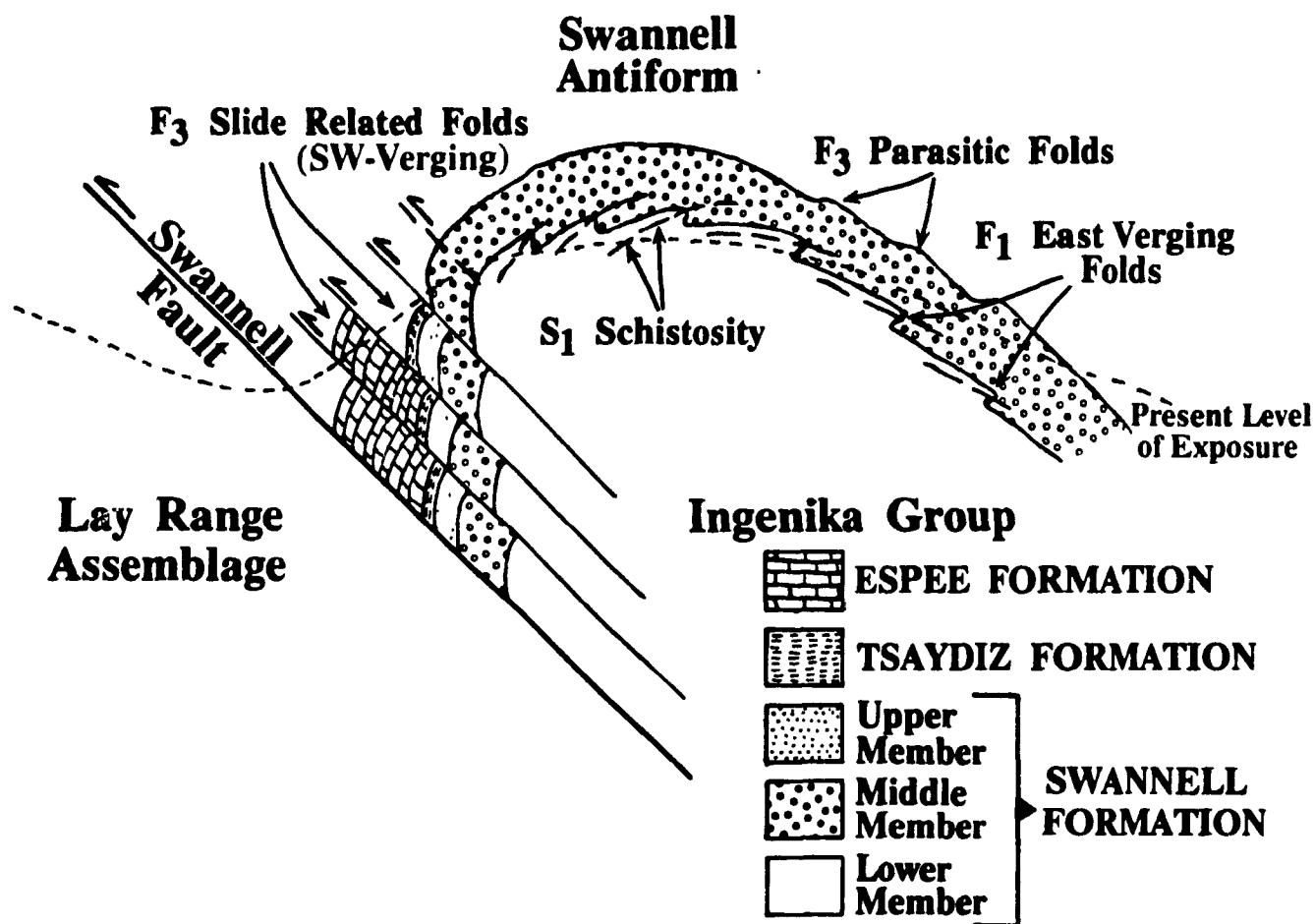


Figure 11: Schematic tectonic profile of Ingenika Range displaying the structural elements that deform the region. Structural data support southwest-directed motion on the Swannell fault.

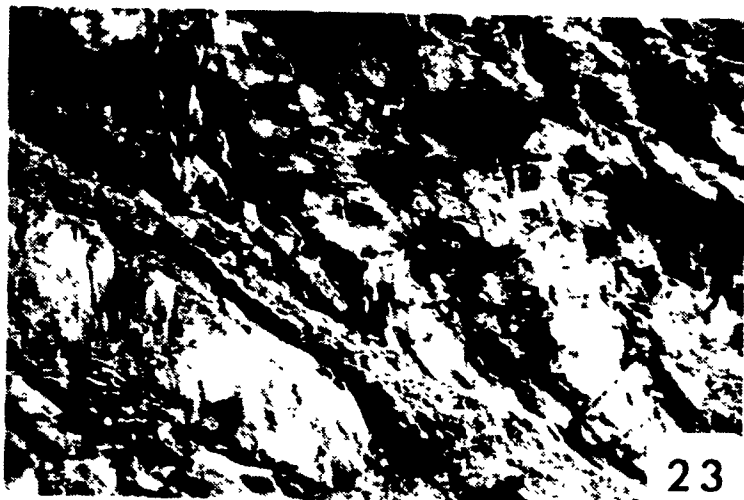


Plate 23: Large-scale bedding-parallel thrust on northeast limb of Swannell antiform. View to the north; person for scale.



Plate 24: Bedding-parallel thrusts located in schistose lithologies on northeast limb of antiform. Photo looking north; hammer for scale.

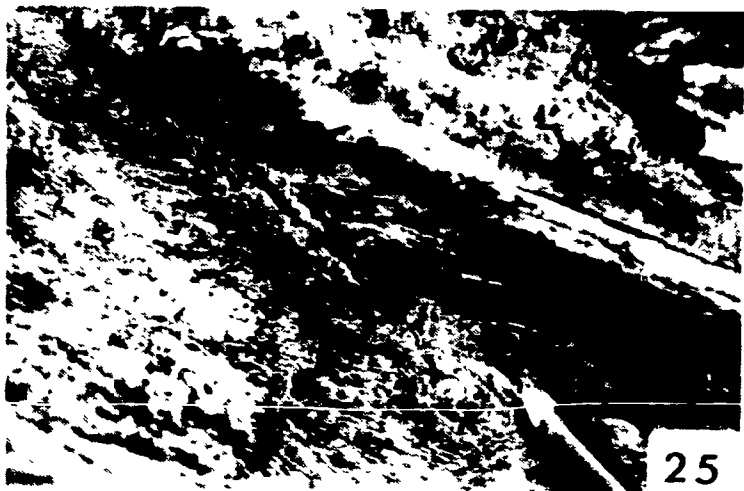


Plate 25: Small-scale drag folds related to movement on southwest-verging slide planes. Photo looking northwest; pencil for scale.



Plate 26: Small-scale drag fold. Pencil tip for scale.



Plate 27: Small-scale shear kink from southwest limb of Swannell antiform. Photo looking northeast.



Plate 28: Kink fold consistent with sinistral shear. View to the northeast.

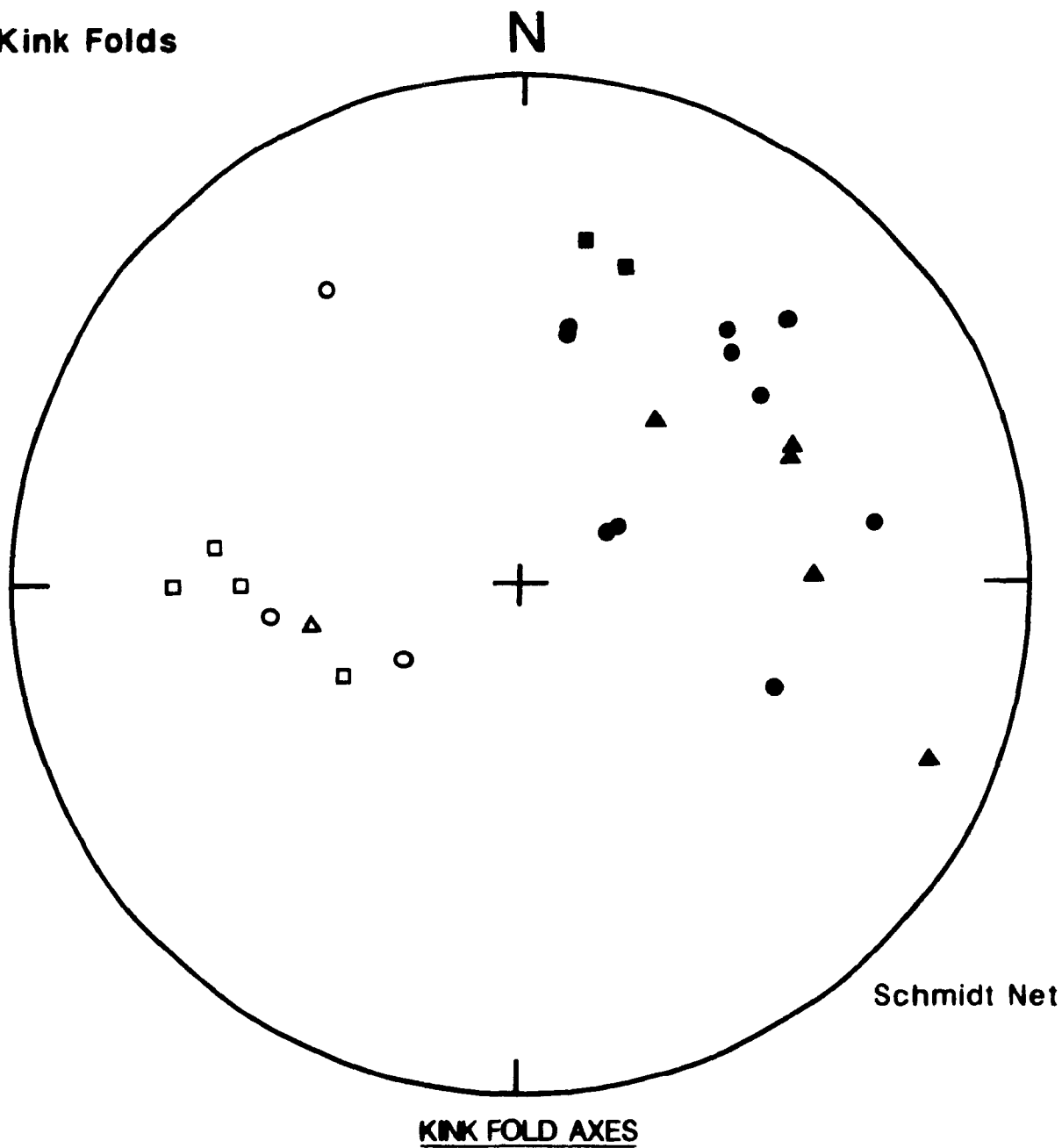
Some information about relative motion on the Swannell fault may be inferred from structural data for the kinks, although interpretation is difficult since the folds have been superimposed on beds of many different attitudes. To help alleviate this problem, only data for kinks that overprint beds having the regional southwest-dipping limb orientation or the northeast-dipping slide orientation were used.

A stereonet plot of the structural data of kinks (Figure 12) shows that regardless of the sense of symmetry of the minor folds, kinks superimposed on beds dipping southwest have west plunging fold axes and those that overprint northeast dipping strata plunge towards the east. The attitudes of the axial planes (043/63SW and 083/73SW; Figure 13) coincide with the orientations of shear directions in a stress field that could only be established by imposing dextral motion on the Swannell fault (Figure 14). This is consistent with the interpretations of Eisbacher (1972). He inferred dextral motion on steep northwest trending faults near Ware, British Columbia from kink folds that deform late Cretaceous to early Tertiary sediments of the Sifton Formation in the Northern Rocky Mountain Trench.

Structural data for a large-scale (25 metre) dextral kink indicate refolding of an earlier crenulation lineation around an axis plunging 25° at a trend of 140° (Figure 15). Although these data are broadly consistent with observations from small kinks, larger kink folds are typically more difficult to interpret since they superimpose beds of many different attitudes.

Late-stage dextral motion on the Swannell fault may account for the presence of kink folds, but it cannot produce the sinistral bend observed in the axial trace of the Swannell antiform (Figures 3 and 5). The curve in the axial plane may have been produced by later sinistral motion on the Swannell fault, but no minor structures were observed to support this. It is more probable that the curve is due to

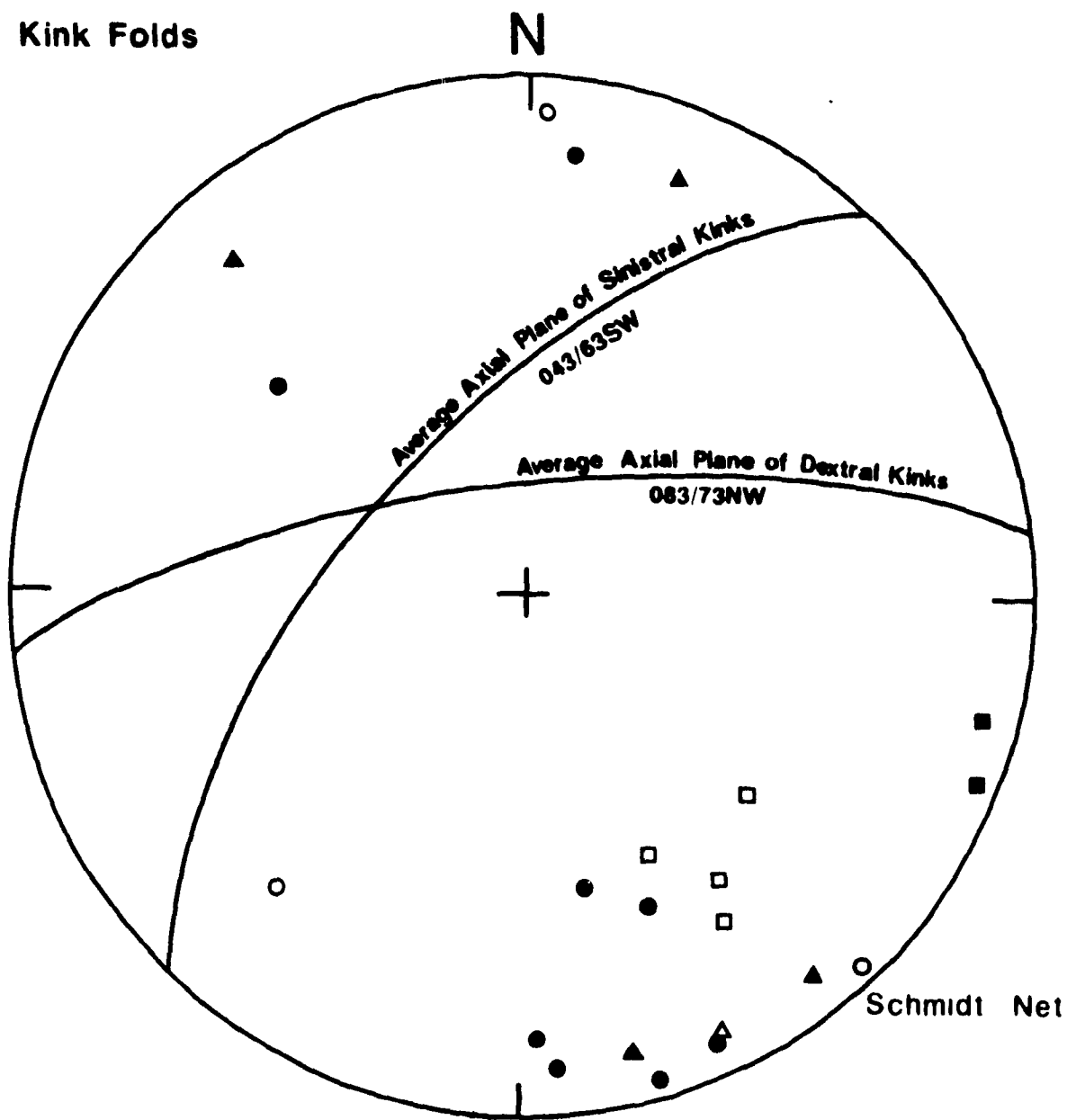
Kink Folds



- | | | |
|-----------------------------|-----------------------------|------------------------|
| ○ Z-kink on regional strata | □ S-kink on regional strata | △ ? on regional strata |
| ● Z-kink on slide strata | ■ S-kink on slide strata | ▲ ? on slide strata |

Figure 12: Equal-area stereonet plot of fold axes of dextral and sinistral shear kinks superimposed on strata with regional southwest-dipping limb orientations and northeast-dipping slide orientations.

Kink Folds

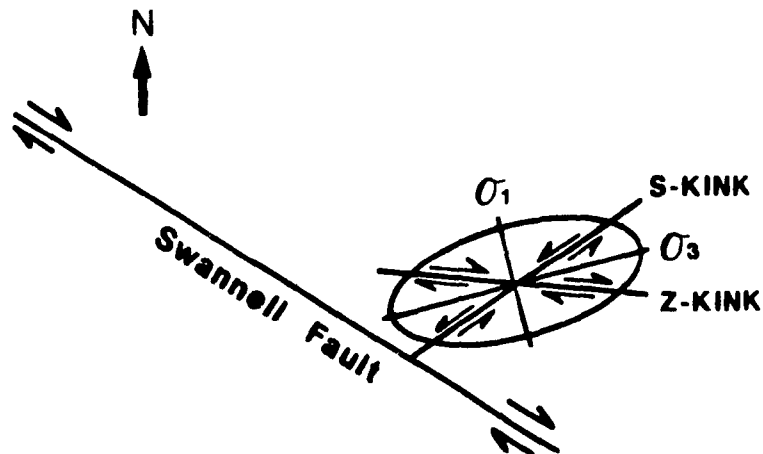


POLES TO AXIAL PLANES OF KINK FOLDS

- | | | |
|-----------------------------|-----------------------------|------------------------|
| ○ Z-kink on regional strata | □ S-kink on regional strata | △ ? on regional strata |
| ● Z-kink on slide strata | ■ S-kink on slide strata | ▲ ? on slide strata |

Figure 13: Attitudes of axial planes of dextral and sinistral shear kinks.

A. DEXTRAL MOTION ON SWANNELL FAULT



B. SINISTRAL MOTION ON SWANNELL FAULT

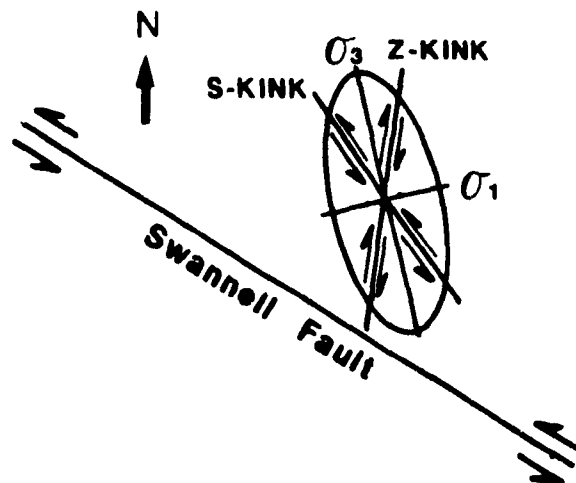


Figure 14: Possible stress fields that could be established on the southwest limb of Swannell antiform by imposing dextral and sinistral motion on the Swannell fault. Attitudes of axial planes of kink folds (Figure 13) are only consistent with shear directions developed as a result of dextral motion on the Swannell fault.

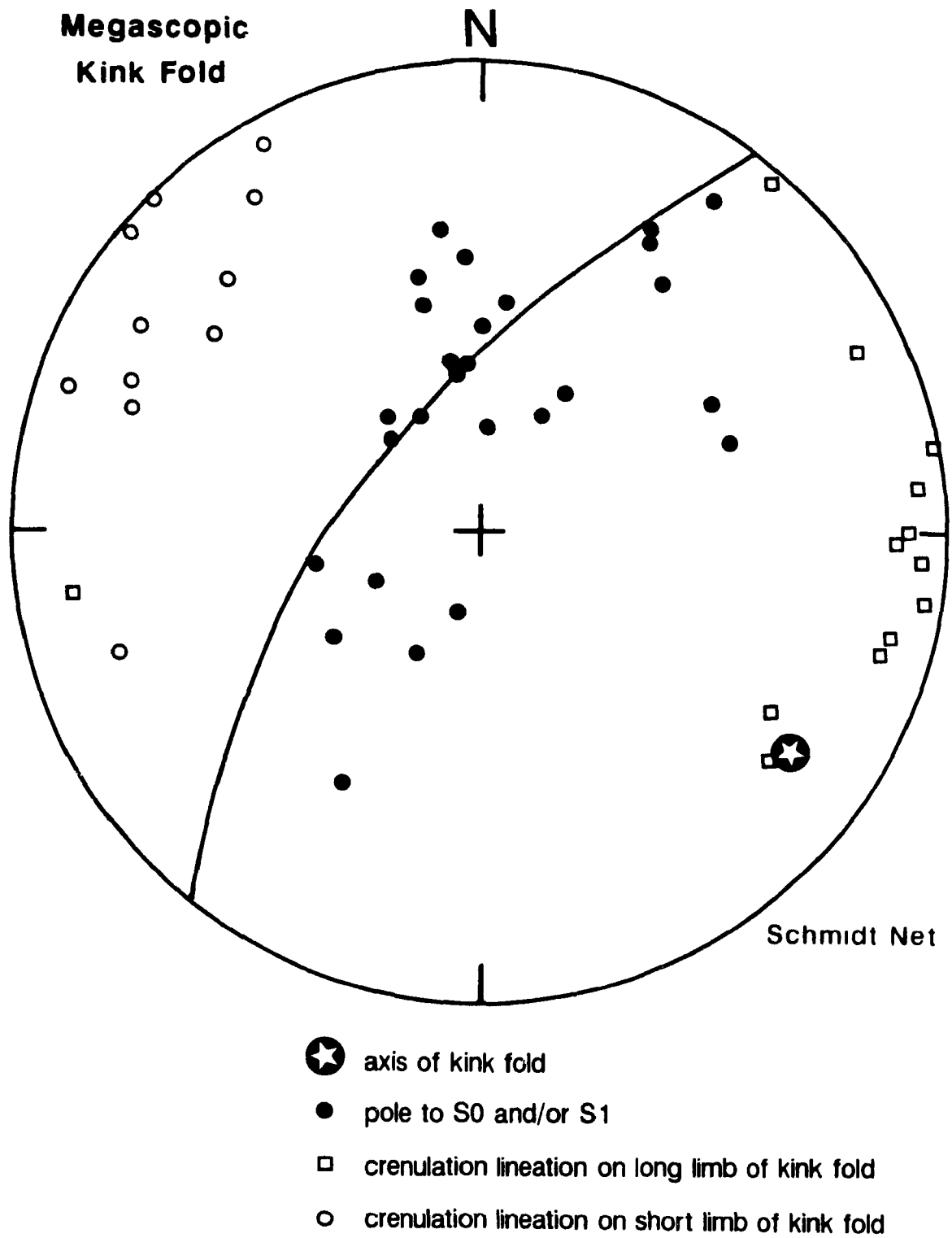


Figure 15: Structural data of megascopic kink fold from southwest limb of Swannell antiform.

an earlier phase of deformation. Rich (1934) demonstrated that the simplest manner in which to generate a bend in a sole antiformal trace was to change the position of a ramp structure in the footwall. The sinistral bend in the axial planar trace of the Swannell antiform may have been produced in this way during the third phase of deformation when rocks of the Ingenika Group were moving southwesterly over the Lay Range Assemblage.

Other late stage structures include fractures of various attitudes and minor open folds and broad flexures that have sub-horizontal east trending fold axes.

3.6 STRUCTURAL SUMMARY

Four phases of colinear deformation that are demonstrably pre-, syn-, and post-metamorphic are present in the Ingenika Range. Structural styles in the region strongly reflect structural and stratigraphic levels. D_1 and D_2 deformations are most evident in the deeper level, higher grade rocks of the infrastructure, while later post-metamorphic folds and fabrics (D_3 and D_4) are most apparent in the lower grade, higher level rocks of the suprastructure. In addition, D_1 and D_2 macroscopic and microscopic structures appear to corroborate a progressive deformational history for the Ingenika Range and indicate that a major reversal of structural vergence was instigated prior to the attainment of peak metamorphic conditions.

CHAPTER IV

METAMORPHISM AND GEOTHERMOBAROMETRY

4.1 INTRODUCTION

The Ingenika Range has undergone a single phase of progressive metamorphism with peak conditions in the upper greenschist to lower amphibolite facies (Gabrielse, 1972a; Mansy and Dodds, 1976; Parrish, 1976b; Mansy, 1986; and Bellefontaine, this report). This metamorphic study was undertaken in an effort to establish the orogenic history of the region by estimating the pressure and temperature conditions that affected the Ingenika Range and by determining the relationship between metamorphism and deformation in the study area.

4.2 DISTRIBUTION OF METAMORPHIC ISOGRADS

Mineral isograds were previously mapped in the Ingenika Range by Mansy (1986) on the basis of the first appearance of index minerals. Chlorite, biotite, garnet and staurolite isograds strike northwest and are folded by the post-metamorphic Swannell antiform (Figure 16). Metamorphic isograds were not remapped in this study since those previously mapped by Mansy (1986) were found to be quite accurately located in the field.

The metamorphic grade of the rocks generally corresponds to their stratigraphic and structural levels. The highest grade rocks outcrop in the core of the antiform and lower grade rocks are exposed on the limbs. There is also a general increase in metamorphic grade from northwest to southeast; staurolite bearing rocks occur at the southeastern limit of the study area.

The isograds are widely and evenly spaced on the east limb of the fold, while those on the southwest limb are much closer together. This close spacing of

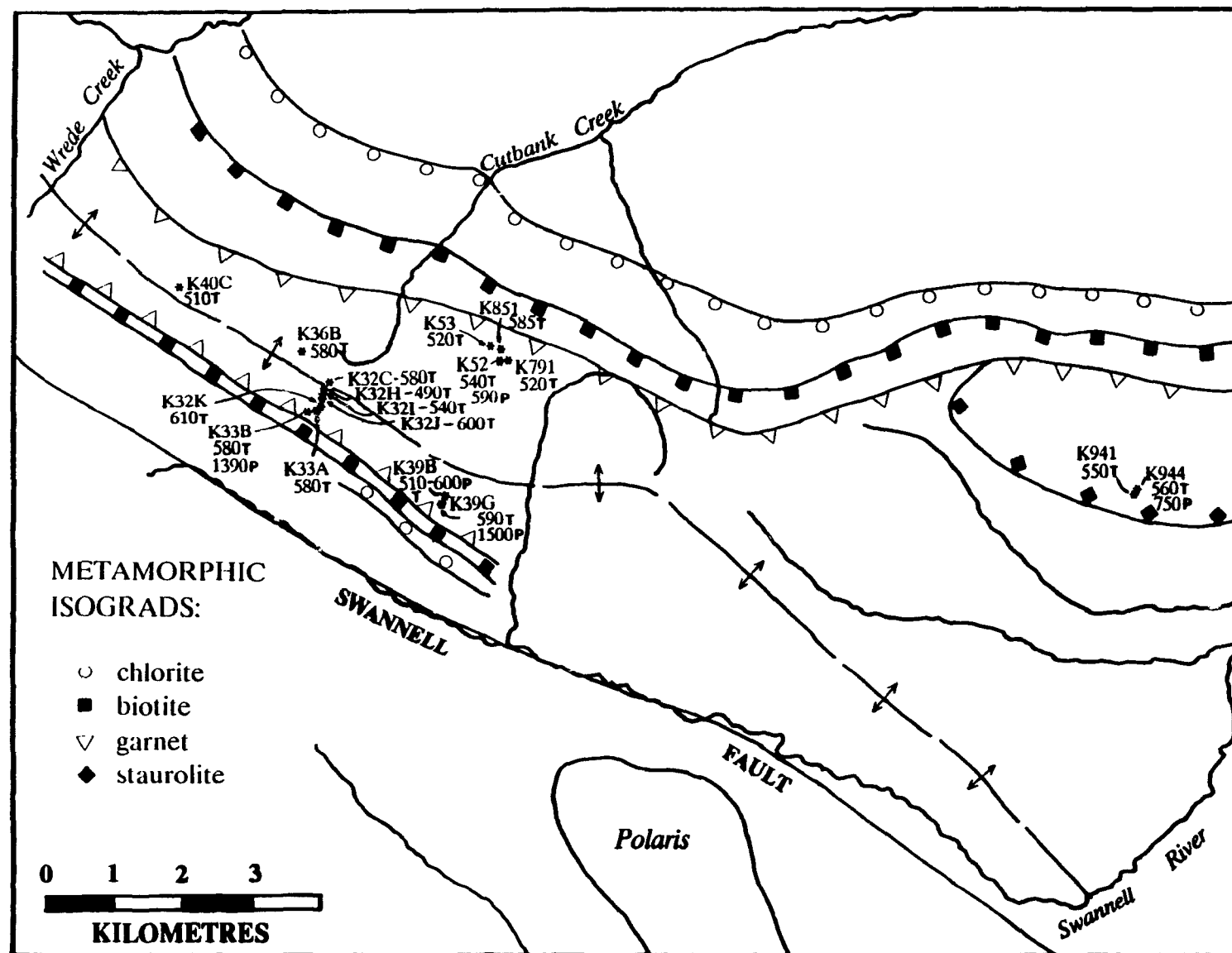


Figure 16: Map showing the distribution of metamorphic isograds in the the Ingenika Range and the location of samples used in geothermometry calculations. Sample numbers all begin with the letter K; temperature results are in degrees celsius and are denoted by the letter T. Estimates of pressures are in MPa and are shown by the letter P.

metamorphic isograds on the southwest limb can be explained by the structural complexities discussed in section 3.4.1. It is believed that rocks of higher metamorphic grade were juxtaposed to lower-grade metamorphic rocks to the southwest by movement along southwest-directed, post-metamorphic thrust faults (Figure 11).

4.3 PETROLOGY

The study area is dominated by semi-pelitic, quartz-rich schists that are typically aluminum poor. Metamorphic mineral assemblages (Table 1) are characteristic of upper greenschist facies and samples K941 and K944 contain staurolite which is diagnostic of the beginning of the amphibolite facies (Winkler, 1979). Retrograde metamorphism does not appear to have been substantial in the study area. Minor retrograde chlorite and sericite occurs on the rims of several garnet and staurolite crystals. Reaction rims were not observed in thin section; thus there is no obvious evidence of disequilibrium between mineral phases.

Geological mapping in 1987 and 1988 led to the idea that metamorphism was synchronous with the first phase of deformation (D_1) in the Ingenika Range (Bellefontaine, 1989). This was based on the presence of syntectonic rolled fabrics in garnet porphyroblasts (visible in outcrop) and the fact that the only other phase of deformation recognized in the area (D_2 ; referred to as D_3 in this report) was obviously post-metamorphic. Subsequent thin section studies (this report) on oriented samples suggested a more complex tectonic history involving an additional phase of deformation. When thin sections were oriented so as to be viewed down the mineral lineation (ie. to the northwest), internal fabrics in all garnets consistently showed a top to the southwest sense of rotation (Plate 13; Plate 29). This, in addition to other textural evidence discussed in the following section,

suggests that metamorphism was synchronous with southwestly-vergent structures instead of with the northeasterly-verging structures associated with D_1 . These observations have been extrapolated to a larger scale to infer a phase of southwest-verging, syn-metamorphic deformation (D_2) that was previously unrecognized in the Ingenika Range.

Increasing metamorphic grade in the rocks is marked by the disappearance of turbid grain boundaries, a general increase in grain size and the development of index minerals such as chlorite, biotite, garnet and staurolite; aluminosilicate minerals were not found anywhere in the Ingenika Range. Rocks of lower metamorphic grade contain a single schistosity (S_1) that is generally parallel to bedding and is crenulated in places. It is defined by splintery laths of chlorite, brown biotite and muscovite/sericite. Porphyroblastic minerals such as garnet and staurolite did not grow synchronous with the formation of S_1 fabrics (D_1 deformation). Higher-grade rocks in the core of the antiform may contain a second schistosity (S_2) in addition to the bedding-parallel S_1 . This foliation is also defined by phyllosilicate minerals, and syn-metamorphic porphyroblastic growth of garnet and staurolite is evident in thin section (Plate 30). Quartz typically displays undulose extinction and has a weak dimensional preferred orientation parallel to S_1 schistosity.

Garnets are the most abundant porphyroblasts in the rocks. They range in diameter from less than 1 millimetre to 2 centimetres and are typically deep wine-red. They commonly contain helicitic inclusion trails of quartz and ilmenite with less common chlorite, biotite and tourmaline. The inclusion trails preserve an early S_1 schistosity that may be relatively straight (Plate 29) or crenulated. There are also several textural varieties of garnet that have grown within schistosity planes. Their appearance depends strongly on the nature of the schistositities they have overgrown.

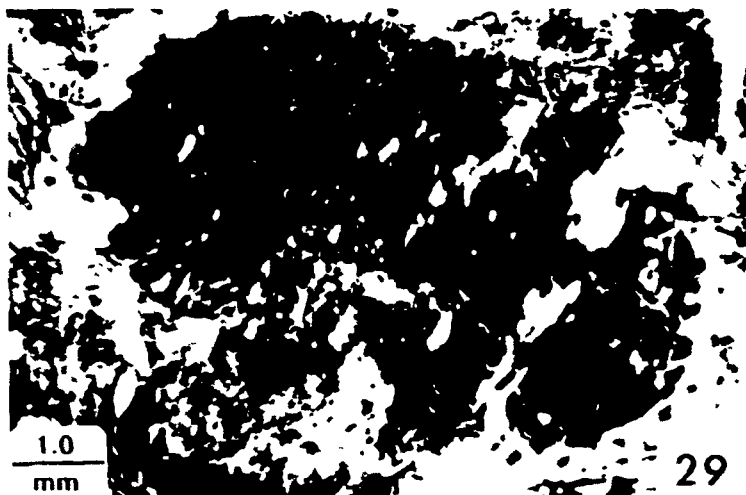


Plate 29. Large garnet porphyroblast containing a straight inclusion trail continuous with S_1 schistosity. Pressure shadows of quartz and orientation of S_1 in garnet indicate top to the left (southwest) rotation.



Plate 30: "Spider-garnet" that has formed after chlorite and/or muscovite in S_1 and S_2 schistosity planes.



Plate 31 Euhedral garnet in garnet-biotite-sericite schist



Plate 32 Biotite overgrowing S_1 schistosity defined by ilmenite in garnet-biotite-sericite schist

Plate 13 shows a large syn-tectonic (D_2) garnet that has overgrown an S_1 schistosity to produce a stringy, skeletal porphyroblast. The sense of rotation of the fabrics in the garnet is towards the southwest (top to left in photo). Another textural variant is produced when garnet overgrows both S_1 and S_2 schistositities (Plate 30). The result is a "spider-like" porphyroblast with arms of garnet extending into both schistosity planes. Idioblastic garnets were also observed in thin section (Plate 31) as well as one porphyroblast possessing a poorly developed snowball texture. Textural zoning is evident in some of the more idioblastic garnet crystals.

Syn-tectonic staurolite porphyroblasts occur in the southeasternmost portion of the map-area. Helicitic trails of inclusions preserve both straight and crenulated S_1 schistositities within the porphyroblasts. Staurolite also occurs as idioblastic crystals and less commonly as skeletal xenoblasts. Many staurolite crystals contain poikiloblastic garnet and biotite.

4.4 RELATIONSHIP OF METAMORPHISM TO DEFORMATION

Data from the study area indicate that the earliest deformation (D_1 , east-verging) recognized in the Ingenika Range preceded peak metamorphic conditions. A strong planar fabric defined by phyllosilicate minerals (S_1) is parallel to compositional layering in the rocks (S_0). The presence of syn-tectonic porphyroblasts that display southwest-verging rotational fabrics and the occurrence of skeletal porphyroblasts in two schistosity planes (S_1 and S_2) indicate a second phase of southwest-directed deformation (D_2) that was synchronous with peak metamorphic conditions. Late crenulations and kinking are also apparent in thin section.

For the most part it appears that deformation outlasted metamorphism in the thesis area. This is evidenced by the continued rotation of garnet porphyroblasts

after their formation and flattening of schistosity planes around many porphyroblasts (Plate 30). Contrary evidence that supports post-deformational metamorphism is the occurrence of pale pink, idioblastic garnets and large, zoned biotite porphyroblasts that overgrow and cross-cut the deformed primary foliation (S_1) in sample K32H (Plates 31 and 32). Several explanations exist for this rare porphyroblast development. First, the garnet and biotite crystals may be part of a retrograde mineral assemblage. Since the bulk chemistry of the sample appears to be different from most other samples (ie. the matrix is composed almost entirely of sericite) it is possible that the porphyroblasts grew after the peak of metamorphism; ie. during a retrograde event. Another possible explanation is that this sample records an additional phase of regional or contact metamorphism. The possibility of multiphase regional metamorphism was previously suggested by Mansy and Dodds (1976) and Bellefontaine (1989). Although no intrusive rocks were found in the Ingenika Range, the potential for a cryptic intrusion still exists. The Cretaceous Mount Whudzi pluton intrudes the axial region of a large anticlinorium in the northern Swannell Ranges (Mansy, 1986).

4.5 GEOTHERMOBAROMETRY

4.5.1 Introduction

Temperature and pressure conditions in a metamorphic terrain may be estimated using various mineralogic thermometers and barometers. The semipelitic nature of the mineral assemblages in the Ingenika Range (Table 1) limits metamorphic investigations to the use of the garnet-biotite geothermometer and the plagioclase-biotite-garnet-muscovite geobarometer. These well-calibrated geothermobarometers are discussed in the following sections and are used in an

MINERAL ASSEMBLAGES IN INGENIKA RANGE

SAMPLE NUMBER	QTZ	MUS	BIO	CHL	PLA	KSP	HBL	GAR	STA	ILM
K32C	x	x	x	x	x		x	x		x
*K32H		x	x					x		x
K32I	x	x	x	x				x		x
K32J	x	x	x	x	x		x	x		x
K32K	x	x	x	x	x			x		x
K33A	x	x	x	x	x			x		x
K33B	x	x	x	x	x	x		x		x
*K36B	x	x	x	x	x			x		x
K39B	x	x	x	x	x		x	x		x
K39G	x	x	x	x	x	x		x		x
*K40C	x	x	x	x				x		
K52	x	x	x	x	x	x		x		x
K53	x	x	x	x				x		x
K791	x	x	x	x				x		x
*K851	x	x	x	x				x		x
*K941	x	x	x					x	x	x
K944	x	x	x		x			x	x	x

TABLE 1: Mineral assemblages of semi-pelitic samples used in geothermobarometry calculations. Accessory minerals include tourmaline, calcite, rutile, apatite, epidote, and zircon. An asterisk (*) denotes samples containing retrograde chlorite and/or sericite rims around garnet porphyroblasts.

Abbreviations used in table

BIO = biotite
 CHL = chlorite
 GAR = garnet
 HBL = hornblende
 ILM = ilmenite
 KSP = alkali feldspar
 MUS = muscovite
 PLA = plagioclase
 QTZ = quartz
 STA = staurolite

attempt to estimate the peak metamorphic conditions that affected the Ingenika Range.

4.5.2 Mineral Chemistry

Microprobe analyses were conducted on most of the mineral phases present in the rocks. A discussion of microprobe methodology and mineral stoichiometries is presented in Appendix A. Due to the fact that mineral phases used in this study were almost never in contact, analyses were commonly conducted on matrix biotite, plagioclase and muscovite as close to garnet porphyroblasts as possible. In addition both the rims and cores of garnet and biotite crystals were analysed due to their potential for compositional zoning. The following discussion of mineral chemistries from the study area is based largely on comparison with data from Deer, Howie and Zussman (1966), Ferry and Spear (1978) and Hodges and Spear (1982).

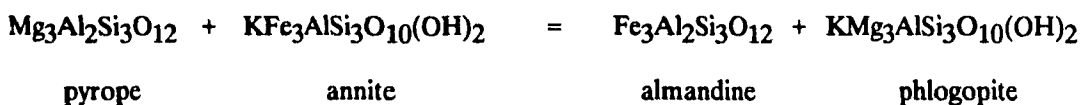
Garnets in the study area are almandine-rich ($\text{FeO} = 28\text{-}33 \text{ wt.}\%$) and many have significant quantities of grossular ($\text{CaO} = 4\text{-}8 \text{ wt.}\%$). Several porphyroblasts are compositionally and texturally zoned. Although detailed compositional traverses were not conducted across garnets, microprobe analyses from rim, core and internal localities show that they have a normal prograde zonation pattern (Hollister, 1966). Garnet cores have higher contents of Ca and Mn and lower contents of Mg and Fe than their rim counterparts. This mineral zoning preserves prograde metamorphic conditions in the study area; garnet rims should yield peak-metamorphic conditions.

Biotites display a relatively constant composition with high MgO (8-14%) and low TiO (1-2%) contents. In addition, several large, porphyroblastic biotites which are chemically zoned were found in sample K32H. They possess Fe-rich cores and Mg-rich rims.

Several staurolite crystals in Samples K941 and K944 are texturally but not chemically zoned. They have uniform chemistries with FeO values ranging from 12 to 13.5 wt.%. Microprobe analyses of amphiboles in Samples K32C, K32J and K39B show them to be common hornblende. The presence of very small, unzoned albite crystals has been documented in several samples, yet overall it is rare in these rocks.

4.5.3 Garnet-Biotite Geothermometer

The presence of garnet and biotite in most of the semi-pelitic schists of the Ingenika Group make the garnet biotite geothermometer an obvious choice for calculating temperatures in the study area. Several different calibrations of the garnet-biotite geothermometer have been proposed by Thompson (1976), Ferry and Spear (1978) and Hodges and Spear (1982). All are based on the temperature sensitive partitioning of Fe and Mg between garnet and biotite:



Thompson's (1976) calibration for the fractionation of Fe and Mg between garnet and biotite is based on the comparison of natural mineral assemblages with phase equilibria. However this method does not account for the effects of pressure on the system (Hodges and Spear, 1982). A more recent calibration that specifically accounts for pressure effects was introduced by Ferry and Spear (1978). It is based on the experimental partitioning of Fe and Mg in synthetic garnet and biotite and assumes that Fe and Mg mix ideally in biotite-garnet solid solutions. However, as the authors note, the application of this geothermometer should be limited to

systems that do not contain significant amounts of Ca, Mn and Ti; that is only if the following conditions apply:

$$\frac{(\text{Ca} + \text{Mn})}{(\text{Ca} + \text{Mn} + \text{Fe} + \text{Mg})} \leq 0.20 \text{ in garnet}$$

and

$$\frac{(\text{Al}^{\text{vi}} + \text{Ti})}{(\text{Al}^{\text{vi}} + \text{Ti} + \text{Fe} + \text{Mg})} \leq 0.15 \text{ in biotite}$$

This geothermometer is not suitable for rocks in the study area since mineral compositions of garnet and biotite do not fall within these limits. As well, Ghent (1976) and subsequent workers have stressed the fact that component mixing in garnet (and plagioclase) solid solutions is not ideal and that this non-ideality must be accounted for when conducting thermobarometric investigations.

Hodges and Spear (1982) account for the non-ideality of fractionating components in garnet (and plagioclase) by applying a consistent set of solution models and an empirical Ca correction. Since this method accounts for non-ideal behavior it has been used to calculate metamorphic temperatures for the study area. The results of garnet-biotite geothermometry are presented in Table 2 and are discussed in section 4.6.

4.5.4 Plagioclase-Biotite-Garnet-Muscovite Geobarometer

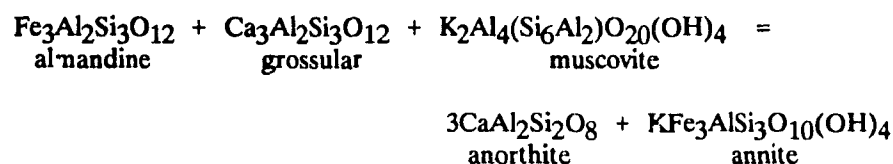
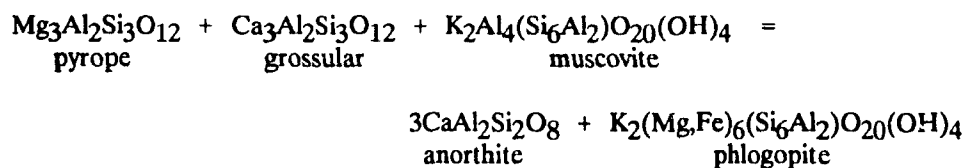
Due to the limitations of mineral assemblages in the thesis area, the plagioclase - biotite - garnet - muscovite geobarometer is the only assemblage that may be used to estimate pressure conditions. This geobarometer was developed by Ghent and Stout (1981) and involves equilibria (listed below) in which there is a

RESULTS OF GEOTHERMOMETRY

METAMORPHIC ZONE	SAMPLE NUMBER	CALCULATED TEMPERATURE (°C)	
G A R N E T Z O N E	K32C - core	550	
	- rim	580	
	K32H - core	450	
	- rim	490	
	K32I - core	470	
	- rim	540	
	K32J - core	600	
	- rim	600	
	K32K - rim	610	
	- core	500	
	- core	500	
	- rim	560*	
	K33A - rim	600*	
	K33B - core	570	
	- rim	580*	P
	K36B - core	540	
	- rim	580	
	K39B - core	420	
	- rim	460	
	- rim	510''	P
	K39G - core	600	
	- rim	580	P
	K40C - core	510	
	K52 - core	540	
	- rim	540*	P
	K53 - core	500	
	- rim	520	
	K791 - core	510	
	- rim	520	
	K851 - core	530	
	- rim	540	
	- rim	585''	
STAUROLITE ZONE	K941 - rim	550*	
	K944 - rim	510*	
	- rim	560	P

TABLE 2. Estimates of metamorphic temperatures for garnet - biotite pairs from the Ingenika Range calculated using the method of Hodges and Spear (1982). Experimental error is ± 50 degrees celsius. An asterisk (*) denotes garnet-biotite pairs that are in contact; a double prime symbol (") means minerals are in close contact. The letter P shows samples used in geobarometry calculations.

change in Al coordination from 6 to 4 and in Mg-Fe coordination from 8 to 6. This exchange is strongly pressure dependent.



Either of these reactions can be used to estimate pressure conditions, but they require an independent estimate of temperature which introduces large uncertainties. Hodges and Crowley (1985) revised the calibration of Ghent and Stout (1981) by using better mixing data. They proposed a method by which to calculate the propagation of uncertainties in external parameters into uncertainties in reaction enthalpy and entropy by using linear regression methods and different activity models.

Pressure conditions in the Ingenika Range have been calculated using the application of Ghent and Stout (1981) as modified by Hodges and Crowley (1985). Temperature estimates needed in this calibration were calculated using the technique of Hodges and Spear (1982). The geobarometry results are presented in Table 3.

RESULTS OF GEOBAROMETRY

SAMPLE NUMBER	PRESSURE (MPa)
K33B	1390
K39B	600
K39G	1500
K52	590
K944	750

TABLE 3: Pressure estimates from the simultaneous solution of Hodges and Spear (1982) and Ghent and Stout (1981, as modified by Hodges and Crowley, 1985) based on the assemblage plagioclase - biotite - garnet - muscovite. Error estimates associated with this calibration are in the order of ± 100 MPa (Ghent and Stout, 1981) but may be as high as ± 270 MPa according to Hodges and Crowley (1985)

4.6 RESULTS OF THERMOBAROMETRY

Pressures and temperatures calculated using mineral rims are assumed to yield peak metamorphic conditions for the Ingenika Range since most samples from the area contain normally zoned porphyroblasts that preserve prograde metamorphic conditions. The only exception to this appears to be sample K39G in which the core analysis of a garnet-biotite pair yields a higher temperature than its rim counterpart. It was previously suggested in section 4.4. that Sample K32H may preserve a retrograde metamorphic assemblage. However, normal zoning in garnet and biotite within the sample records increasing temperature conditions. This indicates that either metamorphism outlasted deformation in some parts of the Ingenika Range, or that some of the rocks were subjected to an additional phase of metamorphism perhaps associated with a nearby buried intrusive.

The rims of garnet-biotite pairs in the garnet zone yield temperatures ranging from 460°C to 610°C. Rim pairs from the staurolite zone produce temperatures varying from 510°C to 560°C. The experimental error associated with these results is $\pm 50^\circ\text{C}$ (Hodges and Spear, 1982).

Temperature results for the Ingenika Range are similar to those estimated by Parrish (1976b) for the Chase Mountain area. Estimates of 510°C to 530°C were obtained from the region based on phase equilibria in pelites, semi-pelites, and calc-silicates. Geothermometry studies by Mansy (1986) yielded slightly lower temperatures of approximately 430°C and 440°C for two locations in the Ingenika Range using the methods of Ferry and Spear (1978; Figure 16).

Metamorphic pressures could be calculated only on 5 samples from the study area. Two of these five samples produced pressures in the order of 1400 and 1500 MPa which are unreasonably high given the apparent medium-grade nature of the rocks. The most probable explanation for this is chemical disequilibrium between

RESULTS FROM THE INGENIKA RANGE

METAMORPHIC ZONE	SAMPLE NUMBER	CALCULATED TEMPERATURE (°C)	CALCULATED PRESSURE (MPa)
GARNET	K39B	510	600
GARNET	K52	540	590
STAUROLITE	K944	560	750

Table 4. Temperature and pressure estimates for the Ingenika Range

mineral phases. Plagioclase grains from these samples have anomalously low Ca contents and are spatially far removed from other mineral phases used in calculations. The other geobarometry results from the study area appear to be more consistent with pressures expected for lower-amphibolite grade rocks. Two samples taken from the garnet zone near Orion Creek produced pressures of 590 MPa and 600 MPa. The other sample taken in the staurolite zone from the southeastern part of the Ingenika Range yields a significantly higher pressure of 750 MPa.

4.7 METAMORPHIC SUMMARY

The Ingenika Range has probably experienced a single phase of metamorphism that spanned two phases of progressive deformation. Metamorphism was initiated during east-verging D_1 deformation and resulted in the development of a regional, bedding-parallel foliation defined by phyllosilicate minerals. Porphyroblastic minerals such as garnet crystallized syn-kinematically with west-verging D_2 deformation; their internal fabrics consistently show top-to-the-southwest senses of rotation. Normal compositional zoning within these porphyroblasts suggests they probably formed during peak metamorphic conditions. The metamorphic isograds of the region were later folded by the Swannell antiform during D_3 southwest-directed deformation. Late stage structures (D_4) resulted in kinking of some metamorphic minerals.

Estimates of peak metamorphic conditions for the region are shown in Table 4. Temperatures and pressures for two samples in the garnet zone yielded results of 510°C at 600 MPa and 540°C at 590 MPa. A calculation of metamorphic conditions in the staurolite zone gave a temperature of 560°C with a pressure estimate of 750 MPa.

The age of metamorphism in the study area is not known with certainty. However, geochronological studies in nearby regions offer some constraints on the timing of regional metamorphism in the northern Omineca Belt. This information has been extrapolated to the Ingenika Range in an effort to estimate the timing of peak metamorphism. These data are presented and discussed in Chapter V.

CHAPTER V

DISCUSSION AND CONCLUSIONS

5.1 INTRODUCTION

The tectonic history of the Ingenika Range is important since the region lies at the suture between cratonic North America and Superterrane I. Structural elements of both the Omineca and Intermontane Belts are used in combination with geochronological data in an attempt to produce a tectonic model for the suture zone in north-central British Columbia. The ultimate goal of this study is to develop an understanding of how and when collision occurred in the northern Cordilleran orogen.

5.2 GEOCHRONOLOGY OF THE INGENIKA RANGE

The timing of deformation and metamorphism in the Ingenika Range is relatively well constrained by geochronological studies by other workers in the region. A summary of the tectonic history based on this information is presented in Table 5.

The first phase of deformation (D_1 - east-verging, pre-peak metamorphic) is probably Early Jurassic to Middle Jurassic and is constrained by the penetratively deformed Polaris ultramafic intrusive complex exposed in the Lay Range west of the Swannell fault. Mylonitic fabrics in a west-dipping fault zone show top-to-the-northeast senses of motion which are consistent with D_1 east-verging deformation in the Ingenika Range (Nixon et al., 1990b; and this report). Preliminary results of uranium-lead dating on the intrusive complex indicate an Early Jurassic age (G.T. Nixon, pers. comm. 1990).

TECTONIC EVOLUTION OF THE INGENIKA GROUP			
EOCENE	D4	POST - METAMORPHIC	Brittle kink folds consistent with dextral motion on Swannell and Rocky Mountain Trench Faults
LATE JURASSIC to EARLY CRETACEOUS	D3	POST - METAMORPHIC	NW - trending, SW - verging Swannell anticline and other regional-scale upright anticlinoria, thrust motion on Swannell fault and minor faults Reactivated D2 structures
MID-JURASSIC	D2	SYN - METAMORPHIC	SW-directed tectonic transport, associated with significant crustal thickening Metamorphism to lower amphibolite grade
POST -EARLY JURASSIC	D1	PRE - METAMORPHIC	NW - trending, NE- verging folds, not associated with major structural thickening

Table 5: Tectonic history of the Ingenika Group at the latitude of the study area.

The timing of peak metamorphic conditions and the second phase of deformation (D_2 - west-verging, syn-metamorphic) is constrained to be Middle Jurassic. This is based on a K-Ar whole rock age of 174 Ma from a phyllite exposed on the lower Osilinka River (Ferri and Melville, in prep.) and from a Rb-Sr (muscovite) age of 166 Ma from Chase Mountain located approximately 15 kilometres southeast of the study area (Figure 2). Much younger K-Ar and Rb-Sr ages from the cores of metamorphic culminations in the Swannell and Sifton Ranges (Wanless et al., 1979; Parrish, 1976b; Stevens et al., 1982; Ferri and Melville, in prep.) suggest that some of these rocks did not cool until Middle Cretaceous to Tertiary time.

D_3 deformation (west-verging, post-metamorphic) is most likely Late Jurassic to Early Cretaceous and is probably coincident with major uplift in the region (Parrish, 1976b; 1979). Southwest-directed movement on the Swannell fault and the formation of the Swannell antiform are probably this age. The Swannell fault was probably also active during D_2 west-verging deformation.

Brittle, late, kink folds (D_4) are likely Eocene in age and are related to minor dextral strike-slip motion on the Swannell fault. Similar kink development in the Late Cretaceous to Eocene Sifton Formation in the Northern Rocky Mountain Trench are related to block faulting and dextral motion along the Rocky Mountain Trench Fault (Eisbacher, 1972). Although the Swannell fault appears to have had minor, late, dextral movement, it appears to be predominantly a west-directed thrust fault.

5.3 IMPORTANT OBSERVATIONS NEAR TERRANE SUTURE

The importance of the structural history of the Ingenika Range has already been stressed. In addition, structural observations of surrounding areas are

important to consider since they impose further constraints on tectonic interpretations. The following discussion summarizes many important observations from the Omineca, Intermontane and Foreland Belts (including the study area) which are believed to be significant for a regional synthesis of the terrane boundary.

5.3.1 Northern Omineca Belt - Swannell Ranges

A structural panel that extends from the Swannell fault to the Northern Rocky Mountain Trench is characterized by large-scale southwest-verging folds and faults. They have been previously documented by Gabrielse (1971, 1972a, 1975), Mansy (1971, 1972, 1974, 1986) and Mansy and Dodds (1976). Bellefontaine and Hynes (1990) and Bellefontaine (this report) have shown that metamorphism is coincident with west-verging deformation. In addition, Ferri and Melville (in prep.) and Evenchick (1985, 1988) have described fabrics and folds that may also be west-verging. South of the Ingenika Range, Ferri and Melville (in prep.) and Parrish (1976b, 1979) have demonstrated that peak metamorphic conditions are synchronous with an east-directed structural vergence. The transition from east- to west-vergent structural prominence in the Swannell Ranges appears to coincide with the study area. The diachronous nature of metamorphism with respect to east and west-directed folding may be a result of the exposure of deeper stratigraphic and structural levels south of the Ingenika Range. Rocks in the Chase Mountain area preserve kyanite and sillimanite bearing assemblages (Parrish, 1976b) whereas strata in the Wolverine Complex near Manson Creek are probably lower in the stratigraphic sequence (lower parts of the lower member of the Swannell Formation) and have metamorphic assemblages that include sillimanite and garnet (Ferri and Melville, in prep.).

5.3.2 Foreland Belt - Northern Rocky Mountains

In contrast to west-verging folds and faults that predominate west of the Northern Rocky Mountain Trench, strata in the Rocky Mountains east of the trench are involved in structures that consistently show northeast-directed asymmetry (Gabrielse, 1971, 1975). Thus, the Northern Rocky Mountain Trench represents a zone of large-scale structural divergence within stratigraphically similar rocks (Gabrielse, 1971, 1975; Eisbacher, 1972). Mapping by McMechan (1987) near Mt. Selwyn, approximately 200 kilometres southeast of the Ingenika Range, has shown that metamorphism predates the formation of major folds and faults in the area and is Latest Jurassic to Early Cretaceous (Leech et al., 1963; Wanless et al., 1979). This suggests that main stage deformation and metamorphism in the Rocky Mountains of northern British Columbia did not occur until after deformation and metamorphism of the Omineca Belt to the west.

5.3.3 Intermontane Belt - Lay Range

Another zone of structural divergence coincides with the Swannell fault. It separates west-verging Proterozoic strata of the northern Omineca Belt from the east-verging faults and fabrics of the Late Paleozoic and Triassic Lay Range Assemblage of the Intermontane Belt. The following brief description of the geology of the Lay Range is from Nixon et al. (1990a, 1990b)

The Early Jurassic Polaris ultramafic complex intrudes/and is in fault contact with mafic volcanic rocks and associated sediments of the Harper Ranch Group. These rocks have been regionally metamorphosed to upper greenschist to lower amphibolite grade. A southwest-dipping mylonitic fault zone within the metasediments contains well developed C/S fabrics and shear bands that indicate the hangingwall was displaced upward and to the northeast relative to the footwall.

These ductile fabrics are defined by dynamically recrystallized grains of chlorite, biotite, quartz and plagioclase which suggest that major fault movements in the Polaris complex took place during regional greenschist metamorphism. The age of metamorphism is confined to be post Early Jurassic and is probably synchronous with metamorphism in the Ingenika Range.

5.4 SYNTHESIS AND INTERPRETATION

East-directed folding in the Ingenika Range is probably related to the initial obduction of Superterrane I onto the distal portions of the North American continental margin. This is consistent with numerous other regions along the suture zone in which the Slide Mountain and Eastern terranes are in thrust contact with continental rocks. Examples of this occur in the Sylvester Allochthon near Cassiar (Nelson and Bradford, 1989), near Manson Creek (Ferri and Melville, in prep.) and in central British Columbia near Quesnel (Rees, 1987). This northeast obduction of allochthonous rocks probably began no earlier than the end of the Early Jurassic. As previously stated, in the thesis area this age is supported by the deformed Early Jurassic Polaris ultramafic intrusive complex. Additional evidence comes from deformed rocks of the Rossland Group near Nelson in southern British Columbia. Here, Toarcian age (190 Ma.) sediments of the Hall Formation are the youngest rocks in Terrane I that are involved in compressional deformation (Tipper, 1984; Höy and Andrew, 1989). This deformation is also bracketed by the post-tectonic late Middle Jurassic Nelson Batholith (Ghosh, 1986; Carr et al., 1987; Höy and Andrew, 1989). These more quantitative age constraints from southern British Columbia may substantiate a similar age for east-verging structures in the Ingenika Range if deformation associated with the collision of Terrane I is not strongly diachronous along the length of the Cordillera.

By early Middle Jurassic time a reversal in structural vergence occurred in the Ingenika Range. West-verging folds and faults were associated with significant structural thickening to produce regional amphibolite-grade metamorphism in the Ingenika Range. Although metamorphism in the Lay Range is probably the same age as in the Ingenika Range, structures in the Lay Range continued to progress to the east during the Middle Jurassic. These data, along with preceding evidence, suggest a maximum gap of 16 million years between east-verging and west-verging structures in the Ingenika Range. This may attest to the progressive nature of deformation in the region.

Regional metamorphism and deformation did not extend east of the Northern Rocky Mountain Trench until the Late Jurassic to Early Cretaceous. At this time, the deformational front stepped eastwards towards the craton and supracrustal rocks became involved in east-verging structures typical of the Rocky Mountains. These structures continued to propagate towards the foreland from Cretaceous to Tertiary time (Price and Mountjoy, 1970; Price, 1985).

While regional metamorphism occurred in the northern Rocky Mountains, the Ingenika Range witnessed southwest-directed, post-metamorphic thrust motion on the Swannell fault and the development of the post-metamorphic Swannell antiform during Late Jurassic to Early Cretaceous time.

5.5 TECTONIC MODEL

The preceding data from the Ingenika Range and surrounding areas are consistent with two models that have been proposed to explain the presence of southwest-directed thrust systems and regional zones of structural divergence in the southern Omineca Belt. Both models involve the initial obduction of allochthonous rocks of Terrane I onto the paleomargin of North America resulting in the

development of east-verging fold systems (Figure 17A). With continued compression (Figure 17B), further shortening may be accommodated by either an east- or west-dipping basement shear (Brown et al., 1986). Price (1986), proposed a model in which the early obduction of the accreted terrane is followed by the tectonic wedging of allochthonous rocks (Terrane I) between para-autochthonous supracrustal rocks and their autochthonous basement. In this manner, the southwest-verging structures are antithetic to the sense of basement shortening (Figure 17Ci). In the model developed by Brown et al. (1986), northeastward obduction of Superterrane I is succeeded by an eastward decoupling and underthrusting of basement rocks. The resulting west-verging structures are synthetic to the basement shear (Figure 17Cii).

Although results from the thesis area cannot be completely reconciled with these two models due to the lack of knowledge of basement geometries, a 'wedge-flake' model consistent with Price (1986) is preferred because it does not invoke regional-scale crustal decoupling as suggested by Brown et al. (1986). Tectonic wedging and delamination occur at all scales from the microscopic to the lithospheric and numerous examples occur in compressional fold belts around the world (Oxburg, 1972; Price, 1986). The model of Brown et al. may explain the occurrence of southwest-verging structures in southern British Columbia, however, regional-scale crustal decoupling along the entire length of the Cordillera may be fortuitous.

The existence of an eastward underplating wedge in the thesis area is suggested by concurrent, syn-metamorphic east and west-verging deformation in the Ingenika and Lay Ranges. This, in addition to the apparent lack of southwest-verging structures in the Lay Range, implies that there may have been a significant structural discontinuity between the two regions during Middle Jurassic time. A

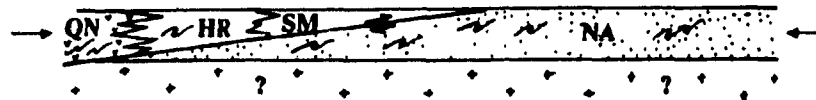
'wedge model' requires that this discontinuity be a west-directed thrust fault. An analogous fault in the study area may be the southwest-verging Swannell fault. Thus, allochthonous rocks of oceanic affinity, and possibly para-autochthonous rocks of displaced continental margin may have acted as an eastward indenting wedge resulting in the development of a backthrust crustal flake above the Swannell fault. In the study area, this delaminated flake of crustal rocks may have overridden the indenting wedge by as much as 60 kilometres. This estimate is based on the distance between the Swannell fault and the limit of southwest-vergent structures at the Northern Rocky Mountain Trench. A schematic tectonic history of the suture zone based on a model of tectonic wedging and crustal delamination is presented in Figure 17.

5.6 DISCUSSION

The evaluation of any terrane boundary is a difficult undertaking. Tectonic sutures are complex zones characterized by intense deformation, regional metamorphism, magmatism, uplift and erosion (Monger et al., 1982). The Mid-Jurassic suture between North America and Superterrane I is perhaps the best example of this. It is characterized by a zone of structural divergence; a direct manifestation of regional-scale northeast- and southwest-verging structures (Price, 1986). Similar east and west-directed thrust systems have been documented along the Late Cretaceous Superterrane II - Superterrane I boundary (Journeay and Csontos, 1989; Schiarizza et al., 1989; Rubin et al., 1990). It is proposed that the findings of this study may attest to the processes of tectonic wedging, delamination and backthrusting at the Terrane I - North American boundary during the Middle Jurassic. If so, then this type of model may have more widespread applications for other tectonic sutures. Opposing thrust systems and zones of

A) LATE EARLY JURASSIC — INITIAL OBDUCTION OF SUPERTERRANE I

- pre-metamorphic east-verging structures in North America and Intermontane Superterrane

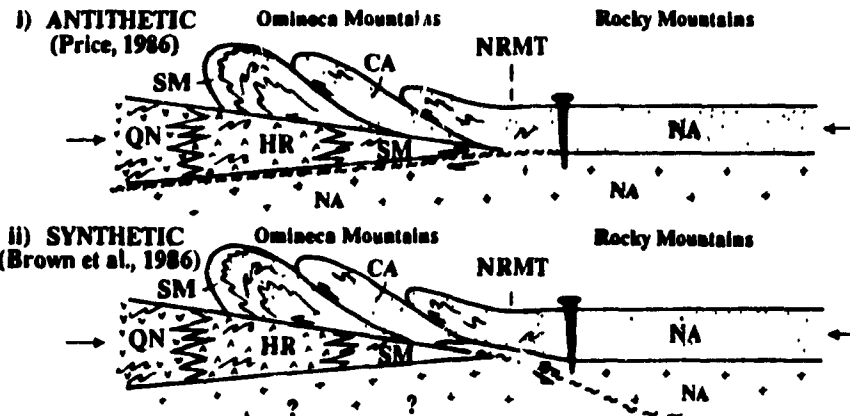


B) POST LATE EARLY JURASSIC(?) — INITIATION OF WEST-VERGING STRUCTURES



C) EARLY(?) MIDDLE JURASSIC — BACK THRUSTING

- syn-metamorphic west-verging structures in Cassiar Terrane
- syn-metamorphic east-verging structures in Superterrane I



D) LATE JURASSIC - EARLY CRETACEOUS — EAST-DIRECTED DEFORMATION IN FORELAND

Omineca Mountains
- uplift and post-metamorphic west-verging deformation
- development of anticlinoria

Rocky Mountains
- metamorphism and east-verging deformation

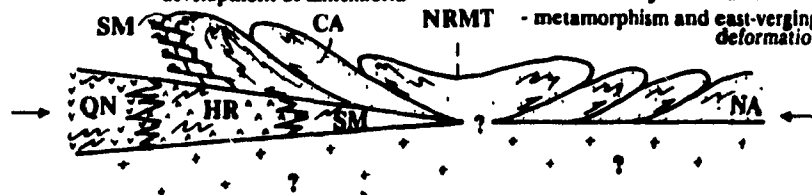


Figure 17: Schematic tectonic history of the Terrane I - North American suture zone at the latitude of the Ingenika Range. Basement geometry is not inferred in diagram A, B or D. Diagram C represents two possible models to produce large-scale backthrusting. Sketch i is based on Price (1986) and involves antithetic backthrusting and basement shortening; sketch ii involves synthetic crustal shortening concurrent with backthrusting (Brown et al., 1986). Abbreviations: NA = North America, CA = Cassiar Terrane, SM = Slide Mountain, HR = Harper Ranch, QN = Quesnellia, NRMT = Northern Rocky Mountain Trench.

structural divergence appear to be common features that are intimately related to collisional tectonics in the Cordilleran Orogen, and are still not fully understood.

5.7 CONCLUSIONS

The Upper Proterozoic Ingenika Group exposed in the Ingenika Range has undergone a progressive deformational history involving pre-, syn- and post-metamorphic structures. Early Jurassic northeast-vergent deformation (D_1) occurred prior to the attainment of peak metamorphic conditions and is most likely related to the initial obduction of Superterrane I onto the western margin of North America. In the study area the Middle Jurassic was marked by a reversal of structural vergence (D_2 - southwest-vergent) concurrent with amphibolite grade regional metamorphism. Peak metamorphic conditions were in the order of 550°C with an approximate pressure of 750 MPa. Syn-metamorphic structures in the Lay Range continued to show northeast-directed asymmetry during this time.

Regional metamorphism and deformation in the Rocky Mountains did not occur until the Late Jurassic to Early Cretaceous when the deformational front progressed eastwards towards the craton. At the same time, uplift, post-metamorphic folding and thrust faulting probably occurred in the Ingenika Range resulting in the development of the Swannell antiform and southwest-directed thrust motion on the Swannell fault. This thrust fault appears to have emplaced rocks of North American affinity over allochthonous rocks of Terrane I. It is also believed that the Swannell fault was active during Middle Jurassic time, when it may have acted as the bounding fault between backthrust cratonic rocks and an underlying eastward-indenting wedge. A simple 'wedge-flake' model can explain the contrasting tectonic histories of the Ingenika Range, the Lay Range and the Rocky Mountains, but, it cannot be reconciled with models proposed for the southern

Omineca Belt due to unknown basement geometries. Regardless of these uncertainties, it appears that collision along the Superterrane I - North American suture (and perhaps other sutures) may have involved some method of tectonic wedging, delamination and large-scale backthrusting.

REFERENCES

- Armstrong, J.E. 1946. Aiken Lake (South half), British Columbia. Geological Survey of Canada, Paper 46-11, Preliminary Map.
- Armstrong, J.E. and Roots, E.F. 1948. Aiken Lake map-area, British Columbia. Geological Survey of Canada, Paper 48-5, 46 p.
- Bellefontaine, K.A. 1989. Tectonic evolution of upper Proterozoic Ingenika Group, north-central British Columbia. British Columbia Ministry of Energy, Mines and Petroleum Resources, Geological Fieldwork, 1988, Paper 1989-1, pp. 221-226.
- Bellefontaine, K. A. and Hynes, A. 1990. Structural evolution of the Ingenika Group: an example of flake tectonics at the Omicea-Intermontane belt boundary. Geological Association of Canada, Program with Abstracts, Volume 15, pp. A8-A9.
- Bellefontaine, K.A. and Minehan, K. 1988. Summary of fieldwork in the Ingenika Range, north-central British Columbia. British Columbia Ministry of Energy, Mines and Petroleum Resources, Geological Fieldwork, 1987, Paper 1988-1, pp. 195-198.
- Brown, R.L., Journeay, J.M., Lane, L.S., Murphy, D.C. and Rees, C.J. 1986. Obduction, backfolding and piggyback thrusting in the metamorphic hinterland of the southeastern Canadian Cordillera. Journal of Structural Geology, Volume 8, pp. 255-268.
- Campbell, R.B., Mountjoy, E.W., and Young, F.G. 1973. Geology of McBride area, British Columbia. Geological Survey of Canada, Paper 72-35, 104 p.
- Carr, S.D., Parrish, R.R. and Brown, R.L. 1987. Eocene structural development of the Valhalla complex, southeastern British Columbia. Tectonics, Volume 6, pp. 175-196.

- Deer, W.A., Howie, R.A., and Zussman, J. 1966. An introduction to the rock forming minerals. Longman, London, 528 p.
- Dymek, R.F. 1983. Titanium, aluminum and interlayer cation substitutions in biotite from high-grade gneisses, West Greenland. *American Mineralogist*, Volume 68, pp. 880-899.
- Eisbacher, G.H. 1972. Tectonic overprinting near Ware, Northern Rocky Mountain Trench. *Canadian Journal of Earth Sciences*, Volume 9, pp. 903-913.
- Eisbacher, G.H. 1981. Sedimentary tectonics and glacial record in the Windermere Supergroup, MacKenzie Mountains, northwestern Canada. Geological Survey of Canada, Paper 80-27, 40 p.
- Evans, G.S. 1923. Brisco-Dogtooth map area, British Columbia. Geological Survey of Canada, Summary Report 1932, part A, pp. 106-176.
- Evenchick, C.A. 1985. Stratigraphy, metamorphism, structure and their tectonic implications in the Sifton and Deserters Ranges, Cassiar and northern Rocky Mountains, northern British Columbia. Unpublished Ph.D. Thesis, Queen's University, Ontario, 189 p.
- Evenchick, C.A. 1988. Stratigraphy, metamorphism, structure, and their tectonic implications in the Sifton and Deserters Ranges, Cassiar and Northern Rocky Mountains, northern British Columbia. Geological Survey of Canada, Bulletin 376, 90 p.
- Ferri, F. and Melville, D. 1988. Manson Creek mapping project. British Columbia Ministry of Energy, Mines and Petroleum Resources, Geological Fieldwork, 1987, Paper 1988-1, pp. 169-180.
- Ferri, F. and Melville, D. 1989. Geology of the Germansen Landing area, British Columbia (93N/10, 15). British Columbia Ministry of Energy, Mines and Petroleum Resources, Geological Fieldwork, 1988, Paper 1989-1, pp. 209-220.

- Ferri, F. and Melville, D. 1990. Geology between Nina Lake and Osilinka River, north-central British Columbia (93N/15, north and 94C/2 south half), British Columbia Ministry of Energy, Mines and Petroleum Resources, Geological Fieldwork, 1989, Paper 1990-1, pp 101-114.
- Ferri, F. and Melville, D. In Prep. Geology of Germansen Landing/Manson Creek area.
- Ferri, F., Melville, D. and Arksey, R. 1989. Geology of the Germansen Landing area, British Columbia, 93N/10, 93N/15. British Columbia Ministry of Energy, Mines and Petroleum Resources, Open File 1989-12.
- Ferry, J.M. and Spear, F.S. 1978. Experimental calibration of the partitioning of Fe and Mg between biotite and garnet. Contributions to Mineralogy and Petrology, Volume 66, pp. 113-117.
- Gabrielse, H. 1962. Cry Lake map-area, British Columbia. Geological Survey of Canada, Map 29-1962.
- Gabrielse, H. 1963. McDame map area, Cassiar district, British Columbia. Geological Survey of Canada, Memoir 319, 138 p.
- Gabrielse, H. 1971. Operation Finlay, north-central British Columbia. Geological Survey of Canada, Paper 71-1A, pp. 23-26.
- Gabrielse, H. 1972a. Operation Finlay (94C east half, 94E,94F west half). Geological Survey of Canada, Paper 72-1A, pp. 26-29.
- Gabrielse, H. 1972b. Younger Precambrian of the Canadian Cordillera. American Journal of Science, Volume 272, pp. 521-536.
- Gabrielse, H. 1975. Geology of Fort Grahame E1/2 map-area, British Columbia. Geological Survey of Canada, Paper 75-33, 28 p.

- Gabrielse, H. 1985. Major dextral transcurrent displacements along the Northern Rocky Mountain Trench and related lineaments in north-central British Columbia. Geological Society of America Bulletin, Volume 96, pp. 1-14.
- Gabrielse, H. and Dodds, C.J. 1974. Operation Finlay. Geological Survey of Canada, Paper 74-1A, pp. 13-16.
- Gabrielse, H. and Dodds, C.J. 1982. Faulting and plutonism in northwestern Cry Lake and adjacent map area, British Columbia. In Current Research, Part A, Geological Survey of Canada, Paper 82-1A, pp. 321-323.
- Gabrielse, H., Dodds, C.J. and Mansy, J.L. 1976. Operation Finlay. Geological Survey of Canada, Paper 76-1A, pp. 89-90.
- Gabrielse, H., Dodds, C.J., Mansy, J.L. and Eisbacher, G.H. 1977. Geology of Toadoggon River (94E) and Ware west-half (94F west-half) map area. Geological Survey of Canada, Open File 483.
- Gabrielse, H. and Mansy, J.L. 1978. Structure style in northeast Cry-Lake map area, British Columbia. In Current Research, part A, Geological Survey of Canada, Paper 78-1A, pp. 33-34.
- Gabrielse, H. and Mansy, J.L. 1980. Structural style in northeastern Cry-Lake map area, British Columbia. In Current Research, part A, Geological Survey of Canada, Paper 80-1A, pp. 33-35.
- Gabrielse, H., Monger, J.W.H., Wheeler, J.O. and Yorath, C.J. (in press). Morphological belts, tectonic assemblages and terranes. In Chapter 2, Tectonic framework, In The Cordilleran Orogen: Canada, Edited by H. Gabrielse and C.J. Yorath. Geological Survey of Canada, Geology of Canada, Number 4.
- Gabrielse, H. and Yorath, C.J. (in press). Chapter 18, Tectonic synthesis, In The Cordilleran Orogen: Canada, Edited by H. Gabrielse and C.J. Yorath. Geological Survey of Canada, Geology of Canada, Number 4.

- Ghent, E.D. 1976. Plagioclase, garnet, Al_2SiO_5 , quartz: a potential geothermometer-geobarometer. *American Mineralogist*, Volume 61, pp. 710-714.
- Ghent, E.D. and Stout, M.Z. 1981. Geobarometry and geothermometry of plagioclase-biotite-garnet-muscovite assemblages. *Contributions to Mineralogy and Petrology*, Volume 76, pp. 92-97.
- Ghosh, D.K. 1986. Geochemistry of the Nelson-Rossland area, southeastern British Columbia. Unpublished Ph.D Thesis, University of Alberta, Edmonton.
- Greenwood, H.J., Woodsworth, G.J., Read, P.B., Ghent, E.D. and Evenchick, C.A. (in press). Chapter 16, Metamorphism, In *The Cordilleran Orogen: Canada*, Edited by H. Gabrielse and C.J. Yorath. Geological Survey of Canada, Geology of Canada, Number 4.
- Hodges, K.V. and Crowley, P.D. 1985. Error estimation and empirical geothermobarometry for pelitic systems. *American Mineralogist*, Volume 70, pp. 702-709.
- Hodges, K.V. and Spear, F.S. 1982. Geothermometry, geobarometry and the Al_2SiO_5 triple point at Mt. Moosilauke, New Hampshire. *American Mineralogist*, Volume 67, pp. 1118-1134
- Hollister, L.S. 1966. Garnet zoning: an interpretation based on the Rayleigh fractionation model. *Science*, Volume 154, pp. 1647-1651.
- Höy, T. and Andrew, K. 1989. The Rossland Group, Nelson map area, southeastern British Columbia. British Columbia Ministry of Energy, Mines and Petroleum Resources, Geological Fieldwork, 1988, Paper 1989-1, pp. 33-43.
- Irish, E.J.W. 1970. Halfway River map-area, British Columbia. Geological Survey of Canada, Paper 69-11.

- Irvine, T.N. 1974. Ultramafic and gabbroic rocks in the Aiken Lake and McConnell Creek map areas, British Columbia. Geological Survey of Canada, Paper 74-1A, pp. 149-152.
- Irvine, T.N. 1976. Alaskan-type ultramafic - gabbroic bodies in the Aiken Lake, McConnell Creek and Toodoggone map areas. Geological Survey of Canada, Paper 76-1A, pp. 76-81.
- Journeay, J.M. and Csontos L. 1989. Preliminary report on the structural setting along the southeast flank of the Coast Belt, British Columbia. In Current Research, Part E, Geological Survey of Canada, Paper 89-1E, pp. 177-187.
- Laird, J. and Albee, A.L. 1981. Pressure, temperature and time indicators in mafic schist from northern Vermont. American Journal of Science, Volume 281, pp. 97-126.
- Little, H.W. 1960. Nelson map-area, west half, British Columbia. Geological Survey of Canada, Memoir 308, 205 p.
- Leech, G.B., Lowden, J.A., Stockwell, C.H. and Wanless, R.K. 1963. Age determinations and geological studies (including isotopic ages - report 4). Geological Survey of Canada, Paper 63-17, pp. 42-43.
- Mansy, J.L. 1971. The Ingenika Group. Geological Survey of Canada, Paper 71-1A, pp. 26-28.
- Mansy, J.L. 1972. Stratigraphy and structure of the Ingenika Group in Finlay and Swannell Ranges. Geological Survey of Canada, Paper 72-1A, pp. 29-32.
- Mansy, J.L. 1974. Operation Finlay. Geological Survey of Canada, Paper 74-1A, pp. 17-18.
- Mansy, J.L. 1986. Géologie de la Chaîne d'Omineca des rocheuses aux plateaux Intérieurs (Cordillère Canadienne) son évolution depuis le Précambrien. Unpublished Ph.D. Thesis, l'Université des Sciences et Techniques de Lille.

- Mansy, J.L. and Dodds, C.J. 1976. Stratigraphy, structure and metamorphism in northern and central Swanneil Ranges. Geological Survey of Canada, Paper 76-1A, pp. 91-92.
- Mansy, J.L. and Gabrielse, H. 1978. Stratigraphy, terminology and correlation of upper Proterozoic rocks in Omineca and Cassiar Mountains, north-central British Columbia. Geological Survey of Canada, Paper 77-19, 17 p.
- McMechan, M.E. 1987. Stratigraphy and structure of the Mount Selwyn area, Rocky Mountains, northeastern British Columbia. Geological Survey of Canada, Paper 85-28, 34 p.
- Minehan, K. 1989a. Takla group volcano-sedimentary rocks, north-central British Columbia: a summary of fieldwork. British Columbia Ministry of Energy, Mines and Petroleum Resources, Geological Fieldwork, 1988, Paper 1989-1, pp. 227-232.
- Minehan, K. 1989b. Paleotectonic setting of Takla Group volcano-sedimentary rocks, Quesnellia, north-central British Columbia. Unpublished M.Sc. Thesis, McGill University, Montreal, 102 p.
- Monger, J.W.H. 1973. Upper Paleozoic rocks of the western Canadian cordillera. Geological Survey of Canada, Paper 73-1A, pp. 27-29.
- Monger, J.W.H. 1977. The Triassic Takla Group in McConnell Creek map-area, north-central British Columbia. Geological Survey of Canada, Paper 76-29, 45 p.
- Monger, J.W.H. and Paterson, I.A. 1974. Upper Paleozoic and Lower Mesozoic rocks of the Omineca Mountains. Geological Survey of Canada, Paper 74-1A, pp. 19-20.

- Monger, J.W.H., Price, R.A. and Tempelman-Kluit, D.J. 1982. Tectonic accretion and the origin of the two major metamorphic and plutonic welts in the Canadian Cordillera. *Geology*, Volume 10, pp. 70-75.
- Monger, J.W.H., Wheeler, J.O., Tipper, H.W., Gabrielse, H., Harms, T., Struik, L.C., Campbell, R.B., Dodds, C.J., Gehrels, G.E., and O'Brien, J. (in press). Chapter 8, Upper Devonian to Middle Jurassic assemblages, *In* The Cordilleran Orogen: Canada, Edited by H. Gabrielse and C.J. Yorath. Geological Survey of Canada, *Geology of Canada*, Number 4.
- Nelson, J.L. and Bradford, J.A. 1989. Geology and mineral deposits of the Cassiar and McDame map area, British Columbia. British Columbia Ministry of Energy, Mines and Petroleum Resources, *Geological Fieldwork*, 1988, Paper 1989-1, pp. 323-338.
- Nixon, G.T., Hammack, J.L., Ash, C.H., Connelly, J.N., Case, G., Paterson, W.P.E. and Nuttall, C. 1990a. Geology of the Polaris ultramafic complex. British Columbia Ministry of Energy, Mines and Petroleum Resources, Open File 1990-13.
- Nixon, G.T., Hammack, J.L., Connelly, J.N., Case, G. and Paterson, W.P.E. 1990b. Geology and noble metal geochemistry of the Polaris ultramafic complex, north-central British Columbia. British Columbia Ministry of Energy, Mines and Petroleum Resources, *Geological Fieldwork*, 1989, Paper 1990-1, pp. 387-404.
- Oxburgh, E.R. 1972. Flake tectonics and continental collision. *Nature*, Volume 239, pp. 202-204.
- Parrish, R.R. 1976a. Structure and metamorphism in southern Swannell Ranges, British Columbia. Geological Survey of Canada, Paper 76-1A, pp. 83-86.
- Parrish, R.R. 1976b. Structure, metamorphism and geochronology of the northern Wolverine Complex near Chase Mountain, Aiken Lake map-area, British Columbia. Unpublished M.Sc. Thesis, The University of British Columbia, 89 p.

- Parrish, R.R. 1979. Geochronology and tectonics of the northern Wolverine Complex, British Columbia. *Canadian Journal of Earth Sciences*, Volume 16, pp. 1428-1438.
- Price, R.A. 1986. The southeastern Canadian Cordillera: thrust faulting, tectonic wedging, and delamination of the lithosphere. *Journal of Structural Geology*, Volume 8, pp. 239-254.
- Price, R.A., Monger, J.W.H., and Roddick, J.A. 1985. Cordilleran cross-section: Calgary to Vancouver. In *Field Guides to Geology and Mineral Deposits in the Southern Canadian Cordillera*. Edited by Tempelman-Kluit, D.J., Geological Society of America, Cordilleran Section, Annual Meeting, Vancouver, pp. 3-1 - 3-85.
- Price, R.A. and Mountjoy, E.W. 1970. Geologic structure of the Canadian Rocky Mountains between the Row and Athabasca Rivers - a progress report. Geological Association of Canada, Special Paper No. 6, pp. 7-26.
- Rees, C.J. 1987. The Intermontane-Omineca belt boundary in the Quesnel Lake area, east-central British Columbia: tectonic implications based on geology, structure, and paleomagnetism. Unpublished Ph.D. thesis, Carleton University, Ottawa, 409 p.
- Ressor, J.E. 1973. Geology of the Lardeau map-area, east-half, British Columbia. Geological Survey of Canada, Memoir 369, 129 p.
- Rich, J.L. 1934. Mechanics of low-angle overthrust faulting as illustrated by the Cumberland thrust block, Virginia, Kentucky, and Tennessee. In *North American Thrust-Faulted Terranes*, American Association of Petroleum Geologists, 1984, Reprint Series No. 27, pp. 1-13.
- Root, E.F. 1954. Geology and mineral deposits of the Aiken Lake map-area, British Columbia. Geological Survey of Canada, Memoir 274, 246 p.

- Rubin, C.M., Saleeby, J.B., Cowan, D.S., Brandon, M.T., and McGroder, M.F. 1990. Regionally extensive mid-Cretaceous west-vergent thrust system in the northwestern Cordillera: Implications for continent-margin tectonism. *Geology*, Volume 18, pp. 276-280.
- Schiarizza, P., Gaba, R.G., Glover J.K. and Garver, J.I. 1989. Geology and mineral occurrences of the Tyaughton Creek area. British Columbia Ministry of Energy, Mines and Petroleum Resources, Geological Fieldwork, 1988, Paper 1989-1, pp. 115-130.
- Slind, O.L. and Perkins, G.D. 1966. Lower Paleozoic and Proterozoic sediments of the Rocky Mountains between Jasper, Alberta and Pine River, British Columbia. *Bulletin of Canadian Petroleum Geology*, Volume 14, pp. 442-468.
- Stevens, R.B., Delabio, R.N. and Lachance, G.R. 1982. Age determinations and geological studies: K-Ar isotopic ages, Report 16. Geological Survey of Canada, Paper 82-2, 56 p.
- Taylor, G.C. and Stott, D.F. 1973. Tuchodi Lakes map-area, British Columbia. Geological Survey of Canada, Memoir 373, 37 p.
- Thompson, A.B. 1976. Mineral reactions in pelitic rocks: II, calculation of some P-T-x (Fe-Mg) phase relations. *American Journal of Science*, Volume 276, pp. 425-454.
- Tipper, H.W. 1984. The age of the Jurassic Rossland Group of southeastern British Columbia. In *Current Research, Part A*, Geological Survey of Canada, Paper 84-1A, pp. 631-632.
- Wanless, R.K., Stevens, R.D., Lachance, G.R. and Delabio, R.N. 1979. Age determinations and geological studies, K-Ar isotopic ages, Report 14. Geological Survey of Canada, Paper 79-2, pp. 9-10.

- Wheeler, J.O. and McFeely, P. 1987. Tectonic assemblage map of the Canadian Cordillera and adjacent parts of the United States of America. Geological Survey of Canada, Open File 1565.
- Wheeler, J.O., Brookfield, A.J., Gabrielse, H., Monger, J.W.H., Tipper, H.W. and Woodsworth, G.J. 1988. Terrane map of the Canadian Cordillera. Geological Survey of Canada, Open File 1894.
- Winkler, H.G.F. 1979. Petrogenesis of metamorphic rocks. Springer-Verlag, New York.
- Young, F.G., Campbell, R.B. and Poulton, T.P. 1973. The Windermere Supergroup of the southeastern Cordillera. In Belt Symposium 1973, Volume 1, Department of Geology, The University of Idaho and Idaho Bureau of Mines and Geology, Moscow, Idaho, pp. 181-203.

APPENDIX A

A.1 Analytical Procedures

Polished thin sections were made of rock samples containing semi-pelitic assemblages. Mineral compositions were analysed using the Cameca-Camebax wavelength dispersive electron microprobe at McGill University. Analyses were conducted at specimen currents between 8 and 10 nanoamps with counting times of 30 seconds.

Mineral stoichiometries were calculated using microcomputer programs written by G. Poirier. A test for the ferric iron content of several garnets from the Ingenika Range was estimated using the procedure of Laird and Albee (1981) and was found to be very low. Therefore all iron in garnets used in geothermobarometric studies and listed in this appendix is assumed to be ferrous. Biotite stoichiometries were based on 14 cation sites using the method of Dymek (1983) in which a calculation is iterated until vacancies for every Ti and every second Al^{vi} are created. Fe^{2+} is then converted to Fe^{3+} to balance the difference in charge.

Mineral formulae for plagioclase were calculated using 32 oxygens whereas muscovite stoichiometries were established on the presence of 14 cations.

A.2 Analyses

Thin sections containing semi-pelitic assemblages were chosen for microprobe analyses. Data presented in the following tables have been used for geothermobarometric studies. The results have been organized by thin section/sample number and by mineral pairs that were used in calculations. Garnet (gar) and biotite (bio) crystals were analysed in a core spot (core) and on a rim locality (rim). Mineral phases were almost never in contact; analyses were conducted on matrix biotite, plagioclase (plag), and muscovite (musc) as close to garnet porphyroblasts as possible.

	SAMPLE K32C				SAMPLE K32H			
	gar-core	bio-core	gar-rim	bio-rim	gar-core	bio-core	gar-rim	bio-rim
	32C-2	32C-8	32C-1	32C-9	32H1-4	32H1-3	32H1-7	32H1-4
SiO2	38.11	37.91	38.24	36.38	38.51	38.25	37.63	38.02
TiO2	0.07	1.57	0.08	1.60	0.12	1.43	0.05	1.59
Al2O3	20.68	18.49	20.72	18.63	20.34	18.69	20.32	18.68
Fe2O3	0.00	0.00	0.00	0.00	0.00	0.00	0.00	0.00
Cr2O3	0.00	0.00	0.00	0.00	0.00	0.00	0.00	0.00
FeO	30.16	17.82	31.06	18.82	29.58	18.03	33.46	17.98
MnO	1.58	0.10	1.46	0.08	3.39	0.02	0.69	0.03
MgO	2.16	11.02	2.32	10.53	1.38	10.99	2.10	11.10
BaO	0.00	0.00	0.00	0.00	0.00	0.00	0.00	0.00
CaO	7.42	0.00	6.96	0.01	7.67	0.00	5.32	0.00
Na2O	0.00	0.07	0.00	0.08	0.00	0.20	0.00	0.12
K2O	0.00	9.99	0.00	8.59	0.00	9.76	0.00	9.91
F	0.00	0.00	0.00	0.00	0.00	0.00	0.00	0.00
TOTAL	100.19	96.97	100.84	94.73	100.99	97.37	99.57	97.43
Si	3.040	2.804	3.034	2.756	3.067	2.813	3.041	2.797
Ti	0.004	0.087	0.005	0.091	0.007	0.079	0.003	0.088
AlIV	0.000	1.196	0.000	1.244	0.000	1.187	0.000	1.203
AlVI	1.942	0.415	1.936	0.420	1.907	0.432	1.933	0.418
Fe3+	0.000	0.000	0.000	0.000	0.000	0.000	0.000	0.000
Cr	0.000	0.000	0.000	0.000	0.000	0.000	0.000	0.000
Fe2+	2.012	1.102	2.060	1.192	1.970	1.109	2.261	1.107
Mn	0.107	0.006	0.098	0.005	0.229	0.001	0.047	0.002
Mg	0.259	1.215	0.274	1.189	0.164	1.204	0.253	1.217
Ba	0.000	0.000	0.000	0.000	0.000	0.000	0.000	0.000
Ca	0.634	0.000	0.591	0.001	0.654	0.000	0.460	0.000
Na	0.000	0.010	0.000	0.012	0.000	0.029	0.000	0.018
K	0.000	0.943	0.000	0.830	0.000	0.916	0.000	0.931
Xal	0.668		0.681		0.653		0.748	
Xsp	0.035		0.032		0.076		0.016	
Xpy	0.086		0.091		0.054		0.084	
Xgr	0.211		0.196		0.217		0.152	

	SAMPLE K32I				SAMPLE K32J			
	gar-core	bio-core	gar-rim	bio-rim	gar-core	bio-core	gar-rim	bio-rim
	32I-1	32I-3	32I-2	32I-2	32J-2	32J-1	32J-1	32J-2
SiO2	38.23	36.73	38.20	36.30	38.22	37.17	38.46	37.61
TiO2	0.08	1.42	0.12	1.86	0.10	1.73	0.07	1.46
Al2O3	20.60	17.93	20.66	17.95	20.66	18.26	20.78	17.91
Fe2O3	0.00	0.00	0.00	0.00	0.00	0.00	0.00	0.00
Cr2O3	0.00	0.00	0.00	0.00	0.00	0.00	0.00	0.00
FeO	30.92	18.43	31.88	17.94	30.08	19.48	29.23	18.94
MnO	1.92	0.00	0.27	0.00	1.58	0.11	1.56	0.13
MgO	1.49	10.68	2.09	10.43	2.12	10.06	2.20	10.45
BaO	0.00	0.00	0.00	0.00	0.00	0.00	0.00	0.00
CaO	7.13	0.00	7.64	0.00	7.74	0.01	7.93	0.00
Na2O	0.00	0.15	0.00	0.10	0.00	0.07	0.00	0.04
K2O	0.00	9.60	0.00	9.76	0.00	9.88	0.00	9.88
F	0.00	0.00	0.00	0.00	0.00	0.00	0.00	0.00
TOTAL	100.36	94.96	100.87	94.36	100.50	96.77	100.23	96.43
Si	3.061	2.788	3.031	2.773	3.040	2.782	3.060	2.816
Ti	0.005	0.081	0.007	0.107	0.006	0.097	0.004	0.082
Al/IV	0.000	1.212	0.000	1.227	0.000	1.128	0.000	1.184
Al/VI	1.942	0.393	1.930	0.389	1.934	0.392	1.946	0.396
Fe3+	0.000	0.000	0.000	0.000	0.000	0.000	0.000	0.000
Cr	0.000	0.000	0.000	0.000	0.000	0.000	0.000	0.000
Fe2+	2.070	1.170	2.115	1.416	2.001	1.220	1.945	1.185
Mn	0.130	0.000	0.018	0.000	0.106	0.007	0.105	0.008
Mg	0.178	1.208	0.247	1.188	0.251	1.122	0.261	1.166
Ba	0.000	0.000	0.000	0.000	0.000	0.000	0.000	0.000
Ca	0.611	0.000	0.649	0.000	0.660	0.000	0.676	0.000
Na	0.000	0.023	0.000	0.014	0.000	0.010	0.000	0.006
K	0.000	0.930	0.000	0.951	0.000	0.943	0.000	0.944
Xal	0.692		0.698		0.663		0.651	
Xsp	0.043		0.006		0.035		0.035	
Xpy	0.060		0.082		0.083		0.087	
Xgr	0.204		0.214		0.219		0.226	

	SAMPLE K32K							SAMPLE K33A	
	gar-rim	bio-rim	gar-core	bio-core	gar-core	gar-rim	bio-rim	gar-rim	bio-rim
	32K-6	32K-3	32K-8	32K-2	32K-4	32K-7	32K-4	33A-1	33A-1
SiO ₂	37.94	36.78	37.70	37.50	38.20	37.81	36.70	37.91	36.19
TiO ₂	0.04	2.62	0.07	1.51	0.09	0.05	1.34	0.02	1.38
Al ₂ O ₃	20.39	17.33	20.55	18.50	20.55	20.65	17.92	20.60	17.74
Fe ₂ O ₃	0.00	0.00	0.00	0.00	0.00	0.00	0.00	0.00	0.00
Cr ₂ O ₃	0.00	0.00	0.00	0.00	0.00	0.00	0.00	0.00	0.00
FeO	36.66	22.09	31.51	21.15	29.72	34.37	21.38	36.28	22.32
MnO	0.68	0.05	2.65	0.01	3.77	1.08	0.02	1.09	0.06
MgO	2.42	8.13	1.40	8.80	1.19	2.02	8.68	2.25	7.99
BaO	0.00	0.00	0.00	0.00	0.00	0.00	0.00	0.00	0.00
CaO	2.39	0.00	5.43	0.00	7.23	3.83	0.00	2.00	0.00
Na ₂ O	0.00	0.09	0.00	0.12	0.00	0.00	0.10	0.00	0.11
K ₂ O	0.00	10.00	0.00	9.84	0.00	0.00	9.89	0.00	9.63
F	0.00	0.00	0.00	0.00	0.00	0.00	0.00	0.00	0.00
TOTAL	100.52	97.09	99.32	97.43	100.75	99.81	96.03	100.15	95.42
Si	3.054	2.786	3.062	2.803	3.054	3.057	2.797	3.065	2.790
Ti	0.002	0.149	0.004	0.085	0.006	0.003	0.077	0.001	0.080
Al ^{IV}	0.000	1.214	0.000	1.197	0.000	0.000	1.203	0.000	1.210
Al ^{VI}	1.932	0.333	1.966	0.432	1.935	1.966	0.406	1.961	0.402
Fe ³⁺	0.000	0.000	0.000	0.000	0.000	0.000	0.000	0.000	0.000
Cr	0.000	0.000	0.000	0.000	0.000	0.000	0.000	0.000	0.000
Fe ²⁺	2.467	1.399	2.141	1.322	1.987	2.323	1.363	2.453	1.439
Mn	0.046	0.004	0.182	0.001	0.256	0.074	0.001	0.074	0.004
Mg	0.290	0.918	0.170	0.980	0.142	0.243	0.986	0.271	0.918
Ba	0.000	0.000	0.000	0.000	0.000	0.000	0.000	0.000	0.000
Ca	0.206	0.000	0.473	0.000	0.619	0.331	0.000	0.173	0.000
Na	0.000	0.013	0.000	0.017	0.000	0.000	0.016	0.000	0.016
K	0.000	0.966	0.000	0.938	0.000	0.000	0.962	0.000	0.947
X _{al}	0.820		0.722		0.662	0.782		0.826	
X _{sp}	0.015		0.061		0.085	0.025		0.025	
X _{py}	0.096		0.057		0.047	0.082		0.091	
X _{gr}	0.069		0.159		0.206	0.111		0.058	

	SAMPLE K33B				SAMPLE K36B3			
	gar-core	bio-core	gar-rim	bio-rim	gar-core	bio-core	gar-rim	bio-rim
	33B-2	33B-3	33B-6	33B-4	36B3-2	36B3-1	36B3-1	36B3-2
SiO2	38.31	36.55	37.61	35.93	38.09	36.73	37.51	36.98
TiO2	0.07	1.80	0.05	1.79	0.13	2.03	0.06	1.48
Al2O3	20.83	18.32	20.55	18.56	20.64	17.99	20.48	17.95
Fe2O3	0.00	0.00	0.00	0.00	0.00	0.00	0.00	0.00
Cr2O3	0.00	0.00	0.00	0.00	0.00	0.00	0.00	0.00
FeO	30.50	20.25	33.71	20.56	29.63	21.34	31.17	21.43
MnO	1.61	0.05	1.75	0.05	3.24	0.10	1.75	0.07
MgO	1.63	8.74	2.25	8.86	1.40	8.79	1.72	9.02
BaO	0.00	0.00	0.00	0.00	0.00	0.00	0.00	0.00
CaO	7.46	0.00	3.70	0.00	7.31	0.02	7.06	0.05
Na2O	0.00	0.18	0.00	0.13	0.00	0.06	0.00	0.10
K2O	0.00	9.46	0.00	9.85	0.00	9.34	0.00	9.51
F	0.00	0.00	0.00	0.00	0.00	0.00	0.00	0.00
TOTAL	100.41	95.35	99.61	95.75	100.44	96.42	99.74	96.64
Si	3.058	2.784	3.044	2.740	3.049	2.779	3.020	2.794
Ti	0.004	0.103	0.003	0.103	0.008	0.116	0.004	0.084
AlIV	0.000	1.216	0.000	1.260	0.000	1.221	0.000	1.206
AlVI	1.958	0.429	1.958	0.409	1.945	0.383	1.941	0.392
Fe3+	0.000	0.000	0.000	0.000	0.000	0.000	0.000	0.000
Cr	0.000	0.000	0.000	0.000	0.000	0.000	0.000	0.000
Fe2+	2.036	1.290	2.281	1.312	1.983	1.350	2.099	1.357
Mn	0.109	0.003	0.120	0.003	0.220	0.006	0.119	0.004
Mg	0.194	0.993	0.271	1.008	0.167	0.992	0.206	1.016
Ba	0.000	0.000	0.000	0.000	0.000	0.000	0.000	0.000
Ca	0.639	0.000	0.321	0.000	0.627	0.002	0.609	0.004
Na	0.000	0.027	0.000	0.020	0.000	0.009	0.000	0.015
K	0.000	0.919	0.000	0.958	0.000	0.902	0.000	0.916
Xal	0.684		0.762		0.662		0.692	
Xsp	0.037		0.040		0.073		0.039	
Xpy	0.065		0.091		0.056		0.068	
Xgr	0.214		0.107		0.209		0.201	

SAMPLE K39B								
	gar-core	bio-core	gar-rim	bio-rim	gar	bio	plag	musc
	39B2-1	39B2-5	39B2-2	39B2-6	39B2	39B2	39B2-1	39B2
SiO2	37.93	37.71	38.09	37.5	37.22	37.41	60.08	46.32
TiO2	0.14	1.55	0.11	1.6	0.08	1.66	0.00	0.10
Al2O3	20.50	18.00	20.42	17.87	20.99	18.15	24.68	33.92
Fe2O3	0.00	0.00	0.00	0.00	0.00	0.00	0.00	0.00
Cr2O3	0.00	0.00	0.00	0.00	0.00	0.00	0.00	0.00
FeO	28.65	16.69	29.11	17.33	30.22	15.53	0.00	2.50
MnO	3.55	0.00	3.07	0.04	1.43	0.02	0.02	0.05
MgO	1.25	11.86	1.48	11.49	2.36	12.33	0.00	0.57
BaO	0.00	0.00	0.00	0.00	0.00	0.00	0.00	0.00
CaO	8.03	0.00	7.96	0.00	7.34	0.00	6.91	0.00
Na2O	0.00	0.11	0.00	0.11	0.00	0.04	7.83	0.57
K2O	0.00	9.67	0.00	9.73	0.00	10.11	0.04	10.69
F	0.00	0.00	0.00	0.00	0.00	0.00	0.00	0.00
TOTAL	100.06	95.59	100.24	96.18	99.63	95.26	99.57	94.71
Si	3.046	2.813	3.050	2.822	2.981	2.794	10.751	6.248
Ti	0.009	0.087	0.006	0.092	0.005	0.093	0.000	0.010
AlIV	0.000	1.187	0.000	1.178	0.019	1.206	0.000	1.752
AlVI	1.938	0.395	1.925	0.388	1.960	0.392	5.199	3.635
Fe3+	0.000	0.000	0.000	0.000	0.000	0.000	0.000	0.000
Cr	0.000	0.000	0.000	0.000	0.000	0.000	0.000	0.000
Fe2+	1.924	1.041	1.949	1.078	2.025	0.970	0.000	0.282
Mn	0.241	0.000	0.208	0.003	0.097	0.001	0.004	0.114
Mg	0.150	1.319	0.177	1.274	0.282	1.373	0.000	0.005
Ba	0.000	0.000	0.000	0.000	0.000	0.000	0.000	0.000
Ca	0.691	0.000	0.683	0.000	0.630	0.000	1.326	0.000
Na	0.000	0.016	0.000	0.016	0.000	0.006	2.715	0.149
K	0.000	0.920	0.000	0.923	0.000	0.963	0.010	1.840
Xal	0.640		0.646		0.658			
Xsp	0.080		0.069		0.032			
Xpy	0.050		0.059		0.093			
Xgr	0.230		0.226		0.208			
Xor							0.002	
Xab							0.670	
Xan							0.328	

SAMPLE K39G						
	gar-core	bio-core	gar	bio	plag	musc
	39G2-1	39G2-1	39G2	39G2	39G2-3	39G2
SiO2	37.73	35.92	37.09	35.88	68.52	46.24
TiO2	0.04	2.55	0.07	2.77	0.00	0.27
Al2O3	20.69	18.14	20.80	18.29	19.53	34.38
Fe2O3	0.00	0.00	0.00	0.00	0.00	0.00
Cr2O3	0.00	0.00	0.00	0.00	0.00	0.00
FeO	32.15	22.58	30.91	22.12	0.04	1.71
MnO	3.90	0.05	4.46	0.04	0.00	0.00
MgO	1.76	7.67	1.63	7.75	0.00	0.90
BaO	0.00	0.00	0.00	0.00	0.00	0.00
CaO	4.13	0.00	4.69	0.01	0.38	0.00
Na2O	0.00	0.05	0.00	0.05	11.77	0.63
K2O	0.00	9.77	0.00	10.04	0.07	10.83
F	0.00	0.00	0.00	0.00	0.00	0.00
TOTAL	100.39	96.75	99.65	96.96	100.31	94.95
Si	3.037	2.736	3.005	2.725	11.952	6.205
Ti	0.002	0.146	0.004	0.158	0.000	0.027
AlIV	0.000	1.264	0.000	1.275	4.011	1.795
AlVI	1.961	0.365	1.984	0.363	0.000	3.637
Fe3+	0.000	0.000	0.000	0.000	0.000	0.000
Cr	0.000	0.000	0.000	0.000	0.000	0.000
Fe2+	2.165	1.439	2.095	1.405	0.005	0.192
Mn	0.266	0.003	0.306	0.003	0.000	0.179
Mg	0.212	0.871	0.196	0.878	0.000	0.000
Ba	0.000	0.000	0.000	0.000	0.000	0.000
Ca	0.356	0.000	0.407	0.000	0.070	0.000
Na	0.000	0.007	0.000	0.008	3.980	0.146
K	0.000	0.950	0.000	0.973	0.016	1.854
Xal	0.722		0.697			
Xsp	0.089		0.102			
Xpy	0.071		0.065			
Xgr	0.119		0.136			
Xor					0.004	
Xab					0.978	
Xan					0.019	

	SAMPLE K40C		SAMPLE K52					
	gar-core	bio-core	gar-core	bio-core	gar	bio	plag	musc
	40C-1	40C-2	52-3	52-2	52-24	52-12	52-11	52-11
SiO2	38.20	36.57	37.68	36.46	37.04	36.18	60.78	46.73
TiO2	0.11	1.52	0.04	1.77	0.04	1.91	0.00	0.27
Al2O3	20.60	17.82	20.46	18.33	20.93	18.29	24.74	34.48
Fe2O3	0.00	0.00	0.00	0.00	0.00	0.00	0.00	0.00
Cr2O3	0.00	0.00	0.00	0.00	0.00	0.00	0.00	0.00
FeO	29.23	20.38	30.40	20.46	30.18	19.53	0.21	1.48
MnO	3.14	0.09	4.31	0.26	4.22	0.10	0.04	0.01
MgO	1.37	9.81	1.81	9.49	1.83	9.72	0.00	0.92
BaO	0.00	0.00	0.00	0.00	0.00	0.00	0.00	0.00
CaO	7.54	0.00	4.74	0.00	5.91	0.03	5.95	0.00
Na2O	0.00	0.09	0.00	0.09	0.00	0.02	8.01	0.82
K2O	0.00	9.63	0.00	9.41	0.00	9.82	0.05	10.34
F	0.00	0.00	0.00	0.00	0.00	0.00	0.00	0.00
TOTAL	100.20	95.92	93.45	96.28	100.15	95.59	99.77	95.06
Si	3.062	2.776	3.055	2.755	2.975	2.749	10.825	6.237
Ti	0.007	0.087	0.002	0.101	0.003	0.109	0.000	0.027
AlIV	0.000	1.224	0.000	1.245	0.025	1.251	5.187	1.763
AlVI	1.944	0.370	1.953	0.388	1.954	0.387	0.000	3.655
Fe3+	0.000	0.000	0.000	0.000	0.000	0.000	0.000	0.000
Cr	0.000	0.000	0.000	0.000	0.000	0.000	0.000	0.000
Fe2+	1.960	1.294	2.061	1.293	2.027	1.241	0.031	0.166
Mn	0.213	0.006	0.296	0.016	0.287	0.006	0.006	0.183
Mg	0.164	1.110	0.219	1.068	0.219	1.100	0.000	0.001
Ba	0.000	0.000	0.000	0.000	0.000	0.000	0.000	0.000
Ca	0.648	0.000	0.412	0.000	0.509	0.002	1.135	0.000
Na	0.000	0.014	0.000	0.014	0.000	0.003	2.765	0.000
K	0.000	0.932	0.000	0.907	0.000	0.952	0.012	1.761
Xal	0.657		0.690		0.666			
Xsp	0.071		0.099		0.094			
Xpy	0.055		0.073		0.072			
Xgr	0.217		0.138		0.167			
Xor							0.003	
Xab							0.700	
Xan							0.297	

	SAMPLE K53				SAMPLE K791			
	gar-core	bio-core	gar-rim	bio-rim	gar-core	bio-core	gar-rim	bio-rim
	53-2	52-1	53-3	53-2	791-1	791-2	791-2	791-1
SiO2	37.85	37.34	38.13	37.11	37.92	37.31	37.42	37.75
TiO2	0.04	1.90	0.07	1.60	0.07	2.16	0.07	2.38
Al2O3	20.37	17.82	20.43	18.15	20.67	18.29	20.63	18.92
Fe2O3	0.00	0.00	0.00	0.00	0.00	0.00	0.00	0.00
Cr2O3	0.00	0.00	0.00	0.00	0.00	0.00	0.00	0.00
FeO	29.81	19.33	31.98	19.34	30.06	18.29	31.80	17.66
MnO	4.80	0.15	2.41	0.06	5.09	0.04	4.42	0.10
MgO	1.69	10.23	1.93	10.02	1.85	9.92	2.05	9.33
BaO	0.00	0.00	0.00	0.00	0.00	0.00	0.00	0.00
CaO	4.87	0.00	5.53	0.00	4.61	0.00	3.98	0.00
Na2O	0.00	0.11	0.00	0.09	0.00	0.11	0.00	0.10
K2O	0.00	9.13	0.00	9.32	0.00	8.76	0.00	8.74
F	0.00	0.00	0.00	0.00	0.00	0.00	0.00	0.00
TOTAL	99.42	96.02	100.48	95.70	100.29	94.89	100.36	94.98
Si	3.071	2.803	3.055	2.798	3.049	2.810	3.011	2.825
Ti	0.003	0.107	0.004	1.202	0.004	1.190	0.004	0.134
AlIV	0.000	1.197	0.000	0.000	0.000	0.122	0.000	1.175
AlVI	1.946	0.380	1.927	4.000	1.957	0.430	1.954	0.495
Fe3+	0.000	0.000	0.000	0.411	0.000	0.000	0.000	0.000
Cr	0.000	0.000	0.000	0.091	0.000	0.000	0.000	0.000
Fe2+	2.023	1.213	2.143	0.000	2.021	1.152	2.139	1.105
Mn	0.330	0.010	0.163	0.501	0.347	0.003	0.301	0.006
Mg	0.204	1.145	0.230	1.126	0.222	1.114	0.245	1.041
Ba	0.000	0.000	0.000	1.220	0.000	0.000	0.000	0.000
Ca	0.423	0.000	0.475	0.004	0.397	0.000	0.343	0.000
Na	0.000	0.016	0.000	0.000	0.000	0.017	0.000	0.015
K	0.000	0.875	0.000	2.349	0.000	0.842	0.000	0.835
Xal	0.679		0.712		0.676		0.706	
Xsp	0.111		0.054		0.116		0.099	
Xpy	0.069		0.076		0.074		0.081	
Xgr	0.142		0.158		0.133		0.113	

SAMPLE K851						
	gar-core	bio-core	gar-rim	bio-rim	gar-rim	bio-rim
	851-3	851-2	851-1	851-1	851-2	851-9
SiO2	37.24	38.15	37.84	37.64	36.98	36.53
TiO2	0.13	1.52	0.05	1.66	0.04	1.46
Al2O3	20.50	18.53	20.63	18.90	20.93	19.13
Fe2O3	0.00	0.00	0.00	0.00	0.00	0.00
Cr2O3	0.00	0.00	0.00	0.00	0.00	0.00
FeO	29.18	19.92	32.48	19.65	33.28	20.35
MnO	4.34	0.18	3.43	0.18	3.42	0.19
MgO	1.60	9.55	2.01	9.21	2.26	8.64
BaO	0.00	0.00	0.00	0.00	0.00	0.00
CaO	6.63	0.00	3.77	0.01	3.09	0.02
Na2O	0.00	0.15	0.00	0.12	0.00	0.06
K2O	0.00	9.34	0.00	9.52	0.00	9.50
F	0.00	0.00	0.00	0.00	0.00	0.00
TOTAL	99.62	97.34	100.21	96.88	100.00	95.89
Si	3.007	2.826	3.049	2.803	2.986	2.766
Ti	0.008	0.085	0.003	0.093	0.002	0.083
AlIV	0.000	1.174	0.000	1.197	0.014	1.234
AlVI	1.949	0.444	1.957	0.462	1.975	0.473
Fe3+	0.000	0.000	0.000	0.000	0.000	0.000
Cr	0.000	0.000	0.000	0.000	0.000	0.000
Fe2+	1.971	1.234	2.189	1.224	2.247	1.289
Mn	0.297	0.011	0.234	0.012	0.234	0.012
Mg	0.192	1.055	0.241	1.022	0.272	0.975
Ba	0.000	0.000	0.000	0.000	0.000	0.000
Ca	0.574	0.000	0.326	0.001	0.267	0.002
Na	0.000	0.021	0.000	0.017	0.000	0.009
K	0.000	0.882	0.000	0.904	0.000	0.917
Xal	0.650		0.732		0.744	
Xsp	0.098		0.078		0.077	
Xpy	0.063		0.081		0.090	
Xgr	0.189		0.109		0.088	

	SAMPLE K941		SAMPLE K944					
	gar-rim	bio-rim	gar-rim	bio-rim	gar-rim	bio-rim	plag	musc
	941-2	941-7	944-2	944-1	944-1	994-3	944-2	944-4
SiO ₂	37 70	37 59	37 71	34 70	38 12	38 03	62 27	46 85
TiO ₂	0 00	1 65	0 02	1 47	0 03	1 63	0 01	0 41
Al ₂ O ₃	21 22	19 53	20 96	19 17	20 90	19 18	23 96	35 36
Fe ₂ O ₃	0 00	0 00	0 00	0 00	0 00	0 00	0 00	0 00
Cr ₂ O ₃	0 00	0 00	0 00	0 00	0 00	0 00	0 00	0 00
FeO	34 22	15 62	32 82	19 74	33 16	14 96	0 12	0 80
MnO	0 79	0 05	0 26	0 03	0 21	0 04	0 00	0 06
MgO	3 66	11 89	3 74	11 93	3 82	12 33	0 01	0 20
BaO	0 00	0 00	0 00	0 00	0 00	0 00	0 00	0 00
CaO	3 56	0 00	4 18	0 00	4 22	0 01	5 09	0 02
Na ₂ O	0 00	0 27	0 00	0 05	0 00	0 24	8 53	1 76
K ₂ O	0 00	8 73	0 00	6 95	0 00	9 29	0 06	9 03
F	0 00	0 00	0 00	0 00	0 00	0 00	0 00	0 00
TOTAL	101 15	95 33	99 68	94 03	100 46	95 71	100 07	95 10
Si	2 978	2 778	3 012	2 589	3 023	2 798	11 021	6 200
Ti	0 000	0 092	0 001	0 082	0 002	0 090	0 002	0 041
Al ^{IV}	0 022	1 222	0 000	1 411	0 000	1 202	4 993	1 800
Al ^{VI}	1 952	0 479	1 972	0 275	1 952	0 461	0 000	3 710
Fe ³⁺	0 000	0 000	0 000	0 000	0 000	0 000	0 000	0 000
Cr	0 000	0 000	0 000	0 000	0 000	0 000	0 000	0 000
Fe ²⁺	2.261	0 965	2.193	0 764	2 199	0 920	0 018	0 089
Mn	0.053	0 003	0 017	0 002	0 014	0 002	0 001	0 158
Mg	0 431	1 310	0 445	1 326	0 451	1 352	0 002	0 007
Ba	0 000	0 000	0 000	0 000	0 000	0 000	0 000	0 000
Ca	0 301	0 000	0 357	0 000	0 358	0 001	0 966	0 000
Na	0 000	0 000	0 000	0 007	0 000	0 034	2 928	0 453
K	0 000	0 823	0 000	0 661	0 000	0 872	0 014	1 525
Xal	0 742		0 728		0 728			
Xsp	0 017		0 006		0 005			
Xpy	0 142		0 148		0 149			
Xgr	0 099		0 119		0 119			
Xor							0 004	
Xab							0 745	
Xan							0 251	

APPE

**STRUCTURAL G
INGENIKA RANGE
BRITISH C**

GEOLOGY BY K.
ADDITIONAL SOUF

SYM










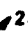






- Bedding
- Schistosity.....
- Crenulation cleavage.....
- Shear zone.....
- F1 fold axis.....
- F2 fold axis.....
- F3 fold axis.....
- Fold axis (unknown generation).....
- East-verging fold.....
- West-verging fold.....
- Crenulation folds and lineations
- S-kink fold axis.....
- Z-kink fold axis
- Axial trace of Swannell antiform (approxin
- Minor antiformal axis.....
- Megascopic kink fold

APPENDIX B

GEOLOGY OF THE E, NORTH-CENTRAL COLUMBIA

K. BELLEFONTAINE
SOURCE: MANSY (1986)

SYMBOLS

.....		22
.....		34
.....		46
.....		63
.....		21
.....		11
.....		22
.....		43
.....		33
.....		43
.....		23
.....		67
.....		31
.....		
.....		
.....		11

11









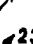








0

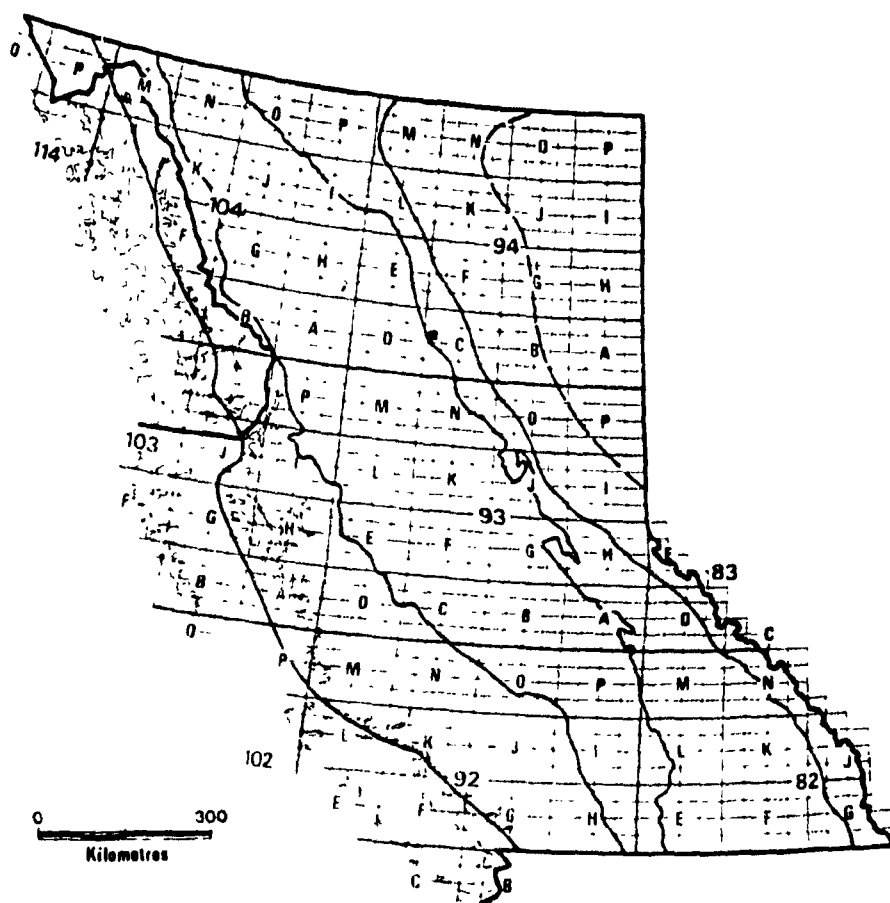
APPENDIX B

STRUCTURAL GEOLOGY OF THE KA RANGE, NORTH-CENTRAL BRITISH COLUMBIA

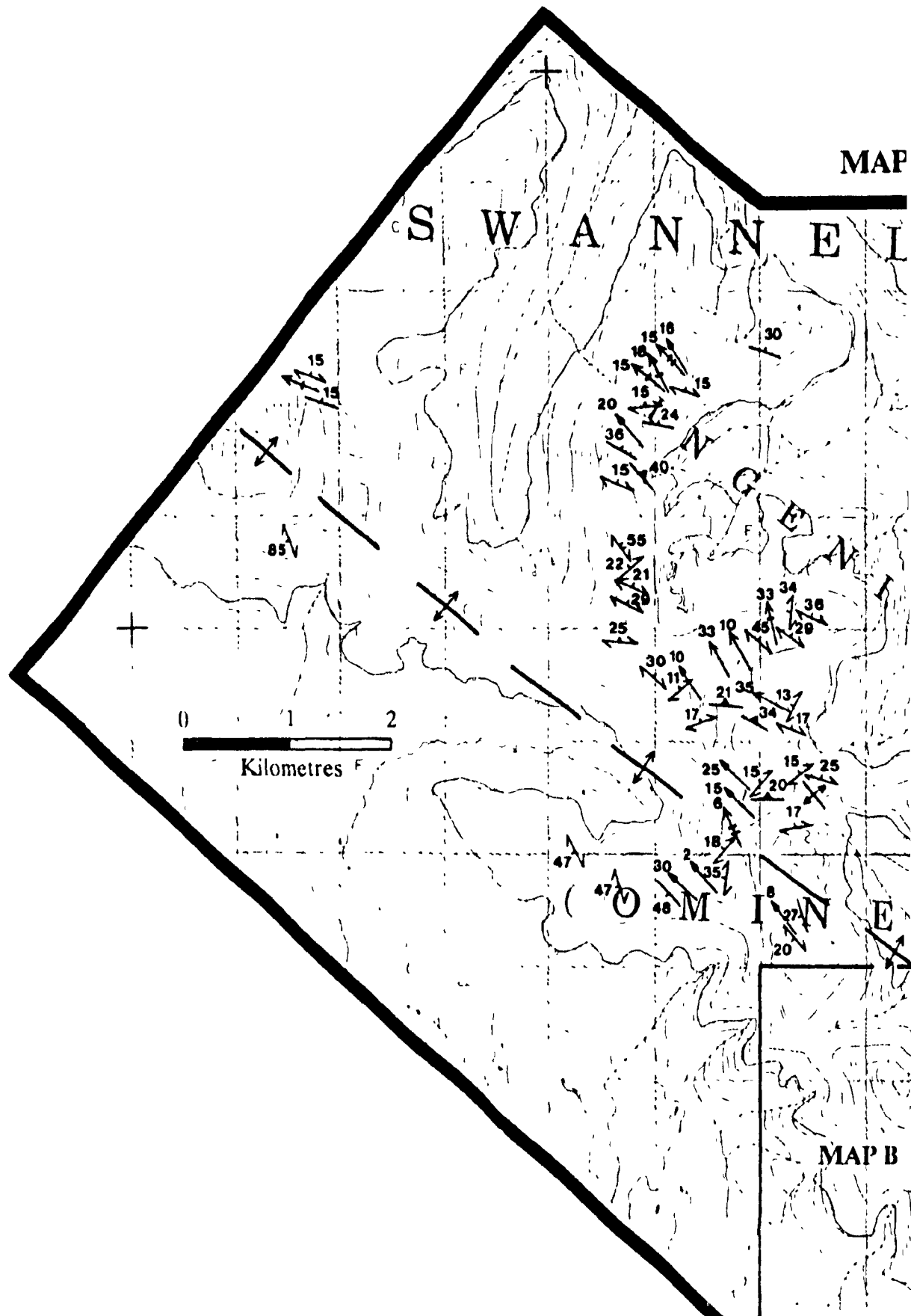
GEOLOGY BY K. BELLEFONTAINE
ADDITIONAL SOURCE: MANSY (1986)

SYMBOLS

.....		22
.....		34
age.....		46
.....		63
.....		21
.....		11
.....		22
own generation).....		43
.....		33
d.....		43
s and lineations.....		23
.....		67
.....		31
vannell antiform (approximate).....		
il axis.....		
fold.....		
.....		11



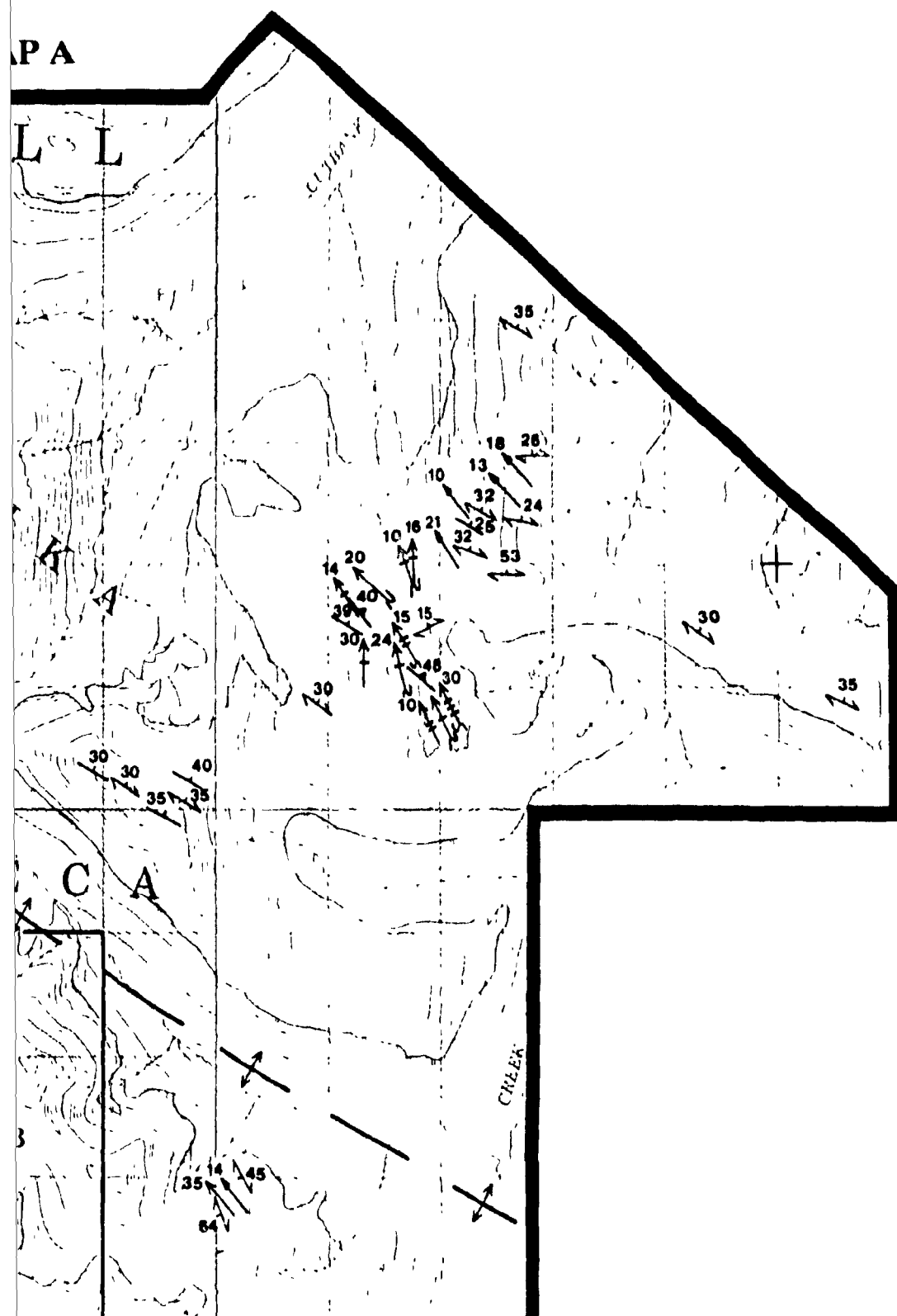
MAP



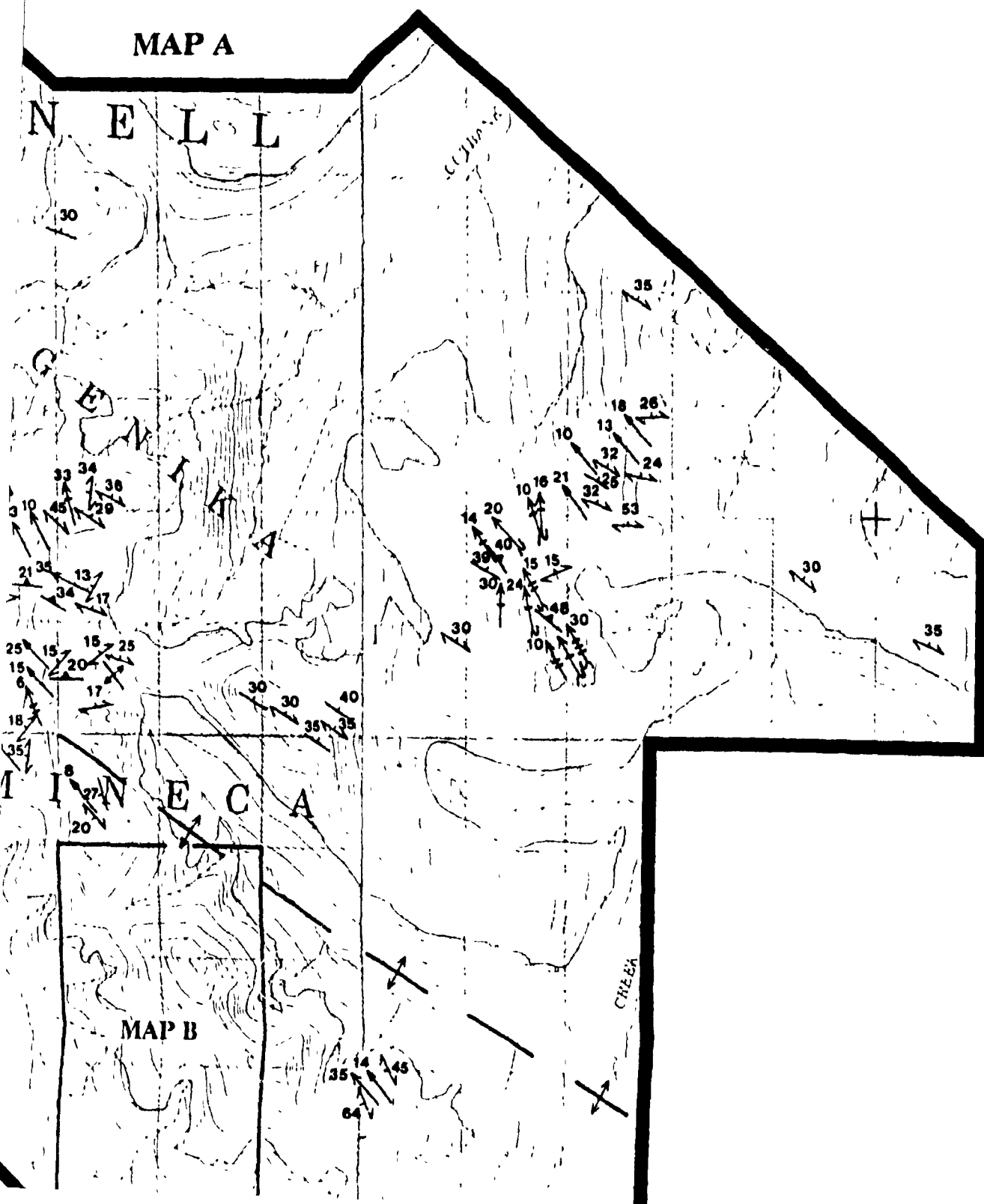
MAP B

PA

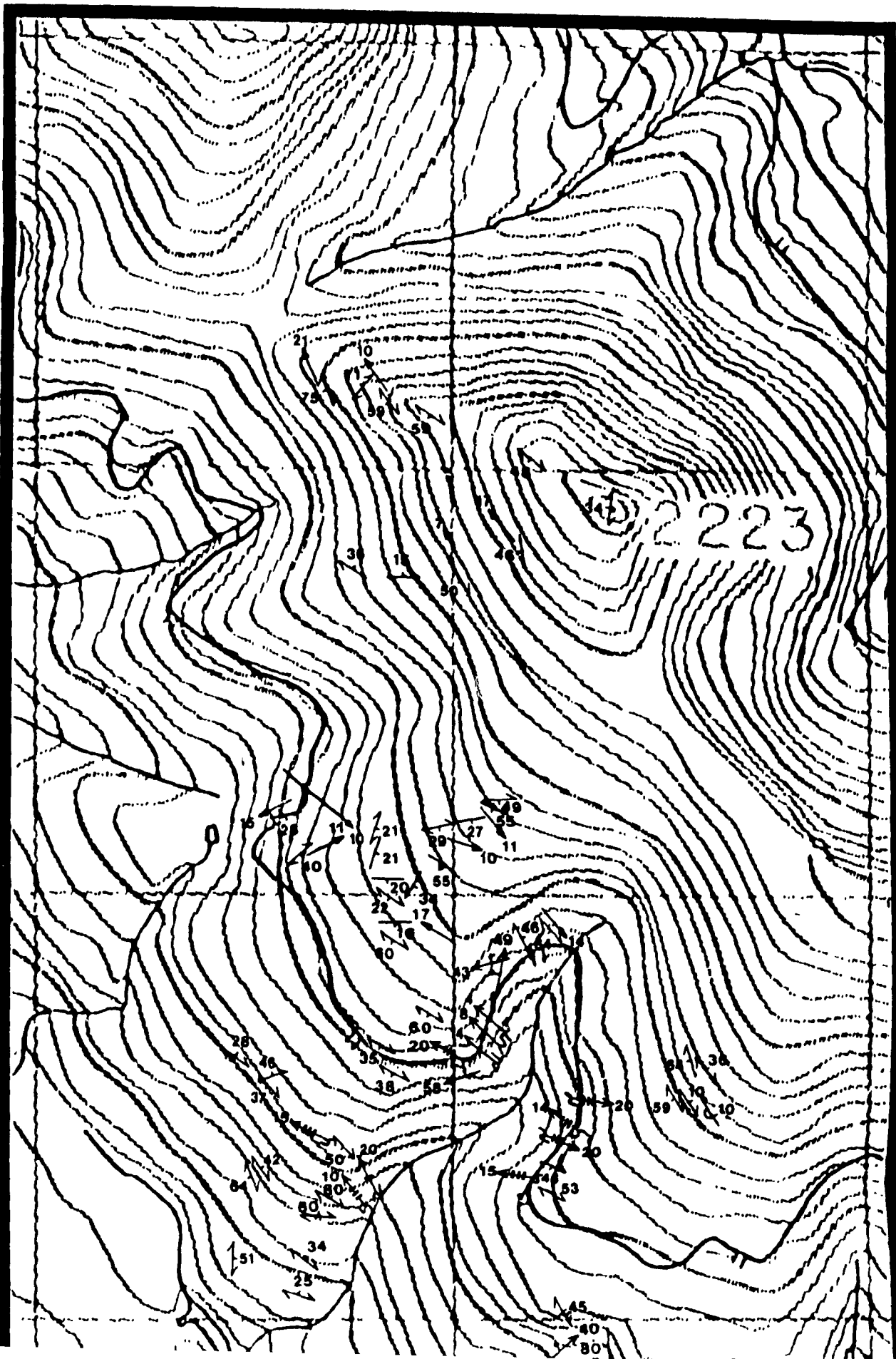
L L



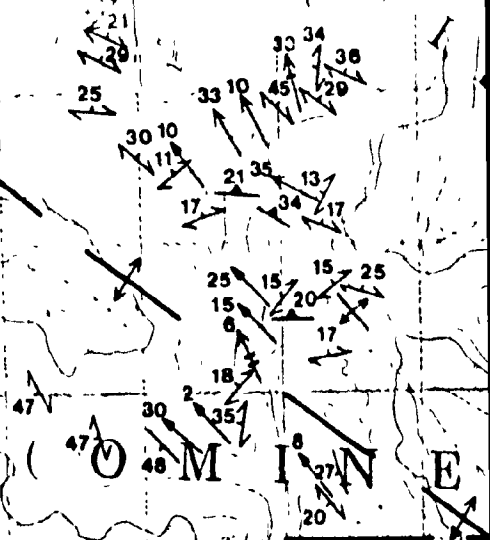
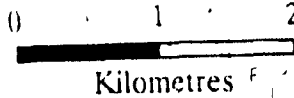
MAP A



MAP B



85V



MAP B



